

**Fritz-Haber-Institut der
Max-Planck-Gesellschaft
Berlin**

12th Meeting of the Fachbeirat

Berlin, 9th - 11th November 2003



Poster Abstracts

**Fritz-Haber-Institut der
Max-Planck-Gesellschaft
Berlin**

12th Meeting of the Fachbeirat

Berlin, 9th - 11th November 2003

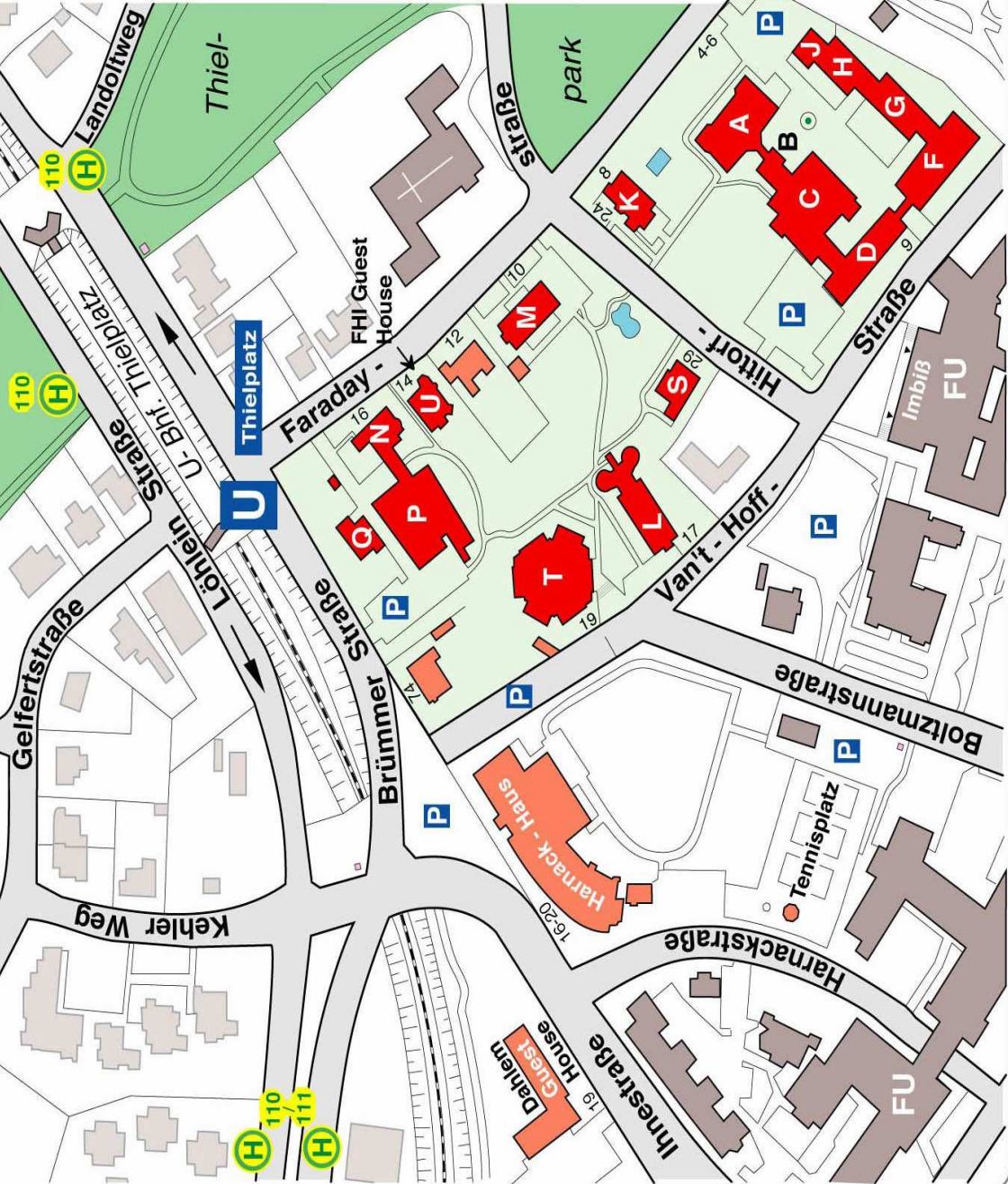
Poster Abstracts

The posters can be found in the following buildings:

	Building
Department of Inorganic Chemistry	F
Department of Chemical Physics	N, P, Q
Department of Molecular Physics	C, D
Department of Physical Chemistry	A, C, F
Theory Department	T

Fritz-Haber-Institut der Max-Planck-Gesellschaft, Faradayweg 4-6, D-14195 Berlin

- A** Physikalische Chemie (G. Ertl)
- B** **Haupteingang** - Telefonzentrale
- C** Zentrale Dienste
Haber-Linde
- D** Molekülphysik (G. Meijer),
Physikalische Chemie (G. Ertl)
- F** Molekülphysik (G. Meijer),
Feinwerktechnik, Betriebsrat
- G** Anorganische Chemie (R. Schlögl),
Physikalische Chemie (G. Ertl)
- H** Bibliothek, Verwaltung
- J** Hörsaal, Holztechnik
- K** Zentrales Beschaffungswesen
- L** Maschinenbau
- M** Haber-Villa: Seminarraum
- N** Ernst-Ruska-Bau:
Anorganische Chemie (R. Schlögl),
Elektroniklabor
- P** Richard-Willstätter-Haus:
Theorie [Geb. II] (M. Scheffler),
Seminarraum
- Q** Chemische Physik (H.-J. Freund)
- S** Seminarraum
- T** PP&B Personal Computer
- U** Theorie [Geb. I] (M. Scheffler),
GNZ Gemeinsames Netzwerkzentrum
Gästehaus, Haustechnik



- N**, **P**, **Q** Chemische Physik (H.-J. Freund)
- S** Seminarraum
- T** PP&B Personal Computer
- U** Theorie [Geb. I] (M. Scheffler),
GNZ Gemeinsames Netzwerkzentrum
Gästehaus, Haustechnik

Department of Inorganic Chemistry

Poster List

Research Area 1: Iron Oxides in Dehydrogenation

- 1.0 Introduction
- 1.1 Iron oxide based model catalysts - preparation and characterization
- 1.2 Iron oxide based model catalysts – adsorption and catalysis

Research Area 2: Zirconia and Heteropoly Acids in Hydrocarbon Activation

- 2.0 Introduction
- 2.1 Active state of heteropoly-acid catalysts of the type
 $H_{3+x-y}Cs_yPV_xMo_{12-x}O_{40} \cdot zH_2O$
- 2.2 Structural dynamics of promoted sulfated zirconia catalysts
- 2.3 Activation, deactivation, and regeneration of sulfated zirconia
- 2.4 New in situ methods

Research Area 3: Vanadium Oxide Catalysts

- 3.0 Introduction
- 3.1 *In-situ* surface characterisation of vanadium-phosphorus-oxide (VPO) bulk catalysts for n-butane oxidation
- 3.2 Micro- and electronic structure of vanadium-phosphorus oxides and vanadium oxides
- 3.3 Preparation and synthesis of VO_x nanowires and nanorods

Research Area 4: Molybdates in C3 selective oxidation

- 4.0 Introduction
- 4.1 Nanostructures as Precursors to In Situ and Chemical Characterisation of a Single Phase Selective Oxidation Catalyst
- 4.2 Structurally Complex Molybdenum Oxide Model Catalysts for the Selective Oxidation of Propene

4.3 Sol-Gel Synthesis and Thin Film Preparation of Molybdenum Oxide based Catalysts

4.4 In situ Structural Characterization of Molybdenum Oxide Catalysts under Partial Oxidation Reaction Conditions

Research Area 5: Copper in C1 Chemistry

5.0 Introduction

5.1 Effect of precipitate ageing of Cu/ZnO catalysts for methanol steam reforming activity

5.2 Cu/ZrO₂ catalysts for methanol steam reforming

5.3 In situ X-ray photoelectron spectroscopy of the methanol oxidation on copper

Research Area 6: Palladium in Model Reactions

6.0 Introduction

6.1 Palladium in Selective Hydrogenation (Athena Project)

6.2 Structural and Catalytic Investigation of Binary Palladium-Gallium Alloys

Research Area 7: Carbon in Catalysis

7.0 Introduction

7.1 Carbon nanotubes and nanobulbs obtained from explosive decomposition of picric acid

7.2 Microstructure and morphology controlled reactivity of environmental carbon

Iron Oxides in Dehydrogenation

This research area deals with the non-oxidative and oxidative dehydrogenation of ethylbenzene (EB) to styrene (St) over iron oxide based catalysts. The study of the oxidative dehydrogenation of EB over carbon catalysts is now part of the new research area “Carbon in Catalysis” (D.S. Su).

Poster (1.1): FeO(111), Fe₃O₄(111) and α -Fe₂O₃(0001) as well as K-promoted Fe₃O₄ model catalyst films were in the past prepared on Pt(111) substrates. Now, comparative studies were made on Ru(0001). New effects like growth of self-assembled ordered arrays of Fe₃O₄(111) islands were observed. Further, K-containing phases like K_xFe₂₂O₃₄(0001)-(2x2) and KFeO₂ were characterized by STM. First steps towards an increased sample complexity were taken by film growth on a stepped Pt substrate. In an attempt to prepare ZrO₂ films, it was found that a FeO layer is a suitable interfacant.

Poster (1.2): The studies of the adsorption and desorption properties of the gases relevant for EB dehydrogenation by isosteric methods were extended to St. All data obtained are critically reviewed.

Studies of EB dehydrogenation with our home made single-crystal flow reactor with pre- and post-reaction surface analysis were systematically continued on unpromoted Fe₂O₃(0001) and on K-promoted K_xFe₂₂O₃₄(0001) films. The initial activity of Fe₂O₃ is as high as on K-promoted films but deactivation by oxide reduction and by carbonaceous deposits is faster. The high initial activity can be maintained by the addition of traces of oxygen.

*Poster 1.1***Iron oxide based model catalysts - preparation and characterization**

The activities concerning the preparation and characterization of epitaxially grown iron oxide and potassium-iron oxide films concentrated on the following topics:

Film growth on Ru was studied by STM and AES. Iron oxide film growth on Ru(0001) is similar to growth on Pt(111). However, the stronger interaction of both O and Fe with Ru causes some differences with remarkable consequences. The initial FeO(111) films align exactly with the substrate atomic rows. Up to four Fe-O bilayers (only 2.6 bilayers on Pt) grow before the growth mode changes. The dipole of the polar FeO(111) film normal to the surface is reduced by huge in-plane expansions for 3 and 4 bilayer thick films. Annealing a 4 bilayer thick film in O₂ causes formation of metastable self-assembled nano arrays of Fe₃O₄(111) islands [1,2].

STM was used to study the growth and structure of K-containing ternary phases. XPS experiments had shown that a series of different ternary K-Fe-O bulk phases is formed when a thick metallic potassium layer, deposited on Fe₃O₄ or Fe₂O₃, is annealed stepwise [3]. The film forming at the temperature of the technical EB dehydrogenation (870 K) consists of K-β-ferrite (K_xFe₂₂O₃₄, 0.67 < x < 2), covered by a thin KFeO₂ layer. STM and AES investigations confirm this [4]. The analogy to the layered structure of the working real catalyst as proposed by Muhler et al. [5] is striking.

STM studies of iron oxide film growth on atomically stepped Pt substrates show restructuring, step-triplicating and a modified Stranski-Krastanov growth mode for Fe₃O₄.

Finally, in cooperation with project 3 (research area 2), the growth of ZrO₂ thin films was studied. On clean Ru(0001) it was not possible to grow an ordered and closed film. This was only possible after depositing a thin FeO film as interfacial layer. We suggest that the in-plane expansion capability of FeO allows for an adjustment of its lattice constant to that of ZrO₂ thus reducing the mismatch energy [6].

*Poster 1.2***Iron oxide based model catalysts – adsorption and catalysis**

In order to obtain energetic and kinetic data for adsorption and desorption of the gases relevant in catalytic dehydrogenation of EB, measurements in adsorption-desorption equilibrium (isosteric methods) were applied during the last 6 years. New results, mainly for St, are discussed within a review of all data obtained so far [7].

Extensive studies of the catalytic activity of single crystalline model catalysts were performed with our single crystal micro flow reactor with GC-MS analysis [8]. The early results presented two years ago [9] are now followed up by detailed investigations [10]. While the reaction temperature (870 K) and the overall flow rate was kept constant, the substrates and the reactant gas mixture were varied. Unpromoted, α -Fe₂O₃(0001) and Fe₃O₄(111), and K-promoted K_xFe₂₂O₃₄(111) (0.67 < x ≤ 2) samples were compared. In order to understand the role of H₂O and O₂ in the reaction, the catalytic activity was measured with EB alone, EB+H₂O and EB+H₂O+O₂ in the reaction gas mixture.

In all cases, activity started without induction period and at a level similar for α -Fe₂O₃(0001) and K_xFe₂₂O₃₄(111). Deactivation of α -Fe₂O₃(0001) occurs over a period of 60-90 min and goes along with a reduction of the oxide and with formation of carbonaceous deposits (CD's). Water in the feed limits reduction to the magnetite state, without water, reduction to metallic Fe⁰ is observed. Deactivation can be avoided by addition of traces of O₂ which prevents reduction and burns CD's. Activity and deactivation of K-promoted catalysts depends on the K content. For too low contents, deactivation by formation of CD's is fast, for too high contents, the activity drops, possibly due to site blocking by K.

Deactivation reduces the catalytic activity of hematite by a factor of 6-10. We believe that the final activity is characteristic for CD's and corresponds to the steady state activity observed in studies performed on unpromoted real catalyst.

We conclude that the active sites on unpromoted and promoted catalysts require accessible Fe³⁺. The prospects to develop a process with unpromoted hematite and traces of O₂ in the feed are checked in cooperation with the group of G. Kolios (Inst. Chem. Engineering, Univ. Stuttgart).

References

1. G. Ketteler and W. Ranke, *Physical Review B* **66** (2002) 033405-1 - 033405-4.
2. G. Ketteler and W. Ranke, *Journal of Physical Chemistry B* **107** (2003) 4320.
3. Y. Joseph, G. Ketteler, C. Kuhrs, W. Ranke, W. Weiss, and R. Schlögl, *Physical Chemistry Chemical Physics* **3** (2001) 4141.
4. G. Ketteler, W. Ranke, and R. Schlögl, *Journal of Catalysis* **212** (2002) 104.
5. M. Muhler, J. Schütze, M. Wesemann, T. Rayment, A. Dent, R. Schlögl, and G. Ertl, *Journal of Catalysis* **126** (1990) 339.
6. G. Ketteler, W. Ranke, and R. Schlögl, submitted (2003).
7. W. Ranke and Y. Joseph, *Physical Chemistry Chemical Physics* **4** (2002) 2483.
8. C. Kuhrs, M. Swoboda, and W. Weiss, *Topics in Catalysis* **15** (2001) 13.
9. C. Kuhrs, Y. Arita, W. Weiss, W. Ranke, and R. Schlögl, *Topics in Catalysis* **14** (2001) 111.
10. O. Shekhah, W. Ranke, A. Schüle, G. Kolios, and R. Schlögl, submitted (2003).

Zirconia and Heteropoly Acids in Hydrocarbon Activation

Introduction

The following hypotheses apply to sulfated zirconia (SZ) and heteropoly acid derived materials (HPA): (i) the catalysts may be bifunctional with e.g. a redox and an acid function, (ii) the bulk structure appears to be important for the catalytic performance, (iii) the active phase is generated only during activation or reaction, this is obvious for SZ from the reaction profiles and has been shown for HPA in previous work of the AC department.¹ These points were addressed in our recent research.

Heteropolyacid-based catalysts of the type $Cs_xH_{4-x}PVMo_{11}O_{40}$ with $2 < x < 3$ are used in the industrial production of methacrylic acid from methacrolein.² In order to also understand the role of vanadium, we have selected $H_3PMo_{12}O_{40}$, $H_4PVMo_{11}O_{40}$, and their Cs salts for our experiments. Structural investigations were conducted with in situ X-ray diffraction and in situ EXAFS spectroscopy with propene as reactant. Further information was derived from optical spectra. Surface sites on differently activated samples were probed with carbon monoxide at liquid nitrogen temperature using IR spectroscopy as analytical technique (*Poster 2.1*).

After extensive investigation of the bulk structure and the nature of the promoters in as-calcined promoted sulfated zirconia catalysts, we are now investigating the structural dynamics of these systems under different kinds of duress, i.e. under mechanical, thermal, and "chemical" stress. (*Poster 2.2*).

Rapid deactivation is a serious problem for sulfated zirconia catalysts. We are conducting investigations to reveal the nature of surface deposits, the number of persistently active (and poisoned) sites, and the best procedure for regeneration. We also seek to prepare materials that are less prone to deactivation such as ordered mesoporous sulfated zirconia (*Poster 2.3*).

Formation of the active phase during activation or reaction makes in situ studies compulsory. In the past two years, progress has been made in the development of two in situ methods: high temperature UV-vis-NIR spectroscopy³ and appearance potential mass spectrometry with molecular beam sampling (*Poster 2.3*).

¹ G. Mestl, T. Ilkenhans, D. Spielbauer, M. Dieterle, O. Timpe, J. Kröhnert, F.C. Jentoft, H. Knözinger and R. Schlögl, Appl. Catal. A: General, **210** (2001) 13.

² T. Okuhara, N. Mizuno, M. Misono, *Adv. Catal.* **41** (1996) 113.

³ J. Melsheimer, M. Thiede, R. Ahmad, G. Tzolova-Müller, F.C. Jentoft, Phys. Chem. Chem. Phys., accepted.

Poster 2.1

Active state of heteropoly-acid catalysts of the type $H_{3+x-y}Cs_yPV_xMo_{12-x}O_{40} \cdot zH_2O$

In situ XRD and XAS experiments combined with MS showed that under reducing atmosphere (propene or hydrogen), in $H_3[PMo_{12}O_{40}] \cdot 13H_2O$ and $Cs_2H[PMo_{12}O_{40}]$ migration of molybdenum cations from the Keggin ion onto interstitial sites takes place above ≈ 573 K, resulting in thermally stable partially reduced lacunary Keggin ions. In $Cs_3[PMo_{12}O_{40}]$ all interstitial sites are occupied by Cs cations, and no partial reduction or decomposition with temperature was observed. Under catalytic oxidation reaction conditions (propene and oxygen), the onset of activity of $H_3[PMo_{12}O_{40}] \cdot 13H_2O$ and $Cs_2H[PMo_{12}O_{40}]$ at ~ 573 K correlates with a partial reduction of Mo and characteristic changes in the local structure of the Keggin ion, which indicate that similar to the treatment in propene, migration of Mo ions from the Keggin ions onto interstitial sites and formation of lacunary Keggin ions takes place. Evidently, the undistorted Keggin ion in the as-prepared heteropolyoxomolybdates should be regarded as a precursor of the active catalyst.

The model for the description of electron transfer optical bands of $H_4PVMo_{11}O_{40} \cdot yH_2O$ was refined and now accounts for the multinuclearity (Keggin ion) of the compound, its structural transformation during crystal and constitutional water loss. The vibronic coupling constants and the crystal field splittings have been calculated with allowance for covalency effects. For the first time the parameters characterizing corner- and edge-sharing electron transfer have been estimated and shown to be values of the same order of magnitude. The absorption coefficient has been calculated by summation over spectra arising from all possible single electron transfers between adjacent sites. It was shown that the dominant contribution to the spectra at 422 K comes from the intervalent transitions in binuclear $(MoH_b)MoO_{11}$ species with an acidic proton (H_b) residing on a bridging oxygen.

Adsorption of CO at 77 K on activated Cs salts of $H_{3(4)}P(V)Mo_{12(11)}O_{40}$ resulted in several bands. A band at $2162\text{-}2164\text{ cm}^{-1}$ is assigned to CO adsorbed on OH groups as it was observable after treatment at 523 K but not after treatment at 673 K, and it was not detected for the Cs-rich and thus H-poor compounds. A band at $2152\text{-}2155\text{ cm}^{-1}$ arises from adsorption of CO on Cs.⁴ Its relative intensity increased with increasing Cs content. A band at $2137\text{-}2140\text{ cm}^{-1}$ was unspecific. Two so far unreported bands were located at $2144\text{-}2147\text{ cm}^{-1}$ in the spectra of $Cs_3HPVMo_{11}O_{40}$ & $Cs_4PVMo_{11}O_{40}$, and at $2130\text{-}2135\text{ cm}^{-1}$ in the spectra of $Cs_2H_2PVMo_{11}O_{40}$ & $Cs_4PVMo_{11}O_{40}$. These bands could indicate weak Lewis acid sites in the form of coordinatively unsaturated Mo or V cations in defective Keggin units, consistent with the structural evolution upon heating as observed by XRD and XAS.

⁴ T. Saito, G. Koyano, and M. Misono, Chem. Lett. 11 (1998) 1075.

*Poster 2.2***Structural dynamics of promoted sulfated zirconia catalysts**

Sulfated zirconia catalysts are easily modified by simple laboratory procedures such as grinding, milling, or pressing. We have observed the formation of a considerable fraction of the monoclinic zirconia phase (from originally entirely tetragonal material) as a result of the above mentioned treatments. These changes to the bulk structure occur despite the presence of sulfate and manganese, both of which exert a stabilizing effect on the tetragonal structure. Surface area and sulfate content remained largely unaffected. The catalytic activity decreased dramatically through the mechanical stress treatments. Milled sulfated zirconia was less active throughout the entire reaction profile than untreated sulfated zirconia. For Mn-promoted sulfated zirconia, particularly the initial high activity was affected by milling but not so much the long-term activity. These results underline the sensitivity of the bulk structure and the active sites of zirconia catalysts, and demonstrate that these samples must be analyzed with great caution.

Sulfated zirconia catalysts undergo structural changes during thermal treatment. SZ and promoted SZ (Mn, Fe) show three steps in the TG curve when they are heated from room temperature to 1473 K and then cooled after 30 min holding time. During the endothermic loss of water at about 373 K also O₂ is set free in an amount equal to about one O per S. The second weight loss is heat neutral and occurs around 1023 K. Sulfate is decomposed to give SO₂ + O₂, corresponding to a formal loss of SO₃. The third weight loss, also formally SO₃, is associated with the exothermic phase change from tetragonal to monoclinic zirconia. For SZ it appears during cooling approximately at 1023 K, promoted samples show it during heating between 1223 and 1473 K depending on the type (better incorporation of Mn than Fe into the zirconia lattice) and amount of promoter. It seems that there is the following correlation for promoted samples: The higher the temperature of the phase change, the higher the long-term activity of the catalyst in *n*-butane isomerization.

In situ XAS experiments show that Mn in promoted sulfated zirconia is reduced during treatment in He, H₂, and even in 50% O₂. As we presume that Mn is predominantly present inside the zirconia lattice, the results point towards an active participation of the zirconia bulk. The local (6 Å) structure around the Mn changes during activation. After reduction treatment (703 K, 30 min, 50% H₂) a good fit of the EXAFS is obtained with 4 oxygens at 2.12 Å and 2 at 2.44 Å, suggesting octahedral coordination. High symmetry around Mn²⁺ is also indicated by EPR. However the average Mn valence is non integer and so even the reduced sample most likely has more than one Mn species. Although catalysts with a higher Mn valence were characterized by a higher maximum activity the actual catalyst performance did not correlate with the Mn oxidation state over the reaction profile.

*Poster 2.3***Activation, deactivation, and regeneration of sulfated zirconia**

Sulfated zirconia catalysts, when exposed to alkanes, typically first undergo an induction period during which the activity is insignificant. The conversion then rises quickly, passes through a maximum, and declines. We have generated sulfated zirconia in such different stages of activity in flow reactor experiments and have then "quasi-in-situ" probed the remaining sites for *n*- and isobutane adsorption by microcalorimetry and TAP experiments (U Leipzig). Isotherms show a decrease in the number of sites with increasing time on stream, heats of adsorption additionally indicate qualitative changes to the sites. The TAP profiles support these observations in that they also show a change in the interaction of butanes with the pre-reacted surface.

Unsaturated surface deposits were detected by in situ UV-vis spectroscopy on tetragonal ("conventional") and ordered mesoporous (MCM-41-type) sulfated zirconia during *n*-butane and *n*-pentane isomerization. In order to further identify the nature of these deposits, which had been tentatively assigned to allylic cations, the deactivated materials were reacted at 298 K first with oxygen and then with water vapor. The gas phase was monitored by MS. In oxygen stream, only minor changes were observed in the spectra of deactivated tetragonal zirconia; in water, intense bands developed at about 380, 455, and 550-560 nm, and the original band of the surface deposit at 310 nm was reduced in intensity. For ordered mesoporous sulfated zirconia, exposure of the deactivated sample to oxygen induced an overall intensity decrease between 250 and 450 nm. Only the sample that was deactivated in *n*-pentane isomerization had surface species that reacted with water: a band at 302 nm was diminished and new bands at 382 and 457 nm formed. Assignment of these bands, which can only arise from molecules with extensive π -systems, is in progress, under consideration of the MS data, which in some of the above experiments yielded weak signals.

Sulfated zirconia was also regenerated after *n*-butane isomerization. A series of consecutive reactivation experiments were conducted, using 50% oxygen at 723 K and alternatingly a short (1 h) and a long (71–88 h) reactivation procedure. The short exposure to oxygen produced a more active and the long exposure a less active catalyst. The catalyst could be switched back and forth between these states. The different responses to oxygen on a scale of hours suggest solid state (bulk) reactions, and this assumption was further confirmed by comparison with literature data⁵ on the oxidation kinetics of sub-stoichiometric zirconia.

⁵ S. Aronson, J. Electrochem. Soc. 108 (1961) 312.

*Poster 2.4***New in situ methods**

The new UV-vis-NIR setup was designed to obtain high quality spectra over the full wavelength range of 250 -2500 nm at temperatures up to 723 K. Key feature is an about 120 mm long light conductor made from quartz, which focuses the light from the source onto the sample and transfers the diffusely reflected light back onto the detectors via the integrating sphere. At this distance, the reactor with the powder bed can be placed into the isothermal zone of a tubular furnace. The light conductor is formed in a tapered way, which reduces the area emitting noise-generating thermal radiation from the hot sample and the amount of sample necessary. This setup was used to measure spectra of zirconia and molybdena catalysts while they were heated in different atmospheres for activation or calcination, and spectra of zirconia catalysts during alkane isomerization.

There are many examples of heterogeneously catalyzed reactions, especially such running at higher temperatures, where gas phase species were found to play a remarkable role in the mechanism. Goal of the project is to develop a mass spectrometric method to sample and analyze the gas phase above a catalyst surface in situ for reactive intermediates, particularly radicals. To reach this goal a tubular reactor consisting of two concentric, resistively heated Pt-tubes has been designed and is under construction. The reaction – given the versatility of Pt as a catalyst, the choices are numerous – will proceed on the Pt-surfaces in the slit between the inner and outer tube. The inner tube can contain a thermocouple or can be used as drain for the exhaust gases. In situ sampling is realized through an orifice of about 250 μm diameter drilled into the reactor wall. The entire reactor will be placed in an HV-chamber and the orifice will serve as internal nozzle through which the gas expands adiabatically. Any reactive molecule desorbing from the catalyst surface will be frozen and subsequent reactions are prevented. High throughput pumps are required to keep the pressure downstream of the nozzle below 10^{-3} mbar to avoid any shock wave structure in the expansion (Fenn type interface).⁶ A differentially pumped arrangement of skimmer and sampler cone forms a molecular beam that is aligned with the ion source of the mass spectrometer. The beam molecules are either identified by characteristic masses or in case of radicals by the threshold ionization technique. This method takes advantage of differences in ionization potentials and allows distinction of radicals from other species with the same mass/charge ratio.

⁶ R. Campargue, *J. Phys. Chem.* **88** (1984) 4466.

V oxides for selective oxidation

Vanadium oxides and vanadium-phosphorus oxide (VPO) systems are extensively used as catalysts in mild oxidation of hydrocarbons. Vanadium pyrophosphate (VPP) is active and the only one commercialized ternary vanadium phosphorus oxide in the selective oxidation of n-butane to maleic anhydride (MA). Besides that, vanadium containing systems attract scientific interest due to their electrochemical properties and their interesting magnetic behaviors leading to a wide range of applications reaching from cathode material in lithium-ion batteries to model systems for spin ladders and high TC components.

The previous research up to the 11th Fachbeirat meeting in 2001 revealed that butane oxidation over VPP is most probably not structure sensitive and there is no simple correlation between structure and activity, due to the presence of amorphous surface structure. All the research works published may suggest that VPP is only necessary in the n-butane to MA selective oxidation as bulk phase to support the active surface of working VPO catalysts. *In situ* spectroscopic techniques (*in situ* XPS and *in situ* XAS) are developed and used to study the active surface of working VPO catalysts during the n-butane oxidation to MA using a proton transfer reaction mass spectrometer to monitor the catalytic activity of the material simultaneously to the spectroscopic characterisation of the catalyst's surface. The experimental results on working catalysts stress the dynamic nature of the VPO surface. The surface structure of working VPO catalysts is different from a crystalline single phase like vanadyl pyrophosphate (*Poster 3.1*).

One other significant phenomenon in VPP catalysts is the presence of various V⁵⁺ phases (in form of VOPO₄) and the preparation- and activation-dependent microstructure and micromorphology of the resulting catalysts. TEM, EELS and XRD are used to study the geometric structure of VPO prepared with different routes and of the standard V⁵⁺ phases. *Ab initio* band-structure calculations were performed to study the electronic structure of single-valence vanadium oxides with respect to the differences in oxidation state and geometric structure (*Poster 3.2*).

Due to the structure complexity of vanadium oxides and VPO systems, fundamental catalysis research requires uniform materials offering the opportunity to study selective oxidation on model system with well determined surface morphology and high crystalline order. In an initial work, nanostructured vanadium oxides (nanorods, nanowires) were prepared using wet-chemical methods giving promising perspective for the preparation of pure and nanostructured VPO systems (*Poster 3.3*).

*Poster 3.1***In-situ surface characterisation of vanadium-phosphorus-oxide (VPO) bulk catalysts for n-butane oxidation**

Vanadium-phosphorus-oxide (VPO) catalysts are known to be active in the selective oxidation of *n*-butane to maleic anhydride (MA). Different phases, both crystalline and disordered, are found on the VPO surface influencing the catalytic activity in various ways. We applied *in-situ* X-ray absorption spectroscopy (XAS) and the recently successfully developed *in-situ* X-ray photoelectron spectroscopy (XPS) to study the active surface of working VPO catalysts during the *n*-butane oxidation to MA. The catalytic activity of the material was monitored by proton transfer reaction mass spectrometry (PTR-MS) simultaneously to the spectroscopic characterisation of the catalyst's surface.

The surface structure of the catalyst depends strongly on the temperature and the gaseous environment. The dynamic nature of the surface is revealed by the temperature dependence of the V L₃-edge NEXAFS that represents various surface functional groups. These changes are related to the activity to maleic anhydride of the catalyst. The variation of the spectral shape indicates the presence of structural changes of the catalyst surface. One type of functional group predominates at room temperature, whereas other groups dominate at higher temperatures. The ability of the surface to undergo these changes is different for differently active catalysts. This suggests that these rearrangements are one factor that determines the catalytic performance. The *in-situ* XP spectra revealed changes in the vanadium oxidation state between +4.0 and +4.5 as response on the temperature and the ambient gas atmosphere. A V valence gradient was found by XPS depth profiling technique. In general, the oxidation state was lower at the surface (1 nm information depth) as in deeper layers (3 nm) of the catalyst. The presence of V⁵⁺ centres (7% to 53% of all V atoms) was proven by deconvolution of the V2p_{3/2} XP peak. The involvement of these centres in the anaerobic *n*-butane oxidation could be shown.

Our findings stress the dynamic nature of the VPO surface. The surface structure of working VPO catalysts is different from a crystalline single phase like vanadyl pyrophosphate. The importance of an *in-situ* surface characterisation of this bulk material under *n*-butane reaction conditions became obvious.

*Poster 3.2***Micro- and electronic structure of vanadium-phosphorus oxides and vanadium oxides**

The micro-morphological studies of VPO catalysts reveal the structural complexity of this system: besides a small fraction of amorphous materials at the surface of particles, V^{5+} phases (in form of $VOPO_4$) are always present. This fact can be associated with different catalytic performance (different ratio of V^{5+} phases to VPP matrix). The V^{5+} can exist either as separate single particle or grown as grain on vanadyl pyrophosphate particles. Its characteristic morphology differs from the main VPP phases, but the structure suffers from the high electron beam sensitivity in TEM. The morphological studies of VPO catalysts prepared using various acids, vanadium sources and in different solution with and without refluxing reveal a preparation-dependent microstructure and phase composition. Together with the fact that the catalytic performance of VPO is also preparation- and activation-dependent, our finding doubt again the hypothesis that vanadyl pyrophosphate is the unique active phase during the n-butane to maleic anhydride oxidation since the experiment cannot confirm the established structure/reactivity relationship of VPO system.

Ab initio band-structure calculations were performed to study the electronic structure of single-valence vanadium oxides with respect to the differences in oxidation state and geometrical distortion. The density of unoccupied state is calculated for the modelling of the ELNES obtained in analytical TEM and of the NEXAFS obtained in in-situ XAS. Anisotropy in the electronic structure of V_2O_5 was investigated by performing EELS at different spectrometer collection angles and orientation- and collection angle dependent simulations. A comparison between two polymorphs of V_2O_5 (α - and γ - V_2O_5) allowed the observation of geometric effects on the electronic structure at a fixed vanadium valence state, whereas changes in the oxidation state of vanadium combined with structural changes are observed when comparing V_2O_5 with V_2O_4 , V_2O_3 and VO. This investigations help to give an interpretation of previous experiments in which the electron beam induced reduction process as well as the thermal decomposition of V_2O_5 has been studied.

Vanadium-phosphorus oxides are very prone to electron beam induced decomposition and reduction. A valid interpretation of spectra recorded under low dose criteria can only be given under assistance of EELS spectra that were simulated for a variety of possible vanadium-phosphorus oxide phases.

*Poster 3.3***Preparation and synthesis of VO_x nanowires and nanorods**

Recently the control of the shape in the production of nanoparticles has become a new and interesting research area. In fact it has been demonstrated that physical properties are strongly related to the nanoparticles shapes. Due to the structural complexity of vanadium oxides and VPO systems, fundamental catalysis research requires uniform materials offering the opportunity to study selective oxidation on model systems with well determined surface morphology and high crystalline order containing the oxidation state V⁵⁺. Usually such well-defined model system is difficult to obtain with more conventional PVD methods. Alternative methods are developed for the synthesis of nanostructured vanadium oxides.

A new soft chemistry way to synthesize for the first time divanadium pentoxide (V₂O₅) nanorods and nanowires has been developed by colloidal self assembly made of Sodium bis(ethyl-2-hexyl)sulfosuccinate (AOT)/Isooctane/H₂O. The vanadium oxide nanocrystals are grown in the solution anisotropically, forming a rod-like shape. The length can be tuned easily by keeping the particles in micellar solution after the synthesis from 40 nm to 1 μm. The particles are characterized by transmission electron microscopy, x-ray photoemission spectroscopy, electron energy loss spectrometry, infrared spectroscopy and x-ray diffraction. These techniques show that the nanorods and nanowires consist of divanadium pentoxide and are crystallized in the γ phase.

Using a quite different method, vanadium oxide nanowires are also obtained by a simple hydrolysis of aqueous NH₄VO₃ solution at refluxing temperature, in which carbon nanotubes are introduced. The carbon nanotubes are found for the first time to induce an anisotropic nucleation of the layered oxide nanostructures on one side of the curved tube surfaces. The formed oxide nuclei peel away from the tube surface and then grow continuously into long nanowires. The inducement mechanism is confirmed by TEM observations of related intermediate derivatives. The obtained oxide nanowires are free-standing, with lengths up to 20 μm and widths of 5-15 nm. Both hydrated penta-valence and tetra-valence vanadium oxides are present as uni-dimensional objects. The oxide nanowires are thermally stable in morphology at temperatures as high as 400 °C in air, although the wire surfaces become rough and most of the water molecules in the them great potential of practical applications such as in catalysis and functional ceramics crystals are lost, which endow.

Mo oxides in C3 selective oxidation

Molybdenum oxide based catalysts, are extensively used in industry for the synthesis of acrylic acid. Despite their industrial importance there is still a lack of information concerning structure formation during synthesis and the atomic arrangements with respect to different preparation routes and element ratios. It is now commonly accepted that the main catalytic processes occur on centers with a high- but often unidentified- number of defects. The most common methods for defect formation involve introduction of heteroatoms (Poster 4.1.), controlled precipitation (Poster 4.2), Sol gel synthesis (Poster 4.3.), and oxidation/ reduction (Poster 4.4.). The major aim of this project was firstly to identify specific defects in Mo oxides, secondly to control their formation and thirdly to understand their relevance during catalytic reactions.

Poster 4.1. The ternary oxide $(\text{MoVW})_5\text{O}_{14}$ was successfully synthesized. Studies of the coordination chemistry of the molybdate species in the precursor solutions have established that mixing the precursor solutions forms a polymeric network in which the vanadyl species act as a linker between the molybdate species and tungsten favors formation of a pentagonal bipyramid as its main structural motif.

Poster 4.2. Controlling the precipitation of molybdenum oxide in aqueous solution is a method to arrive at structurally complex solids suitable as model catalysts for selective oxidation studies. The precipitation parameters are identified and are reviewed for their relevance on the final product properties.

Poster 4.3. The sol gel process of Mo oxide formation has been observed by in situ UV vis spectroscopy for the first time. Careful adjustment of the hydrolysis parameters allows us to control the formation of molybdenum clusters in solution. With this method thin Mo oxide films on a Si (100) wafer have been successfully prepared which will serve as model surfaces for catalytic studies.

Poster 4.4. In situ bulk studies of MoO_3 have been performed to elucidate structure-reactivity relationships and reveal the “real” structure of MoO_3 under partial oxidation reaction conditions. Oxidation of MoO_2 and reduction of MoO_3 have both shown the existence of $\text{Mo}_{18}\text{O}_{52}$ shear structures which are also present in catalytically active Mo oxide under partial oxidation conditions at temperatures below 720 K.

*Poster 4.1***Nanostructures as Precursors to In Situ and Chemical Characterisation of a Single Phase Selective Oxidation Catalyst**

The ternary oxide $(\text{MoVW})_5\text{O}_{14}$ is considered to be highly significant for catalytic, mild selective oxidation reactions [1]. The nature of the active site and the role of tungsten and vanadium are still discussed. A breakthrough was achieved recently by preparing an active single $(\text{MoVW})_5\text{O}_{14}$ phase and thereby showing that no phase cooperation or spill over phenomena are functionally essential for catalytic activity [2]. This structure that is believed to be the active site shows Mo atoms in pentagonal bipyramidal coordination. The degree of catalytic activity was found to be crucially dependent upon the preparation parameters, as compounds with identical XRD patterns showed significantly different catalytic activities.

The aim of this work was to understand the chemistry behind each step of preparation. The starting materials were aqueous solutions of ammonium heptamolybdate (AHM), ammonium metatungstate (AMT) and vanadyl oxalate. Investigations were performed on the pure AHM solution as well as on the mixture. The structural changes in solution are followed by conductivity experiments as well as UV/Vis, ^{95}Mo NMR and ESR spectroscopy.

UV/vis spectroscopy and the conductivity experiments have shown that addition of vanadyl oxalate to ammonium heptamolybdate leads to kinetically controlled protonation- and condensation reactions. Addition of the vanadyl oxalate is the rate-determining step. Whilst quick addition leads to higher polymerisation/condensation products, slower addition leads to a higher proton concentration (lower pH). In parallel protonated AHM is transferred into octamolybdate. Further support is drawn from ^{95}Mo NMR study that formation of $[\text{Mo}_8\text{O}_{26}]^{4-}$ -type species is dominant in the MoVW mixed solutions. These findings are in line with a long series of pH dependent investigations of Polyoxometallate chemistry [3, 4]. ESR showed the existence of associated vanadyl species, while molybdenum and tungsten are all in an oxidation state of (+6). Tungsten atoms are incorporated into the octamolybdate species, leading to the formation of the pentagonal bipyramidal motive.

*Poster 4.2***Structurally Complex Molybdenum Oxide Modell Catalysts for the Selective Oxidation of Propene**

It is commonly accepted that highly specific local electronic structures of the active metal sites are essential for the catalytic performance [3]. A measure for the local electronic structure in Mo^{VI} and Mo^V polyhedra is the variation of terminal Mo-O bond distances. A broader variation of such distances is commonly achieved by introduction of defects through reduction or oxidation, (see Poster 4.4) or introduction of heteroatoms (see Poster 4.1). However, in order to minimise chemical complexity and to optimise synthetic strategies towards catalytically relevant molybdates it is desirable to explore the potential of controlled precipitation chemistry coupled with avoiding the usual high-temperature calcination that eliminates all non-orthorhombic binary molybdates. The present study investigates the sequence of events during decreasing pH precipitation that is the normal method of preparation. It highlights the potential to synthesise complex connectivity of molybdate polyhedra without having to use thermal defect formation procedures.

Ammonium heptamolybdate (AHM) was employed as Mo source and HNO₃ was used as precipitation agent. Most experiments were carried out at ambient temperature. The concentration of the AHM solution was chosen to be 0.1 molar (equivalent to 0.7 molar in [MoO₄]²⁻). A titration automat (Mettler Toldedo DL 55) was used with 100 ml vessels. The pH data were recorded and analysed digitally. Some preparations were 50 times up-scaled in a home-made four litre computerised semi-technical preparation set-up allowing to control the temperature accurately and to measure simultaneously pH and electrical conductivity. The same concentrations and rates of additions were used than in the small-scale preparations.

Two different materials were obtained in a controlled manner. It can generally be stated that high molybdenum concentrations and low temperature lead to a spontaneous precipitation of a supramolecular compound, which is very similar to the [Mo₃₆O₁₁₂]⁸⁻ reported by Krebs [6] whereas low Mo concentration and high temperature leads to the formation of a hexagonal MoO₃ reported by Garin, J L, Blanc, J M.[7]. Temperature programmed reaction spectroscopy showed a similar behaviour during the onset of catalytic activity for pure Mo oxides and the doped Mo oxides. The major effect of tungsten and vanadium additions is to maintain the structural complexity at high temperatures by stabilizing the active phase against conversion into inactive o MoO₃ [see Poster 4.1].

Poster 4.3

Sol-Gel Synthesis and Thin Film Preparation of Molybdenum Oxide based Catalysts

The reliable synthesis of catalytic systems (oxides) is a key step to an understanding of the catalytic function. To improve our comprehension of the interaction and structural development of the constituents of a heterogeneous catalyst it is necessary to monitor and understand the successive steps during preparation. In this project the versatility of the sol-gel process is used in order to elucidate structure reactivity relationships of molybdenum oxide based catalysts. Thin films of metal oxides were obtained by spin-coating as they represent a good compromise between model- and real-catalysts and a promising material in order to bridge the so-called material gap in heterogeneous catalysis.

Alkoxides typically used in sol-gel chemistry are commercially not available in the case of molybdenum and had to be synthesized. $\text{Mo}(\text{NMe}_2)_4$ and $\text{Mo}(\text{OtBu})_4$ were chosen as precursors due to their facile and characteristic hydrolysis and condensation properties. In order to get information on the hydrolysis and condensation processes during synthesis, these steps were monitored by in situ UV/vis- and Raman-spectroscopy. The combination of both methods revealed a change in the oxidation state from Mo^{+4} to a mixture of Mo^{+4} , Mo^{+5} and Mo^{+6} , followed by a quick (within minutes) condensation process and the formation of polyoxometall species similar to those formed in aqueous solution.

DSC/TG experiments at different gas compositions ($p\text{O}_2=2-10\%$) and temperatures up to 500°C indicate typically a three step thermal transformation from polymeric solids (xerogels) to $\alpha\text{-MoO}_3$. The as prepared xerogels already exhibit a short range ordering indicated by XRD and Raman. The Ramanshift of the Xerogels suggest the formation of larger polycondensates with, even if poor, defined structure.

The thin films are prepared by using the same procedure as for powders and should therefore be comparable. The surface of the films was investigated using SEM, AFM and XPS. AFM measured height of the films could be varied from 20nm to 150nm, depending mainly on concentration of the precursor solution and the spinning velocity. The as prepared films after drying at 120°C show a uniform flat surface. At about 300°C small crystals break through the surface and are exposed to the exterior. At higher temperatures the surface is composed of a closed roughly structured crystalline film preferentially orientated in the (0k0) direction.

*Poster 4.4***In situ Structural Characterization of Molybdenum Oxide Catalysts under Partial Oxidation Reaction Conditions***Introduction*

Molybdenum trioxide, MoO₃, is both an active catalyst for the oxidation of propene and a suitable three-dimensional model system for the more complex molybdenum based mixed oxide catalysts. The defects in the regular layer structure of MoO₃ that may form under reaction conditions, and the structural properties and the role of these defects in partial oxidation reactions are not fully understood yet. Therefore, we have performed bulk structural in situ investigations of MoO₃ to elucidate structure-reactivity relationships and reveal the “real” structure of MoO₃ under partial oxidation reaction conditions.

Results

Reduction of MoO₃ in propene and oxidation of MoO₂ in oxygen were investigated by in situ XRD and XAFS. During the reduction of MoO₃ in propene and the oxidation of MoO₂, only crystalline MoO₃ and MoO₂ were detected by in situ XRD. However, analysis of the in situ XAFS data yielded the formation of “Mo₁₈O₅₂” type shear-structures as intermediate of both the reduction of MoO₃ in propene and the oxidation of MoO₂ in oxygen. The solid-state kinetics of the reduction of MoO₃ in propene exhibits a change in the rate-limiting step both as a function of temperature and as a function of the extent of reduction. Under partial oxidation reaction conditions (273 K to 773 K and propene to oxygen ratio from 1:1 to 1:5), MoO₃ remains the only crystalline phase detected by XRD. The onset temperature for the temperature-programmed reaction of propene and oxygen in the presence of MoO₃ coincides with the onset of the reduction of MoO₃ in He, H₂, or propene. Various in situ experiments indicate that the structural evolution of MoO₃ during TPR, reduction, and treatment in He is similar. At temperatures below ~720 K and independent of the atmosphere used, partial reduction of MoO₃ is observed resulting in the formation of “Mo₁₈O₅₂” type defects in the bulk structure. At temperatures above ~720 K and in oxygen or in an oxidizing atmosphere (sufficiently low propene to oxygen ratio), the “Mo₁₈O₅₂” type defects are re-oxidized to MoO₃. Evidently, the catalytically active molybdenum oxide phase under partial oxidation conditions at temperatures below 720 K does not correspond to the original MoO₃ possessing the undisturbed ideal layer structure of orthorhombic α -MoO₃. Instead, at these temperatures, the catalytically active phase, which is partially reduced and possesses a large amount of “Mo₁₈O₅₂” type defects (crystallographic-shear structures) in the layer structure of MoO₃, develops under reaction conditions. The results presented clearly show the necessity and the large potential of bulk structural investigations of heterogeneous catalysts under reaction conditions.

References

- 1) Hibst, H., Unverricht, S., (BASF) DE 19815281 1
- 2) Knobl, S., Zenkovets, G., Kryukova, G., Ovsitser, O., Niemeyer, D., Mestl, G., Schlögl, R., *Journal of Catalysis*, 2003, **215**, 177
- 3) Tytko, K-H., Glemser, O., *Adv. Inorg. Chem. Radiochem.* 1976, **19**, 239
- 4) Tytko, K-H., Baethe, G., *Z. Anorg. allg. Chem.*, 1983, **503**, 43
- 5) Grasselli, R. K., *Topics in Catalysis*, 2002, **21**, 79
- 6) Krebs, B., Paulat Bösch, I., *Acta Crystallographica* 1982, **B38**, 1710
- 7) Garin, J.L. Blanc, J.M., *Journal of Solid State Chemistry*, 1985, **1**, 98

Copper in C1 Chemistry

Copper based catalysts are extensively used for methanol synthesis and the conversion of methanol to hydrogen and carbon dioxide (reforming) or formaldehyde (selective oxidation). The work performed in this research area focuses on revealing structure-reactivity relationships of various copper systems and rationalizing copper catalyst synthesis in terms of tailoring particular bulk and surface properties to accomplish an improved catalytic performance. The results shown demonstrate that elucidating structure-activity relationships is a necessary prerequisite for a rational catalyst design, together with a detailed knowledge about appropriate preparation and treatment conditions resulting in the right target structure of the heterogeneous catalyst.

Recently, we were able to show that the catalytic activity of binary Cu/ZnO catalysts correlates with the microstrain in the copper particles. In order to tailor microstructural characteristics such as structural disorder, impurities, microstrain, and particle size and, thus, open up pathways to a rational catalyst design, we investigated the effect of precipitate ageing on structure-activity relationships. Microstructural properties of the freshly reduced and activated catalyst were elucidated by using in-situ XRD, XAS, NMR, TEM. (*Poster 5.1*)

The structural and catalytic properties of novel CuO/ZrO₂ catalysts in the methanol steam reforming process were investigated by various characterization methods. The CuO/ZrO₂ catalysts can be activated by an oxidation procedure resulting in partially oxidized copper clusters supported on ZrO₂ which exhibit improved catalytic properties (e.g. stability, selectivity, etc.) compared to a commercial Cu/ZnO/Al₂O₃ catalyst. (50 ml/min) for a short time (5 min) into the feed at reaction condition. (*Poster 5.2*)

Furthermore, the oxidation of methanol on elemental unsupported copper is investigated as a model reaction. There are two main reaction paths: partial oxidation to formaldehyde, and total oxidation. We have simultaneously investigated the surface and near-surface region of a polycrystalline Cu foil and the adjacent gas-phase reactants under reaction conditions using *in situ* X-ray photoelectron spectroscopy (XPS). (*Poster 5.3*)

The research project “*Nano chemistry for the automobiles of the future*” is a joint collaboration of four Max-Planck instituts (MPI) and of the Technischen Universität Berlin, and is funded by the ZEIT-Stiftung (Hamburg). During the first three years of the project we succeeded in preparing and characterizing novel copper catalyst supported on nano-structured zirconium dioxide Cu/ZrO₂. The catalysts exhibit an improved catalytic activity in the steam reforming of methanol compared to Cu/ZnO, a considerable thermal and long-term stability during time on stream and produce significantly less carbon monoxide. (additional poster)

*Poster 5.1***Effect of precipitate ageing of Cu/ZnO catalysts for methanol steam reforming activity***Introduction*

Cu/ZnO based catalysts are frequently employed for methanol synthesis, steam reforming, and water gas shift reaction. Recently, we were able to show that the catalytic activity of binary Cu/ZnO catalysts correlates with the microstrain in the copper particles ^[1]. In order to tailor microstructural characteristics such as structural disorder, impurities, microstrain, and particle size and, thus, open up pathways to a rational catalyst design, we investigated the effect of precipitate ageing on structure-activity relationships. Therefore, Cu-Zn hydroxycarbonate precursors (ratio Cu/Zn = 70/30 mol%) were co-precipitated at constant pH (pH=7). The precipitates were aged for 0, 15, 30 and 120 min in the mother liquid, followed by drying, washing, and calcination for 3 h in air. Microstructural properties of the freshly reduced and activated catalyst were elucidated by using in-situ X-ray-diffraction (XRD) and in-situ X-ray absorption-spectroscopy (XAS) at the Cu K-edge combined with mass spectrometry, ⁶³Cu Nuclear magnetic resonance (NMR) and Electron microscopy (TEM).

Results

The Cu/ZnO catalysts obtained from the precursors aged for longer times (30 and 120 min) exhibited a much-increased H₂ production rate. The decreasing Cu particle size (130 Å = 0 min ageing to 100 Å = 120 min ageing) obtained from a detailed XRD line profile analysis and the resulting higher surface area are not sufficient explain the increase in activity. In addition to the decreasing particle size, the H₂ production rate in methanol steam reforming correlates well with the microstrain in the catalytically active copper phase. The ex-situ NMR investigations of freshly reduced catalysts are in good agreement with the in-situ XRD results. Similar to the X-ray diffraction, the line profile and line breadth of the ⁶³Cu NMR signal is determined by the particle size and microstrain of the copper particles. The short aged precursors (0 and 15 min) revealed a symmetric line broadening due to less strained and bigger Cu particles and the longer aged precursors (30 and 120 min) exhibited a asymmetric line broadening due to strained and smaller Cu nano particles. Analysis of the in-situ EXAFS spectra shows a decrease in the amplitude of the first Cu-Cu shell as function of ageing. It was found by simulating the EXFAS spectra assuming a solid solution of Cu and Zn, that the Zn content in Cu clusters decreases with longer ageing times. This indicates, that the occupancy of Zn atoms on Cu lattice sites diminishes the transmission of strain, induced by epitactical orientation of the Cu/ZnO interface, to the surface. Furthermore, the EXAFS analysis suggests an increasing structural disorder in the medium range order with increasing ageing time (e.g., microstrain).

[1] M.M. Günter, T.Ressler, R.E Jentoft, B.Bems, J. Catal. 2001, 203, 133-149

*Poster5.2***Cu/ZrO₂ catalysts for methanol steam reforming***Introduction*

Conventional Cu/ZnO^{1,2} catalysts that can be used to produce hydrogen for fuel cell applications exhibit an unsatisfactory long-term stability and CO selectivity. Therefore, various starting materials and templates have been used to prepare nanostructured, mesoporous and macroporous Cu/ZrO₂ catalysts. These catalysts have been investigated under methanol steam reforming conditions by XRD (X-ray diffraction) and XAS (X-ray absorption spectroscopy), TG, combined with mass spectrometry, and by and electron microscopy to monitor structural changes, stability and catalytic activity under reaction conditions. Furthermore, a three channel plug flow reactor was used to perform detailed catalytic characterizations of the various Cu/ZrO₂ materials.

Structural Characterization

XRD measurements showed that tetragonal zirconium dioxide (normally metastable at room temperature) is the main zirconia phase and that only some of the catalysts show a minor monoclinic contribution. For most of the catalysts the reduction in 2 vol-% H₂/He or the direct activation in the feed at 523 K resulted in copper metal on ZrO₂ that does not fully correspond to pure copper metal. The deviations from the ideal structure were observed by XAS, and were stronger for the samples after activation in the feed. The initial low activity for MSR (MeOH:H₂O = 2:1) could be significantly improved by a short addition of oxygen to the feed. In most cases this procedure also resulted in an increase of the deviation from ideal copper metal. In addition, after extended times in the MSR feed and elevated temperatures (673 K, 2 vol-% H₂/He), the catalysts were still active or could be reactivated (via this oxygen addition procedure), indicating a superior stability of the material.

Catalytic study

The detailed study of the catalytic properties of the novel CuO/ZrO₂ catalysts confirmed that the activity of the CuO/ZrO₂ catalysts can be improved by introducing oxygen (50 ml/min) for a short time (5 min) into the feed at reaction condition. As to changes of the specific copper surface area of a commercial CuO/ZnO/Al₂O₃ the opposite result was observed. This indicates that the CuO/ZrO₂ catalysts are less susceptible to sintering of the metal particles than the CuO/ZnO/Al₂O₃ catalyst. The measurement of methanol conversion as a function of contact time shows clearly that the macroporous CuO/ZrO₂ catalyst is more active than the commercial CuO/ZnO/Al₂O₃ catalyst. Moreover, the CO concentration plotted as a function of methanol conversion measured over CuO/ZrO₂ catalysts and CuO/ZnO/Al₂O₃ catalyst show that less CO was formed over the CuO/ZrO₂ catalysts, especially significant at higher methanol conversion.

*Poster5.3***In situ X-ray photoelectron spectroscopy of the methanol oxidation on copper***Introduction*

Elemental copper can be used as an unsupported catalyst for the oxidative dehydrogenation of alcohols to aldehydes. In this work the oxidation of methanol is investigated as a model reaction. There are two main reaction paths: partial oxidation to formaldehyde, and total oxidation, which would be thermodynamically favored under equilibrium conditions. We have simultaneously investigated the surface and near-surface region of a polycrystalline Cu foil and the adjacent gas-phase reactants under reaction conditions using in situ X-ray photoelectron spectroscopy (XPS).

Results

In situ XPS spectra were taken at a total methanol and oxygen pressure of 0.6 mbar in the temperature range from 25 to 450 °C. The in situ XPS spectra showed that the chemical composition of the Cu surface depends both on the temperature and on the ratio of methanol to oxygen in the reactant stream. The catalytic reaction started at temperatures above 250 °C. Under oxygen-rich conditions ($O_2:CH_3OH=2:1$), when the catalyst was most selective for the total oxidation reaction, the surface consisted mainly of Cu_2O , as could be determined from valence band and O1s spectra. Under methanol-rich conditions ($O_2:CH_3OH=1:3, 1:6$) the valence band spectra indicated that the surface was metallic. The O1s spectra under these conditions showed a peak at 529.9 eV. Photon energy-dependent depth-profiling investigations revealed that the peak at 529.9 eV is due to sub-surface oxygen. The comparison of the depth-dependent O1s sub-surface peak area with depth-dependent Cu3p peak areas showed that the highest concentration of sub-surface oxygen is found on average about 3 Å below the surface, with O:Cu stoichiometries of up to 1:2. Since in situ XPS probes not only the sample surface but also the gas phase in front of the sample, the chemical composition of the gas phase could be determined from the in situ XPS spectra (in addition to mass spectrometry). Our investigation showed that there was a linear correlation between the formaldehyde yield, and the presence of the sub-surface oxygen species. We have also found that this sub-surface oxygen species can only be investigated in situ. It was not possible to observe this species under vacuum conditions.

In summary, our experiments demonstrate that the pure Cu metal is not an active catalyst for the methanol oxidation reaction, but that a certain amount of oxygen has to be present in the sub-surface region to activate the catalytic reaction. This result demonstrates that for an understanding of heterogeneous catalysts a characterization of the surface alone may not be sufficient, and that sub-surface characterization may also be necessary. In addition, our results stress the necessity to perform experiments under reaction conditions.

Research Area 6: Palladium based catalysts

This research area deals with the hydrogenation reaction on palladium based catalysts. The hydrogenation of propene, ethylene, acetylene and trans-2-pentene have been investigated. The formation of carbon species is observed under hydrogenation conditions of C5 compounds. The dynamic behaviour of the carbon deposited was shown by means of in situ photoelectron spectroscopy.

Poster (6.1): Pd(111) and Pd foil was investigated in hydrogenation of trans-2-pentene. UPS measurements show a change in chemisorption at 220 K in agreement with TDS measurement performed in the CP department. This change is due to the loss of hydrogen. XPS measurements show the formation of carbon on the catalysts surface. In situ XPS measurements demonstrate the dynamic behaviour of the carbon deposit by changing the catalytic conditions.

Poster (6.2): The structure of binary alloys like PdGa and Pd₃Ga₇ offers the possibility to isolate Pd sites. The geometric and electronic structure of Pd on site isolation will be changed by modifying the coordination of the surrounding Ga sphere. The catalytic selectivity might be tailored by changing the coordination. The thermal stability of PdGa and Pd₃Ga₇ in the presence of various atmospheres was investigated by in situ XAS at the Pd and the Ga K-edge and by in situ XRD and by thermal analysis.

*Poster 6.1***Palladium in Selective Hydrogenation (Athena Project)**

In this joint multi-centre project Pd based catalysts are investigated in the hydrogenation of C5 multifunctional molecules, in which special attention is taken by our side on the electronic structure of the working catalyst. The starting molecule to investigate was trans-2-pentene (t-2-P).

UPS of t-2-P on Pd(111) indicates changes in the chemisorption modus at ~ 210-220 K. As the π -bonded molecules desorb (~170 K) the coordination is σ -bonded to the surface. However, the π bond is intact; therefore the chemisorption occurs via loosing hydrogen. At ~220 K the molecule loses the double bond and consequently the bonding to the surface changes, as well. TDS studies (*Department Chemical Physics*) reveals similar adsorption behavior of Pd(111) and supported Pd clusters¹. The latter were active in the hydrogenation of t-2-P.

Ex-situ XPS measurements on t-2-P treated Pd foil demonstrate that the residual carbon species depend on the amount of hydrocarbon introduced. Palladium foil was measured also in our in-situ XPS set-up at UHV conditions, in hydrogen and in mixtures of hydrogen and t-2-P at different temperatures. In the C1s region three main surface components (~284.0, ~284.6 and ~285.2 eV) could be identified by least square fits corresponding to carbon connected to Pd, C to C and C to H, respectively². The surface behaves dynamic³: the type of carbon depends on the experimental conditions (gas phase composition, pressure, temperature). Carbon accumulation from the base pressure shifted the C1s maximum by +0.5 eV (to 284.5 eV) thus increasing the graphitic phase. Hydrogen restructured the C layer as the peak at 284 eV strongly decreased and that at 285.2 increased. Increasing temperature favors C-Pd and removed the C-H component. Introduction of a 2-pentene/hydrogen mixture increased the C1s component at 285.2 eV (also chemisorbed species). MS data recorded during the XP scans show the highest activity at 100°C while the catalytic activity was completely lost at 250°C. Depth profiling on the active state of the catalyst revealed that the carbon component corresponding to the peak at 285.2 eV is at the topmost surface position and that at 284.0 eV is located at the deepest position. The activity lost was accompanied by a stronger interaction of carbonaceous species with the palladium at the inactive state of the sample.

Preliminary in-situ XPS data on the inactive Pd(111) single crystal reveals mainly graphitic carbon to be present at reaction conditions and the proportion of the C-H component is much smaller. The d-band in the valence region of the active Pd foil indicates a likely interaction of palladium with carbon, which was absent for the single crystal, and this might correlate with the activity in hydrogenation.

Poster 6.2

Structural and Catalytic Investigation of Binary Palladium-Gallium Alloys*Introduction*

Palladium constitutes an important catalyst for hydrogenation (e.g. the hydrogenation of acetylene to ethylene or 1,2-butadiene to 1-butene) and for combustion reactions. Typical Pd-catalysts are supported on metal oxides and show high activity but only limited selectivity⁴. The limited selectivity of Pd catalysts may be caused by too neighbouring active sites on the catalyst metal surface⁵. Binary alloys PdGa and Pd₃Ga₇ prepared by the group of Prof. Y. Grin (MPI for Chemical Physics of Solids, Dresden) are stoichiometric compounds with ordered crystallographic structures. These materials are particularly interesting as potential catalysts because of the isolation of the Pd atoms in the structure. In both structures the Pd atoms are surrounded by a coordination sphere of Ga atoms (i.e. coordination number of 7 in PdGa and 8 in Pd₃Ga₇). This site isolation changes the geometry and the electronic structure of the active Pd atoms and may modify adsorption and desorption properties⁶. Therefore, this significant difference in the local structures of Pd metal clusters and the Pd-Ga alloys offers a promising way to tailor the selectivity of palladium catalysts in hydrogenation reactions.

Results

The thermal stability of PdGa and Pd₃Ga₇ in the presence of various atmospheres was investigated by in situ XAS at both the Pd and the Ga K-edge, in situ XRD and by thermal analysis. First catalytic studies were carried out for oxidation and hydrogenation reactions and the surface area was determined by BET measurements and CO adsorption. BET measurements of the ground samples resulted in a surface area of 1-2 m²/g for both alloys. The structural evolution of the alloys in helium, hydrogen, and oxygen in the temperature range from 293 to 593 K shows that the palladium-gallium alloys are stable under these conditions. In contrast to Pd metal no hydrogen and oxygen inclusion is detectable. Also no phase transition in this temperature range and no oxidation within the detection limit of XAS and XRD were observed. Catalytic studies show catalytic activity for propene and ethylene hydrogenation, for CO oxidation as well as high selectivity for acetylene hydrogenation to ethylene. For acetylene hydrogenation, PdGa and Pd₃Ga₇ possess the maximum in activity and selectivity in the temperature range from 275 to 325 °C. In contrast, commercial Pd/Al₂O₃ catalysts exhibit a high activity in the temperature range from 125 to 325 °C, whereas the maximum in selectivity to ethylene hydrogenation is at temperatures of 325 to 425 °C.

References

-
- ¹A. Doyle, Sh. Shaikhutdinov, D. Jackson, H-J Freund, Hydrogenation on metal surfaces: why are nanoparticles more active than single crystals? submitted to Angew. Chem.
²N. M. Rodriguez, P. Anderson, Z. Paál, U. Wild, A. Wootsch, R. Schlögl, J. Catal. 197 (2001) 365.
³G. A. Somorjai, Introduction to surface chemistry and catalysis, John Wiley & Sons, 1994.
⁴D. Duca, F. Frusteri, A. Parmaliana, G. Deganello, Applied Catalysis A-General 1996, 146 269-284.
⁵J. Houzviccka, R. Pestman, V. Ponec, Catalysis Letters 1995, 30 289-296.
⁶D. H. Mei, E. W. Hansen, M. Neurock, Journal of Physical Chemistry B 2003, 107 798-810.

Carbon in Catalysis

Carbon materials are old objects in catalysis research. They are mostly used as catalyst supports (active and activated carbon, carbon black). Since the discovery of nanocarbon (fullerene, nanotube, nanofilament...), carbon draws more interesting in heterogeneous catalysts. Nanocarbon is ideal as catalyst supports due to its high surface area, and is used as a template to prepare nanostructured catalysts like nanotubes of transition metal oxides. The unique geometric and electronic structure of nanocarbon induces the research activity in the department to test the catalytic performance of various as-synthesised nanocarbons without any structural modification.

Oxidative dehydrogenation of ethylbenzen to styrene is chosen as test reaction. The reaction, the styrene process, is thus exothermic so that the working temperature is reduced by at least 150°C and the addition of steam needed in direct dehydrogenation is no longer necessary. This opens up a new horizon in styrene production that is one of the 10 largest industrial processes. Carbon black, graphite, nanofilaments, nanotubes, onions, and ultra-dispersed diamonds, were tested as catalysts for this reaction. All tested nanocarbon are active for the reaction, while onion-like carbon is found to be the most efficient catalyst for the oxidative dehydrogenation reaction on the mass-reference basis.

Nanocarbons are usually prepared by arc-discharge of graphite, metal-catalysed decomposition of hydrocarbon, but there are other preparation routs. As one of alternative methods, carbon nanotubes and nanobulbs can be obtained from explosive decomposition of picric acid. This method can be used to efficiently produce multi-walled carbon nanotubes when cobalt or nickel-containing catalyst precursor is introduced into the reaction system. Under special explosive decomposition-resulted environments, the initially formed carbon nanotubes exhibit a blowing behavior similar to glass blowing and produce hollow spherical graphite nanobulbs, characterized by large dimensions, thin walls, and fully hollow cores. The carbon nanobulbs are expected to exhibit novel properties and application potential in micro- containers, reactors, and other devices (*Poster 7.1*).

Carbon in some forms can also become to risk for the environment and may be harmful to human health. For instance, soot emitted from energy plants or automobiles contributes to air pollution and is a potential risk for human health. We have investigated the microstructure and oxidative behaviour of soot emitted from Euro IV diesel engines. Such engines will be put into service in 2005. We find a microstructure-controlled reactivity toward oxidation of Euro IV soot that can be explained by the typically fullerene-like microstrucure of the primary soot particles. Comparative investigations on different model or reference soot confirm the findings (*Poster 7.2*).

*Poster 7.1***Carbon nanotubes and nanobulbs obtained from explosive decomposition of picric acid**

This work was performed by a co-operation with the Institute of Coal Chemistry, Chinese Academy of Sciences and focused on the structures of the solid products produced from the explosive decomposition of common carbon-containing explosives in the presence of catalysts. The aim is looking for an alternative way for the synthesis of nanostructured carbon materials at large scale.

It was found that the explosive decomposition of picric acid can be used to efficiently produce multi-walled carbon nanotubes when cobalt or nickel-containing catalyst precursor is introduced into the reaction system. Under the explosive environment, the catalyst precursor decomposes and is reduced to in-situ form nanoparticles of parent metal, on which carbon species deposit, nucleate, and grow into tubular structures. By this way tube content as high as 90% can be obtained by adjusting experimental parameters. The resulted tubes are 10-50 nm in diameter and up to several tens micrometers in length and are well structured with concentric graphite layers. This heat-self-served, high-pressure, and simple approach represents a novel and alternative way to carbon nanotubes.

We also found that under the special explosive decomposition-resulted environments, the initially formed carbon nanotubes exhibit a blowing behavior similar to glass blowing and produce hollow spherical graphite nanobulbs. These bulbs have large diameters (150-920) but exhibit relatively thin wall thickness (6-25 nm). The blowing behavior of the tubes is confirmed by careful SEM and TEM observations of related intermediate derivatives. The tube blowing is associated with the high-pressure gases (produced from the explosive decomposition and filled inside the closed tubes), a continuously decreasing system temperature, and the intrinsically low c-axis thermal conductivity of the layered graphitic sheets, which result in temperature and pressure differences between the inside and the outside of tubes and then induce an expansion of tube volume through structural deformations. The blowing is also connected with the structural defects in the layered graphite sheets of the tubes. This finding indicates that CNTs exhibit, at least during their generation, excellent thermoplasticity and expansibility and suggests that it is possible to engineer tubular structures on nano-scale into various shaped devices. The blown spherical bulbs, characterized by large dimensions, thin walls, and fully hollow cores, are expected to exhibit novel properties and application potential in micro- containers, reactors, and other devices.

*Poster 7.2***Microstructure and morphology controlled reactivity of environmental carbon**

Despite significant reduction in the emission rate of soot from diesel engines, the increasing number of diesel engine passenger cars has kept soot emission a major source of air pollution and a potential risk for human health. The microstructure and oxidation behaviour of EuroIV diesel engine soot is investigated and compared with soot produced by arc-discharge of graphite, soot from a black smoke adjusted engine, and microcrystallites of Hexabenzocorone (HBC). We find a microstructure-controlled reactivity toward oxidation of all four samples when heated in 5% O₂ in N₂.

The characteristic of the soot emitted by the EuroIV engine is its fullerenoid-like structure of the fine primary particles, agglomerated in a secondary chain-like structure with final dimensions of up to 500 nanometers. The agglomerates of EuroIV soot do not exhibit a defined profile or regular shape. The primary particles then agglomerate to gain stability by a graphene-type dispersive interaction between bent strands of ribbons. A similar morphology is observed in the fullerenic carbon in soot produced by arc-discharge of graphite. The primary particles show multiple shell structures. The black smoke contains large spherical particles agglomerated to a chain-like secondary structure. The evaluated size-distribution of primary particles gives a median size of 35 nm. HBC-microcrystallites consist of platelets of an extended carbon lamella structure with large strands of well-ordered (parallel to each other) basic structural units, and thus it serves as a well-defined model for the BSU of diesel engine soot.

TG measurements in 5% O₂ to 1073 K show a distinct reactivity for each of the samples. The only gas phase products measured by MS are CO₂ with lesser amounts of H₂O. The TG measurements for the diesel engine soot samples reveal that the EuroIV soot is more easily oxidized than the black smoke soot. This higher reactivity is indicative of the fullerenoid character of the EuroIV soot and its smaller particle sizes. The defective non six-membered rings may produce highly localized olefinic structures prone to the addition of molecular oxidants. The arc discharge soot burns at lower temperatures indicating the reactivity of the fullerenic carbon. The HBC-crystallites with the highest combustion temperature are less reactive towards O₂ due to its well-developed graphitic properties.

Poster list:

- CP 1 Termination of V₂O₃(0001) Thin Films**
M. Abu Al-Haija, A.-C. Dupuis, B. Richter, H. Kuhlenbeck, H.-J. Freund
- CP 2 Adsorption on V₂O₃(0001) Thin Films**
M. Abu Al-Haija, A.-C. Dupuis, B. Richter, H. Kuhlenbeck, H.-J. Freund
- CP 3 Spectro-Microscopic Investigation of Ultra-Thin Organic Film Growth on Ag(111)**
H. Marchetto, Th. Schmidt, U. Groh, H.-J. Freund, E. Umbach
- CP 4 Towards an Understanding Catalysis by Gold**
R. Meyer, C. Lemire, Sh. K. Shaikhutdinov, H.-J. Freund
- CP 5 Metal Model Catalysts Supported on Iron Oxide Films: Structure and Reactivity**
Sh. K. Shaikhutdinov, R. Meyer, D. Lahav, T. Klüner, H.-J. Freund
- CP 6 Hydrogenation on Palladium Surfaces: Nanoparticles vs Single Crystal**
A. M. Doyle, Sh. K. Shaikhutdinov, H.-J. Freund
- CP 7 Atomic Force and Scanning Tunnelling Microscopy Measurements at Low Temperatures**
M. Kulawik, M. Heyde, G. Thielsch, H.-P. Rust, H.-J. Freund
- CP 8 Geometric and Electronic Structure of Line Defects in Al₂O₃ Thin Films on NiAl(110)**
M. Kulawik, N. Nilius, H.-P. Rust, H.-J. Freund
- CP 9 Photon Emission Spectroscopy on Individual Oxide-supported Ag-Au Alloy Particles**
W. Benten, N. Nilius, N. Ernst, H.-J. Freund
- CP 10 The Surface Structure of Co-Pd Bimetallic Particles Supported on Al₂O₃ Thin Films Studied Using IRAS of CO**
A. F. Carlsson, T. Risse, M. Bäumer, H.-J. Freund
- CP 11 Magnetic Properties as a Probe for Structural Changes in Nanoparticle Catalysts**
T. Risse, M. Mozaffari-Afshar, H. Hamann, H.-J. Freund
- CP 12 Structure and Dynamics of Proteins on Planar Surfaces**
K. Jacobsen, T. Risse, W. L. Hubell

- CP 13** **Sum Frequency Generation Spectroscopy of CO-H₂ Interaction and CH₃OH Decomposition on Pd Model Catalysts**
M. Morkel, G. Rupprechter, H.-J. Freund
- CP 14** **PM-IRAS and XPS Spectroscopy on Model Catalysts: Methanol Decomposition on Pd Surfaces**
O. Rodriguez de la Fuente, M. Borasio, P. Galletto, G. Rupprechter, H.-J. Freund
- CP 15** **Reaction Kinetics on Supported Nanoparticles: Local Reaction Rates, Surface Diffusion and Kinetic Bistabilities**
M. Laurin, V. Johánek, S. Schauer mann, J. Hoffmann, A. Grant, B. Kasemo, J. Libuda, H.-J. Freund
- CP 16** **Activity and Selectivity of Specific Sites on Supported Nanoparticles: Molecular Beam Experiments–Time Resolved IRAS–Microcalorimetry**
M. Laurin, V. Johánek, S. Schauer mann, J. Hoffmann, A. Grant, B. Kasemo, J. Libuda, H.-J. Freund
- CP 17** **Two Photon Photoemission Microscopy Using Femtosecond Laser Radiation**
W. Bente n, H. Petek, W. Drachsel, H.-J. Freund
- CP 18** **Photoinduced Desorption of NO from Supported Silver Nanoparticles**
C. Rakete, F. Evers, W. Drachsel, H.-J. Freund
- CP 19** **Prediction of Electronic Excited States of Adsorbates on Metal Surfaces from First Principles**
D. Lahav, T. Klüner, S. Borowski, N. Govind, Y.A. Wang, E.A. Carter
- CP 20** **A Surrogate Hamiltonian Treatment of Laser Induced Desorption of NO/NiO(100)**
S. Dittrich, C. P. Koch, D. Kröner, S. Borowski, T. Klüner, H.-J. Freund, R. Kosloff
- CP 21** **Rotational and Lateral Dynamic of the Photodesorption of CO from Cr₂O₃(0001) – A First-Principles Quantum Dynamical Study**
S. Borowski, T. Klüner, S. Thiel, M. Pykavy, V. Staemmler, H.-J. Freund

Termination of $V_2O_3(0001)$ Thin Films

M. Abu Al-Haija, A.-C. Dupuis, B. Richter, H. Kuhlenbeck, H.-J. Freund

Introduction

Vanadium oxides exhibit a number of interesting physical and chemical properties. This includes a very complicated phase diagram and several phase transitions. Vanadium oxides also exhibit catalytic activity for different reactions, most of them involving transfer of oxygen atoms. The catalysts are usually based on VO_2 or V_2O_5 material. In the framework of the Sonderforschungsbereich 546 which deals with the catalytic activity of vanadium oxides, the preparation, the surface properties and the chemical activity of well ordered $V_2O_3(0001)$ films on Au(111) and W(110) have been studied. The studies reported here aimed at learning about the termination of the $V_2O_3(0001)$ surface.

Results

$V_2O_3(0001)$ films with a typical thickness between 60 and 120 Å were grown by evaporation of vanadium onto Au(111) and W(110) surfaces in an oxygen atmosphere. They exhibit LEED patterns with low background intensity and sharp spots. The occurrence of the characteristic insulator-metal phase transition at low temperature may be viewed as an indication that the properties of the thin films are not too different from those of bulk V_2O_3 . The surface termination has been studied with photoelectron spectroscopy with light from the BESSY II storage ring and with vibrational spectroscopy. If oxygen is available the surface immediately forms vanadyl groups which are stable on the surface even above 1000 K. The vanadyl groups may easily be detected by vibrational spectroscopy. In photoelectron spectra they lead to specific states in the valence band and the $V2p$ region. States corresponding to the latter could also be observed in NEXAFS spectra. The vanadyl terminated surface is rather inert with respect to most adsorbates which is not the case any more if the vanadyl groups are removed by electron irradiation. The so-obtained surface exhibits photoelectron spectra which differ characteristically from those of the vanadyl-terminated surface. Interaction with oxygen transforms the reduced surface back into the vanadyl-terminated one.

Adsorption on $V_2O_3(0001)$ Thin Films

M. Abu Al-Haija, A.-C. Dupuis, B. Richter, H. Kuhlenbeck, H.-J. Freund

Introduction

Vanadium oxides exhibit catalytic activity for a number of chemical reactions usually involving the transfer of oxygen atoms. As part of the activities of the Sonderforschungsbereich 546 in Berlin we have studied the chemical activity of different ordered vanadium oxide surfaces, i.e. $V_2O_5(001)$, $VO_2(110)$, and $V_2O_3(0001)$. They exhibit significantly different chemical activities which may be attributed to the different occupancies of the V3d levels. Here we report on our results on $V_2O_3(0001)$.

Results

$V_2O_3(0001)$ thin films on Au(111) and W(110) were prepared by evaporation of vanadium in an oxygen atmosphere. Their typical thickness was between 60 and 120 Å and they are well ordered as judged from their LEED patterns. Oxygen leads to the formation of vanadyl groups on the surface which may be removed by electron irradiation. Dosage of oxygen re-establishes the vanadyl-termination. The vanadyl-terminated surface appears to be inert with respect to the studied adsorbates (carbon monoxide, oxygen, water, carbon dioxide, propane and propylene). This is at least true for small doses. As shown by Henrich et al, high doses of CO may remove the vanadyl groups. We removed the vanadyl groups by electron irradiation which led to a chemically reactive surface. For CO a molecular adsorbate state as found for $Cr_2O_3(0001)$ could be detected. The molecular axis of these molecules is strongly tilted and the valence band binding energies are unusually high. However, possibly dependent on the degree of surface reduction also formation of CO_2 or carbonated was observed. CO_2 partly transforms into CO, possibly via a bent $CO_2^{\delta-}$ precursor state and H_2O forms OH layers already at low temperature. Currently ongoing experiment deals with the interaction with propane and propane+oxygen co-adsorption. Propane may be catalytically transformed into propylene via an oxy-dehydrogenation reaction on vanadium oxide catalysts. Results of these experiments will be reported.

Spectro-Microscopic Investigation of Ultra-Thin Organic Film Growth on Ag(111)

H. Marchetto, Th. Schmidt*, U. Groh*, H.-J. Freund, E. Umbach*

*Exp. Physik II, Am Hubland, Universität Würzburg

Introduction

The current version of the SMART¹ spectro-microscope is a photo-emission electron microscope (PEEM) equipped with an imaging energy analyzer (OMEGA filter). For the final version a corrector, consisting of an electrostatic tetrode mirror together with a highly symmetric magnetic beam-splitter, will be implemented in autumn 2003. This corrector compensates simultaneously for both, the spherical and chromatic aberrations of the lens system, and will improve the lateral resolution by one order of magnitude and the transmission by two orders. Aiming at a lateral resolution of < 2 nm with an energy resolution of ~ 100 meV² this is worldwide the most ambitious project in the field of spectroscopic x-ray induced PEEM (XPEEM) and low energy electron microscopy (LEEM). Besides electron microscopy as a surface sensitive imaging method, the OMEGA energy filter enables photoelectron spectroscopy and electron diffraction³ as well as combinations thereof (e.g. spectroscopy at individual, nanometer sized surface objects).

Results

The current version of the microscope, installed at the high-brilliance undulator-beamline UE52 at BESSY II, has been used to study ultra-thin organic films on metallic substrates. The temperature-dependent *in-situ* observations of the PTCDA growth on a Ag(111) surface shows a transition of the growth mode from a layer-by-layer (Franck-van der Merwe) to a growth of two or three layers followed by three-dimensional (3D) island growth (Stranski-Krastanov) at about 300 K. The UV-photoemission intensity decreases during the growth of the first layer for both, the growing PTCDA layer and the substrate area in between. This can be explained by the formation of a PTCDA precursor state with relaxed structure⁴. Furthermore, with laterally resolved NEXAFS spectroscopy and by switching the linear polarization of the light one can clearly derive the molecular orientation as flat-lying in both, the 3D islands and the bilayer. Additionally, the circular polarization reveals a natural circular dichroism for the PTCDA crystallites, which is unique and unexpectedly large for these planar and non-chiral molecules.

1. R. Fink et al., J. Electr. Spectrosc. Rel. Phen. **84** (1997) 231.
2. D. Preikszas, H. Rose, J. Electr. Micr. **1** (1997) 1.
3. Th. Schmidt et al., Surf. Rev. Lett. **9** (2002) 223.
4. B. Krause et al., Phys. Rev. B **66** (2002) 235404.

Towards an Understanding Catalysis by Gold

R. Meyer, C. Lemire, M. Naschitzki, Sh. Shaikhutdinov, H.-J. Freund

Introduction

In the last decade, gold nanoparticles have begun to attract attention owing to unique catalytic properties such as low temperature CO oxidation¹. In order to elucidate the reaction mechanism and determine structure-activity relationships we developed well-defined model systems involving gold particles vapor deposited on thin oxide films. Of particular interest are the role of the support and the origin of any differences in catalytic activity and in deactivation behavior between gold catalysts on varying supports. Here we report on the preparation, thermal stability and CO adsorption on gold deposited on Al₂O₃, FeO, Fe₃O₄ and Fe₂O₃ films.

Results

The morphology of the Au deposits was studied by scanning tunneling microscopy (STM), and CO adsorption was examined by temperature programmed desorption (TPD) and infrared reflection absorption spectroscopy (IRAS).

Gold deposition on oxide films leads to formation of three-dimensional particles for all the substrates studied except FeO on which small monolayer islands can be formed at low Au coverage^{2,3}. For Au deposited at low temperatures (< 100 K) TPD experiments show that CO desorption temperature is sensitive to Au coverage. It gradually shifts from ~ 250 to 170 K as gold coverage and hence a mean cluster size increases. Therefore, the results point to a particle size effect with respect to CO adsorption: small particles adsorb CO more strongly. The desorption temperature for the smallest particles may extend to 300 K which has never been observed on gold single crystals.

The effect vanishes for the particles annealed to 400 - 500 K due to gold sintering and particle restructuring, thus resulting in a loss of the low coordinated Au atoms, on which CO may adsorb. On average, the thermal stability depends on the defect structure of support. The TPD results show that the size effect disappears as the particle size exceeds ~ 3 nm as measured by STM².

The nature of the CO adsorption sites has been studied with IRAS³. The IRAS spectra obtained for the annealed samples only reveal a single adsorption state at ca. 2108 cm⁻¹ independent of support and gold coverage. Therefore, the TPD and IRAS data clearly indicate that interaction of CO with gold surfaces is essentially identical and independent on the particle size and dimensions. It seems likely, that the CO adsorption only includes highly uncoordinated surface atoms in accordance with theoretical predictions.

In order to examine the stability of the gold particles in a reactive atmosphere, we have performed *in situ* STM experiments in CO + O₂ environment. The results show that supported gold particles are remarkably stable, at least at room temperature.

1. M. Haruta, *CATTECH*, **6** (2002) 102.
2. Sh. Shaikhutdinov, R. Meyer, M. Naschitzki, M. Bäumer, H.-J. Freund, *Catal. Lett.* **86** (2003) 211.
3. C. Lemire, R. Meyer, Sh. Shaikhutdinov, H.-J. Freund, submitted.

Metal Model Catalysts Supported on Iron Oxide Films: Structure and Reactivity

Sh. K. Shaikhutdinov, R. Meyer, D. Lahav, T. Klüner, H.-J. Freund

Introduction

Metal particles deposited on well-ordered oxide films represent suitable model systems for highly dispersed metal catalysts. It has been previously shown that FeO(111), Fe₃O₄(111) and α -Fe₂O₃(0001) films can be prepared on a Pt(111) substrate in a controllable way by iron deposition/oxidation procedures¹. Here we report on the structure and CO adsorption properties of metals vapor-deposited on the different iron oxide films as studied by scanning tunneling microscopy (STM) and temperature programmed desorption (TPD).

Results

Several interesting phenomena have been observed which may have important implications:

a) On a FeO thin film, Pd forms two-dimensional, monolayer islands while Pd grows three-dimensionally on other oxide films. This wetting phenomenon seems to be a new example of the strong metal-support interaction for metals on reducible oxides. In addition, we have found that CO desorbs from the monolayer Pd(111) islands at much lower temperatures than from a thick Pd overlayer or oxide supported three-dimensional particles. In order to explain these effects, theoretical calculations combined with the high-resolution STM measurements have been performed for determining the atomic structure of the metal/oxide interface².

Interestingly that gold also forms monolayer islands at low coverage, but the growth becomes three-dimensional at increasing coverage³. Therefore, the FeO(111) film can be used as a suitable oxide support for studying the chemical properties of the metal deposits with reduced dimensions.

b) TPD results show that CO reacts with lattice oxygen of Fe₃O₄, presumably at the Pd/oxide periphery. The reactivity is enhanced on the samples pre-treated with oxygen. STM images revealed structural changes of the reducible oxide support induced by Pd dissociating oxygen. This effect may be important in (selective) oxidation reactions.

c) Comparison of the results obtained for the systems involving reducible and non-reducible oxide supports may shed light on the support effects on the catalytic properties of the metal nanoparticles³.

1. W. Weiss, W. Ranke, *Progr. Surf. Sci.* **70** (2002) 1.
2. Sh. Shaikhutdinov, D. Lahav, R. Meyer, et al., *Rhys. Rev. Lett.* **91** (2003) 076102.
3. Sh. Shaikhutdinov, R. Meyer, M. Naschitzki, M. Bäumer, H.-J. Freund, *Catal. Lett.* **86** (2003) 211.

Hydrogenation on Palladium Surfaces: Nanoparticles vs Single Crystal

A.M. Doyle, Sh.K. Shaikhutdinov, H.-J. Freund

Introduction

Hydrogenation of unsaturated hydrocarbons occurs efficiently on noble metal catalysts such as Pt, Rh and Pd. However, real hydrogenation catalysts represent very complex systems for studying reaction mechanisms at the molecular level. Therefore, model systems with a reduced complexity have been invoked ranging from single crystals to metal particles deposited on oxide films¹. The conclusions regarding reaction mechanism and structural sensitivity are often based upon experiments on single crystals². In particular, hydrogenation of alkenes has been shown to be structure insensitive. Here we report on comparative studies of alkene hydrogenation reactions on Pd(111) single crystal and Pd nanoparticles.

Results

We studied the surface chemistry of ethene and different pentene isomers on Pd(111) and Pd particles deposited on a thin alumina film. The particles studied were ~ 5 nm in diameter and consisted primarily of (111) facets. The experiments were performed in ultra-high vacuum on clean and well-defined systems. Using temperature programmed desorption (TPD) technique, we have observed that a number of hydrocarbon transformations, such as dehydrogenation and H-D exchange reaction, occur on both Pd systems. However, the hydrogenation to alkane only occurs on small particles³.

We show that the formation of weakly bonded “sub-surface” hydrogen is a key factor for hydrogenation to occur efficiently. The “sub-surface” hydrogen exists in both Pd systems. However, the particle dimensions are such that this hydrogen is accessible to the adsorbed alkene, and hydrogenation occurs. In contrast, for crystals, the H atoms diffuse so deep into the bulk that they are not accessible to an adsorbed alkene, and therefore hydrogenation does not occur. The findings clearly demonstrate that studies on nanoparticles are required to fully understand elementary processes of catalytic reactions.

We have also proposed a model of overlapping desorption states observed in the TPD spectra, which may predict the hydrogenation activity and the active species involved in the reaction^{3,4}.

1. C. R. Henry, Surf. Sci. Rep. **31** (1998) 231.
2. G. A. Somorjai, ‘Introduction to Surface Chemistry and Catalysis’, Wiley, New York, 1994.
3. A. M. Doyle, Sh. K. Shaikhutdinov, S. D. Jackson, H.-J. Freund, Angew. Chem., 2003, in press.
4. Sh. K. Shaikhutdinov, M. Frank, M. Bäumer, et al., Catal. Lett. **80** (2002) 115.

Atomic Force and Scanning Tunneling Microscopy Measurements at Low Temperatures

M. Kulawik, M. Heyde, G. Thielsch, H.-P. Rust, H.-J. Freund

Introduction

Scanning probe microscopy is one of the most important tools for the investigation of surfaces on the atomic scale in real space. Two very prominent techniques in this field are the scanning tunneling microscopy/spectroscopy (STM/STS) and the atomic force microscopy (AFM). While STM is sensitive to the local density of states of a surface and requires a conductive sample, AFM can be applied also to insulators and reflects mainly the topography. Thus both techniques often deliver complementary information, and a combined AFM/STM sensor is highly desirable in order to correlate electronic and topographic information.

Results

The construction of the second low temperature scanning tunneling microscope has been completed and tested successfully. Several measurements were performed in the STM mode to demonstrate the stability of the machine. A thin alumina film, grown on NiAl(110) was atomically resolved as well as a Ag(111) surface. Furthermore, the surface state of Ag(111) has been imaged in constant current mode, proving good vibrational insulation and low electronic noise. STS measurements on silver atoms at energies above the work function of Ag(111) show the well known field emission resonances, which are caused by electron standing waves formed between the surface and the tip.

For the AFM mode a double tuning fork assembly has been constructed and successfully tested. Two separated detection channels are used to separate the pure vibrational information at one channel and the tunneling current contribution at the other one. Initial measurements confirm the high stability of the double tuning fork AFM/STM sensor. AFM measurements are presented, which reveal step resolution on Ag(111) and NiAl(110) surfaces.

Geometric and Electronic Structure of Line Defects in Al₂O₃ Thin Films on NiAl(110)

M. Kulawik, N. Nilius, H.-P. Rust, H.-J. Freund

Introduction

The electronic and chemical properties of oxides are strongly influenced by defects. The presence of defects governs the nucleation and growth of metal particles on the oxide surface. They provide unsaturated electronic bonds for the potential adsorption of gases and play the decisive role in the catalytic activity of the oxide. Despite this importance, the interrelation between geometric structure, electronic properties and catalytic activity of oxide defects is not well understood.

Results

Using an UHV-STM operating at 4 K, we have investigated the atomic structure of line defects and their influence on the electronic properties for a well-ordered Al₂O₃ film prepared on NiAl(110). The ultra-thin oxide film grows in two reflection domains on the NiAl support, which are separated by antiphase (between equivalent domains) and reflection domain boundaries (between opposite domains). Whereas the latter type shows no order on the atomic level, antiphase domain boundaries are formed by the insertion of a single row of oxygen atoms in the topmost oxide layer. The additional oxygen row is inserted along two characteristic directions with respect to the NiAl lattice, indicating two mechanisms for stress relaxation in the oxide layer.

In STM topographic images taken at low sample bias, the domain boundaries show very little contrast compared to the surrounding defect-free oxide terraces. With increasing positive sample bias, the apparent height of the line defects strongly increases and shows a pronounced maximum at around +2.5 V. This bias dependence is attributed to electronic effects induced by the domain boundaries. Using STS on Al₂O₃ / NiAl(110), two conductance maximums at +2.5 V and +3.0 V could be identified for the domain boundaries, which are absent on defect-free oxide patches. The peaks indicate the presence of unoccupied defect states in the oxide band gap, induced by the disruption of the ideal oxide lattice around the domain boundaries.

Photon Emission Spectroscopy on Individual Oxide-supported Ag-Au Alloy Particles

W. Bente, N. Nilius, N. Ernst, H.-J. Freund

Introduction

The combination of different transition metals to alloy particles often leads to a dramatic enhancement of the catalytic performance of the corresponding cluster-oxide system. The characterisation of size-dependent properties of alloy clusters in an ensemble is difficult when non-local, averaging surface science techniques are used. It often remains unclear, if the different elements completely mix to alloy particles, if they form a shell structure with different composition of inner and outer layers or if they separate to mono-elemental clusters on the surface. Since plasmon-induced light emission is sensitive to the chemical composition of the alloy particles, optical emission and absorption spectroscopy can be used to unravel details of the alloying process.

Results

Using photon emission spectroscopy with the STM, we have investigated Au-Ag alloy particles on a Al_2O_3 thin film grown on NiAl(110). The technique enables experiments on individual particles, which can be characterised and selected according to their size and shape. To improve the performance of the instrument, several constructive changes have been implemented in the setup, such as a new STM control unit and eddy current damping for the vibrational isolation. The properties of W versus PtIr tips have been tested in order to optimise light emission yields from the tunnel junction and chemical stability of the tip-sample system¹. The consequences of the modifications are summarised in the poster. For pure Ag and Au particles, well-defined photon emission peaks at around 320 and 510 nm, respectively, are observed². The occurrence of intermediate peak positions after co-deposition of both materials indicates the formation of alloy clusters on the surface. The influence of the deposition sequence of both materials (Ag \rightarrow Au, Au \rightarrow Ag or instantaneous deposition) and the Ag-Au mass ratio in the clusters are being examined in detail.

1. N. Nilius, N. Ernst, and H.-J. Freund, Phys. Rev. B **65** (2002) 115421.
2. N. Nilius, W. Bente, N. Ernst, and H.-J. Freund, Poster CP 7, Fachbeirat 2001.

The Surface Structure of Co-Pd Bimetallic Particles Supported on Al₂O₃ Thin Films Studied Using IRAS of CO

A.F. Carlsson, T. Risse, M. Bäumer^a, H.-J. Freund

^a*Institut für Angewandte und Physikalische Chemie, Universität Bremen, Bremen, Germany*

Introduction

Building model catalysts for complex catalytic systems is still a challenging task. In the case of supported bimetallic catalysts, such models can be obtained by taking advantage of the nucleation and growth processes during metal vapor deposition of two metals onto a suitable support. For bimetallic Co/Pd aggregates supported on a thin alumina film STM and TPD investigations show the formation of core shell structures. Depending on the sequence of deposition particles with a Pd shell on top of a Co core or large Pd crystallites with a Co skin may be obtained. In this contribution IRAS using CO as a probe molecule was applied to elucidate available binding sites for differently prepared Co/Pd aggregates.

Results

The IRAS measurements reveal a high-coverage state attributable to a M(CO)_n species on pure Co particles in addition to atop sites. Bridge and 3-fold sites are not detected from CO-stretching on the Co particles. Therefore, the previous assignment of the low temperature desorption peak to bridge bound CO based on similarities with single crystal desorption data was reinterpreted based on the IRAS results. IRAS confirms the conclusions from STM and TPD that sequentially deposited Co and Pd form bimetallic particles with a core-shell structure. However, tendency of Pd to segregate to the surface of the bimetallic particles increases the amount of Co required to cover Pd particles is much beyond the expectation of a simple geometric model. Additionally, deposition of Co on top of Pd gives rise to pure Co particles in addition to the bimetallic ones, because of the higher nucleation density of Co as compared to Pd. The IRAS measurements clearly show that atop sites are better preserved at various bimetallic compositions than higher coordinated sites, because they are statistically less vulnerable. Finally, a combination of IRAS and TPD results shows that the stretching frequency of CO to a given site is nearly independent of the bimetallic composition while the binding energy is much more strongly altered by the environment of the adsorption site.

Magnetic Properties as a Probe for Structural Changes in Nanoparticle Catalysts

T. Risse, M. Mozaffari-Afshar, H. Hamann, H.-J. Freund

Introduction

Various techniques have been successfully applied to accumulate structural information on nano particle catalysts. Even though these methods provide data at the atomic level, it has not been possible so far to unravel *all* details necessary to establish structure reactivity relations. One problem is the presence of several interfaces in such systems, i.e. the particle-gas and the particle-support interfaces. It has long been recognized that small changes in the structure influences the magnetic properties drastically. Therefore, monitoring magnetic properties of such systems could help to gain deeper insight. Ferromagnetic resonance (FMR) spectroscopy was used under ultrahigh vacuum (UHV) conditions to characterize the ferromagnetic properties of Ni and Co nano-particles on well defined Al_2O_3 surfaces.

Results

In dispersed catalytic systems thermal stability of the nanoparticles is an important subject. Small Co particles deposited at room temperature on the $\sqrt{31}\times\sqrt{31}\text{R}\pm 9^\circ$ $\alpha\text{-Al}_2\text{O}_3$ (0001) surface. FMR as well as Auger intensities were monitored while the system was annealed stepwise to 870K. While the FMR intensity increases by a factor of 2.5 upon annealing to 570 K the ratio of the Co/O Auger intensity which probes the particle size distribution remains constant. This indicates an internal rearrangement of the particle which results in an increased magnetic moment of the particles. Further increase to 900 K results in an additional increase of the FMR intensity which is, however, mainly due to sintering of the particles as indicated by Auger spectroscopy. It was already shown for several examples that the magnetic properties even though considered a bulk property react sensitively to the adsorption of gases. The changes are even more pronounced for chemical reactions such as oxidation. However, the sensitivity of the method is not restricted to interactions at the metal vacuum interface. This can be shown for oxidised Co particles deposited on a thin alumina film. Annealing of this system results in a reduction of the cobalt oxide phase to metallic cobalt by the underlying NiAl substrate which results in an increased thickness of the oxide film. Subsequent oxidation and annealing cycles indicate a strong decrease of the efficiency of this process most likely due to kinetic limitations. A similar example of a reaction at the metal substrate interface can be observed for oxidised Ni particles deposited on the reconstructed $\alpha\text{-Al}_2\text{O}_3$ (11 $\bar{2}$ 0) surface. Here the oxygen deficiency of the topmost layers of the substrate serve as the reductive agent upon annealing.

Structure and Dynamics of Proteins on Planar Surfaces

K. Jacobsen, T. Risse, W.L. Hubbell^a

^a Jules Stein Eye Institute, University of California Los Angeles, Los Angeles, USA

Introduction

There is currently intense interest in the interaction of proteins with surfaces, and in the properties of surfaces that determine the interaction. However, little is known about the structure and dynamics of the adsorbed proteins, because the number of experimental techniques to address this issue is limited. Up to now structural information on proteins is mainly gained by diffraction techniques, which in turn require a crystalline arrangement of the molecules. Site-directed spin labeling (SDSL), which involves the mutation of a selected native amino acid into a cysteine and subsequent coupling of the spin label to the cysteine residue, has proven to be a powerful tool for the investigation of structure and dynamics of proteins on surfaces irrespective of the geometric arrangement of the molecules.

Results

In this study a monolayer of histidine-tagged T4 Lysozyme (T4L) was selectively tethered to a supported lipid bilayer via chelating headgroups (Ni-NTA). SDSL in combination Electron Paramagnetic Resonance (EPR) spectroscopy of proteins was used to deduce the structure and dynamics of adsorbed spin-labeled protein from the line shape of the EPR spectra. The EPR spectrum reflects the mobility of the side chain uniquely determined by the local structure and backbone dynamics. Various sites at distinct topographical regions throughout the protein were investigated. The EPR spectra of adsorbed T4L resemble those in viscous solution, where the protein rotation is slow on the timescale of EPR. This indicates the conservation of the tertiary fold of T4L upon adsorption as well as a reduction of global tumbling of the protein in the adsorbed state. For molecules oriented in two dimensions, the tensorial nature of the Hamiltonian gives rise to angular dependent EPR spectra, which can be used to extract the orientation of secondary structure elements with respect to the planar surface. Angular dependent spectra were observed for several sites of adsorbed T4L, proving an ordered arrangement of molecules in the monolayer. This information can be used further to determine the topography of the surface bound protein. A detailed discussion of these results will be given.

Sum Frequency Generation Spectroscopy of CO-H₂ Interaction and CH₃OH Decomposition on Pd Model Catalysts

M. Morkel, G. Rupprechter, H.-J. Freund

Introduction

There is an ongoing debate whether surface science results can be truly transferred to catalysis. Deviations may originate from the specific pressure regimes and from structural differences between single crystals and supported metals. We have employed Sum Frequency Generation (SFG) vibrational spectroscopy to monitor molecules adsorbed on well-defined model catalysts under ultrahigh vacuum (UHV) and high-pressure (1 bar), using an SFG-compatible UHV-high pressure reaction cell combined with gas chromatography and mass spectrometry for product analysis^{1,2}. Systems studied include CO adsorption, CO/H₂ coadsorption, CO hydrogenation, and methanol decomposition on Al₂O₃ supported Pd nanoparticles (mean size 6 nm) and Pd(111).

Results

Comparison of high-pressure (1-1000 mbar) CO adsorbate phases on Pd(111) and Pd-Al₂O₃ demonstrated the importance of specific binding sites located on the steps and edges of metal nanoparticles¹. The picture becomes more complex when CO is coadsorbed with hydrogen². On Pd(111), preadsorbed CO effectively prevented the dissociative adsorption of H₂. Preadsorbed hydrogen was able to hinder CO adsorption at 100 K but was replaced from the surface by CO above 125 K due to hydrogen dissolution in the Pd bulk. Using CO/H₂ mixtures below 125 K, CO and hydrogen coexisted on the surface, while at higher temperatures hydrogen was again replaced by CO. SFG spectra acquired under reaction conditions (55 mbar, 550 K) revealed high CO coverages (~ 0.5 ML), which strongly limit hydrogen adsorption, thus explaining the inactivity of Pd(111) for CO hydrogenation². Oxide supported Pd nanoparticles provide additional sites for CO hydrogenation (facets, step-, edge- and corner sites) on which site blocking effects may be less pronounced. Corresponding coadsorption studies are currently performed.

The reverse reaction, i.e. methanol decomposition on Pd nanoparticles and Pd(111) at mbar pressure, was also studied. For both types of catalysts, the decomposition product CO was observed by SFG, but there was a rapid deactivation due to carbon poisoning. No products were detected by gas chromatography even after hours at 500 K.

1. H. Unterhalt, G. Rupprechter, H.-J. Freund, *J. Phys. Chem. B* **106** (2002) 356.
2. M. Morkel, G. Rupprechter, H.-J. Freund, *J. Chem. Phys.* (2003) in press.

PM-IRAS and XPS Spectroscopy on Model Catalysts: Methanol Decomposition on Pd Surfaces

O. Rodríguez de la Fuente, M. Borasio, P. Galletto, G. Rupprechter, H.-J. Freund

Introduction

The interest to connect surface science and catalysis has stimulated the development of in-situ techniques, e.g. Sum Frequency Generation (SFG). Polarization-Modulation Infrared Reflection Absorption Spectroscopy (PM-IRAS) provides an alternative route for studying vibrations of molecules adsorbed on model catalysts at high pressure. PM-IRAS utilizes the polarization modulation of the incident infrared light and is based on the predominance of p-over s-polarized light at a metal surface. The differential reflectance $\Delta R/R$ that is measured with PM-IRAS provides the surface vibrational spectrum while no bulk (gas phase) species are detected¹. Our experimental setup combines a UHV preparation/characterization chamber with a UHV-high pressure cell optimized for the PM-IRAS geometry. Under UHV, X-ray photoelectron spectroscopy (XPS) is used for pre- and post-reaction surface analysis (beside LEED, AES, TDS).

Results

Methanol adsorption/desorption and its time- and temperature-dependent decomposition on well-annealed and defect-rich (ion-bombarded) Pd(111) was examined by XPS and PM-IRAS². Annealing CH₃OH multilayers from 100 K to 700 K mainly resulted in CH₃OH desorption. Dehydrogenation to CO was a minor path and only trace amounts of carbon or carbonaceous species (CH_x; x = 0-3) were produced, i.e. C-O bond scission was very limited. By contrast, an exposure of 5×10^{-7} mbar CH₃OH at 300 K produced CH_x (~8%) on both surfaces but the rate of formation was not enhanced by surface defects. It seems that defects generated by ion-bombardment do not exhibit the high C-O bond scission activity of steps and edges on Pd nanoparticles. On well-annealed Pd(111) isolated carbon atoms were identified by XPS in the early stages of carbon deposition, with carbon diffusion leading to the growth of carbon clusters in the later stages. Since carbon(aceous) species may either originate from C-O bond scission within methanol (or CH_xO) or from a consecutive dissociation of the dehydrogenation product CO, analogous experiments were also carried out with CO. PM-IRAS spectra up to 170 mbar CO, acquired using a UHV-high pressure cell, did not show any indications of CO dissociation, excluding CO as source of carbonaceous deposits.

1. G. A. Beitel, A. Laskov, H. Oosterbeek, E. W. Kuipers, *J. Phys. Chem.*, **100** (1996) 12494.
2. O. Rodríguez de la Fuente, M. Borasio, P. Galletto, G. Rupprechter, H.-J. Freund, *Surf. Sci.* submitted.

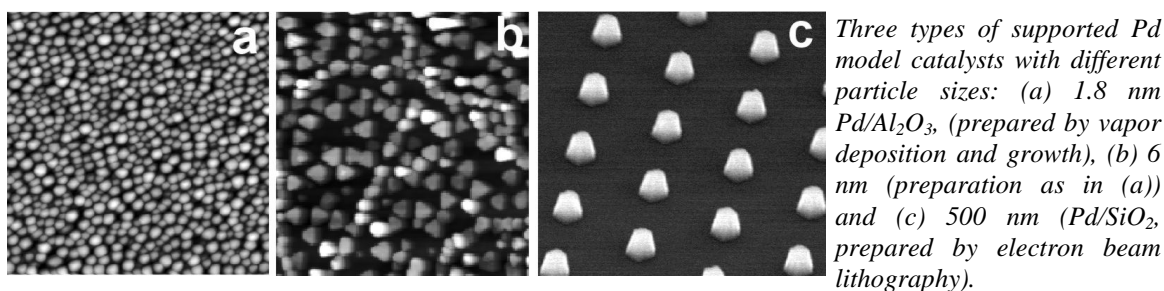
Reaction Kinetics on Supported Nanoparticles: *Local Reaction Rates, Surface Diffusion and Kinetic Bistabilities*

M. Laurin, V. Johánek, S. Schauermann, J. Hoffmann,
A. Grant[§], B. Kasemo[§], J. Libuda, H.-J. Freund

[§] Dept. of Applied Physics and Competence Centre for Catalysis, Chalmers Univ. of Technology, S-41296
Göteborg, Sweden

Introduction

Particle size effects are a common phenomenon in heterogeneous catalysis. In many cases, such effects are related to the presence of specific reactive sites on particles of particular size and structure or to the modification of geometric or electronic properties as a result of the limited size of the particle or the influence of the support. However, there are also kinetic phenomena which exclusively arise as result of the limited size of the reaction system and are not necessarily connected to modified adsorption or reaction properties of individual sites. Here, we investigate two such effects: First, we consider *surface diffusion* which on small particles may be limited by the dimensions of the catalyst particle itself. Secondly, we investigate the behaviour of *kinetic bistabilities* on active particles in the nanometer size range.



Results

Two types of supported Pd model catalysts are employed in this work, which allow us to vary the particle size over an exceptionally broad range from few to several hundred nanometers in diameter: Smaller particles (1 – 6 nm) are prepared by metal vapour deposition and growth under UHV conditions, whereas large particles (500 nm) are prepared by electron beam lithography. As a simple model reaction we consider the oxidation of CO.

In order to investigate the diffusion of atomic oxygen under reaction conditions, we combine multi-molecular beam experiments and an angular-resolved detection of products. It is found that on smaller particles oxygen diffusion is always fast on the timescale of reaction, whereas this is not the case for larger particles and under CO-rich reaction conditions. Diffusion rates under reaction conditions can be derived from this type of data. Moreover, it is shown experimentally that regions with different local coverage can develop on particles above a critical size and the reaction rates on these particles depend on the direction of the incident reactant fluxes.

As a second phenomenon, we systematically investigate kinetic bistabilities, which occur for CO oxidation on Pd and various transition metal surfaces as a result of the asymmetry in adsorption behaviour of the reactants. Systematic molecular beam experiments are performed on the transient and steady-state behaviour as a function of sample temperature, adsorbate fluxes and particle size. Whereas on larger particles well-defined bistability regions are observed, particles of 6 nm size and below show a macroscopically monostable kinetics on the timescale of our experiment. Based on the transient behaviour and microkinetic simulations we suggest that on small particles the macroscopic bistability vanishes as a result of fluctuation induced transitions between the two reactive states. Finally, the influence of defect sites on these transitions is investigated.

Activity and Selectivity of Specific Sites on Supported Nanoparticles: Molecular Beam Experiments – Time Resolved IRAS – Microcalorimetry

V. Johánek, M. Laurin, S. Schauermaun, J. Hoffmann, J. Hartmann,
C. T. Campbell[§], J. Libuda, H.-J. Freund

[§] Dept. of Chemistry, Univ. of Washington, Seattle, WA 98195-1700, USA

Introduction

For many reactions on supported metal catalysts, it is observed that both activity and selectivity sensitively depend on the structure and size of the active particles. Often, such effects are tentatively related to the presence of specific reactive sites, although specific cases are scarce in which the origins of size and structure effects could be uncovered at the atomic level.

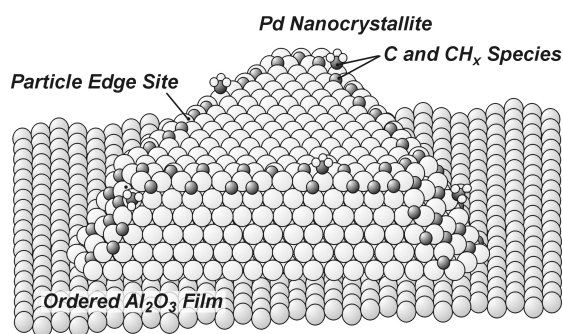
In order to overcome the difficulties arising in classical reactivity studies on real catalysts, we follow a new experimental approach: We combine *supported model catalysts* with a reduced level of complexity and *molecular beam techniques*, providing detailed kinetic data under extremely well-controlled conditions¹. For this purpose, we have developed a molecular beam experiment, which comprises three beam sources, angular-resolved gas phase detection and time-resolved IRAS (IR reflection absorption spectroscopy). In addition, a single-crystal microcalorimetry facility is under development.

Results

In this contribution, we present two examples showing how particle structure, activity and selectivity can be related at the microscopic level. We employ a Pd/alumina model catalyst based on an ordered alumina film, which has been characterized in great detail with respect to its structure and adsorption properties.

As a first example, we investigate the decomposition of methanol, which proceeds via two competing pathways: dehydrogenation to CO and C-O bond scission leading to formation of adsorbed carbon species². Using CO as a probe molecule, the occupation of different adsorption sites on the particles such as facets and edges by the reaction products is analysed. Combining molecular beam experiments and time-resolved IR reflection absorption spectroscopy (TR-IRAS) the corresponding reaction rates are determined. It is shown that C-O bond scission preferentially occurs at particle edges where for the dehydrogenation pathway no similar preference is observed. Thus, the structure of the particle controls selectivity in this reaction system.

As the second example we consider the decomposition of NO³. In contrast to the methanol case, no additional probe molecule is required in this case in order to monitor the distribution of reactants and products over the different particle sites. An enhanced decomposition activity is found for the Pd supported nanocrystallites, indicating preferential N-O bond scission at particle edges and steps. It is shown that the presence of atomic nitrogen and oxygen species in the vicinity of particle edges and steps controls the NO dissociation activity.



Schematic representation of the Pd/alumina model catalyst.

1. J. Libuda, H.-J. Freund, *J. Phys. Chem. B* **106** (2002) 4901.
2. S. Schauermaun, J. Hoffmann, V. Johánek, J. Hartmann, J. Libuda, H.-J. Freund, *Angew. Chem. Int. Ed.* **41** (2002) 2513.
3. V. Johánek, S. Schauermaun, M. Laurin, J. Libuda, H.-J. Freund, *Angew. Chem. Int. Ed.* **42** (2003) 3035.

Two Photon Photoemission Microscopy Using Femtosecond Laser Radiation

W. Bente, H. Petek^a, W. Drachsel, and H.-J. Freund

^aDepartment of Physics and Astronomy, University of Pittsburgh, PA, USA

Introduction

Irradiation of a surface by a fs-laser at a photon energy well below the work function still leads to emission of electrons due to the process of two or multiple photon excitation. This excitation can involve unoccupied intermediate electronic states and thus the two-photon photoemission (2PPE) spectra provide information states above the Fermi level¹. To include spatially resolved information for the study of nonlinear optical effects a conventional photoemission electron microscope (PEEM)² was combined with a fs laser system as excitation source. With the incorporated pump and probe facility the electron dynamics of the studied processes can be observed at a fs time scale.

Results

The partially shielded probe was irradiated at an incidence angle of 15° and a photon energy of 3.1 eV in the PEEM. The image (resolution 500 nm) was recorded by a video camera and the signal digitally stored, the screen current as a measure for the total 2PPE rate was monitored.

In order to determine the actual laser pulse width at the probe location, the auto correlation signal from a Cu(111) crystal was measured for p-polarised light. Due to the sp band gap of 4 eV the emission originates mainly from the occupied surface state at 0.4 eV below E_F via a virtual state and can be considered as instantaneous³. In contrast using s-polarised light the PEEM image is dark with some bright spots, but at the moment it is not clear where they come from. The measured ratio of the averaged intensities cannot be explained by the Fresnel relation.

For an assembly of randomly distributed metal clusters Stockman⁴ predicts ultrafast giant fluctuations of the local field strength after excitation by a fs laser, which should be visible as temporary hot spots in the PEEM. Time resolved (TR) measurements were accomplished for a regular array of square Ag aggregates at a size of 500 nm by 500 nm lithographically prepared on a SiO₂/Si substrate⁵. The PEEM images were full of contrast at highest magnification, the Ag islands were blown up due to electron optical of their 3D-character. The data of the TR investigation corresponded with the expected silver plasmon life time. In a next step an array of randomly distributed Ag cluster prepared at otherwise same conditions was irradiated in the PEEM, with the same result as before. The expected dynamic effect was not observed as predicted, we presume that at island size of 500 nm the condition “cluster dimension \ll wave length“ is not fulfilled. Therefore an investigation for a random distribution of ~10nm Ag cluster is under the way.

The PEEM operated in the 2PPE mode can provide new insights of nonlinear optical behaviour of surfaces in two dimensions which can be fruitfully used for the operation of the SMART with its lateral atomic resolution.

1. H. Petek, S.Ogawa, Prog. Surf. Sci. **56** (1997) 239.
2. W. Engel, M. E. Kordisch, H. H. Rotermund, S. Kubala, A. v. Oertzen, Ultramicroscopy **36** (1991) 148.
3. E. Knösel, T. Hertel, M. Wolf, G. Ertl, Chem. Phys. Lett. **240** (1995) 409.
4. M. I. Stockman, Phys. Rev. Lett. **84** (2000) 1011.
5. Samples were kindly supplied by B. Kasemo, Dept. of Appl. Phys., Chalmers University, Göteborg, Sweden.

Photoinduced Desorption of NO from Supported Silver Nanoparticles

C. Rakete, F. Evers, W. Drachsel, and H.-J. Freund

Introduction

In our group we studied the dynamics of NO photodesorption from oxide layers by quantum state selective detection of the emitted species¹. The observed velocity distribution and the coupling of translation and rotation of the NO molecules could be modelled by wave packet calculations². In comparison to the studied oxide supports, the photodesorption from metals is quenched much stronger, yielding cross sections about three orders lower³. As in case of metallic nanoparticles the excitation of surface plasmons is a very efficient process with a high 2PPE yield⁴, the NO photodesorption from silver clusters should be efficient too. A substrate mediated DIET mechanism is expected, for which the energy conversion from collective electron motion to creation of the intermediate state, the role of spatial confinement, and the dynamics of this process are so far unexplored. In order to tackle these questions a pump-probe experiment was developed, which combines time resolved two photon photoemission and quantum state selective detection of the photodesorbed molecules via resonant-enhanced-multiphoton ionisation (REMPI).

Results

Silver clusters were grown on a thin Al₂O₃ layer on top of a NiAl (110) crystal at 85 K. Typically an average diameter of 5 nm of the aggregates was adjusted, yielding a Mie-resonance centred at 3.6 eV as found in a separate photon STM investigation. The measured 2PPE spectra confirm the same resonance behaviour but display a wider line width due to inhomogeneous broadening. The 2PPE rate at resonance exhibits a sin⁴ dependence on the polarisation angle of the laser light indicating a two plasmon excitation of the Ag clusters. Even at a photon energy of 3.2 eV where the emission rate has dropped to less than 10 % this dependence is still observed. Most of the photo desorption experiments were performed at this energy for laser intensity reasons. In same way as the corresponding 2PPE intensity, the measured NO photo desorption yield depends on the polarisation angle, suggesting that primarily a two plasmon excitation induces the NO desorption. This is further confirmed by the quadratic dependence of the NO desorption rate on laser power. The efficiency of the photo desorption from the clusters is much higher than from Ag(111).as expressed by a cross section of 5x10⁻¹⁷ cm² at a light intensity of 4 mJ/cm². The NO dimers formed on silver at 85 K⁵ will be dissociated by photon interaction, according to (NO)₂ + ħω → NO_{ad} + NO↑.

The quantum state resolved detection yields a mono modal velocity distribution of nonthermal nature for the desorbing NO. The velocity dependence on the probed rotational moment reveals the linear coupling between mean translational energy and the corresponding rotational energy. However the observed occupation of vibrational states at v =1 and 2 does not correlate energetically with the rotational quantum number, and the derived effective temperature of 3500 K is discussed in terms of the lifetime of the NO⁺ intermediate.

Due to the underlying DIET mechanism time resolved measurement of the NO desorption rate in a pump/probe experiment indicates not only a dominating fast process in the fs range, but also a slow one in the ps range, which can be interpreted within the DIMET or friction model.

1. K. Al-Shamery, Appl. Phys. A **63** (1996) 509.
2. T. Klüner, H.-J. Freund, V. Staemmler, R. Kosloff, Phys. Rev. Lett. **80** (1998) 5208.
3. F. M. Zimmermann, W. Ho, Surf. Sci. Rep. **22** (1995) 127.
4. J. Lehmann, M. Merschdorf, W. Pfeiffer, A. Thon, S. Voll, G. Gerber, Phys. Rev. Lett. **85** (2000) 2921.
5. R. T. Kidd, S. R. Meech, D. Lennon, Chem. Phys. Lett. **262** (1996) 142.

Prediction of Electronic Excited States of Adsorbates on Metal Surfaces from First Principles

D. Lahav, T. Klüner, S. Borowski, N. Govind*, Y.A. Wang*, E.A. Carter*

* Department of Chemistry and Biochemistry, University of California, Los Angeles

Introduction

We present the first ab initio prediction of localized electronic excited states in a periodically infinite condensed phase, a heretofore intractable goal. In particular, we examined local excitations within a CO molecule adsorbed on a Pd(111) surface. The calculation allows a CI (Configuration Interaction) treatment of a local region, while its interaction with the extended condensed phase is described via an embedding potential obtained from periodic density functional theory (DFT). Our study lays the foundation of a microscopic understanding of photochemistry and spectroscopy on metal surfaces¹⁻³.

Results

We performed MP2, CASSCF and CI calculations on clusters embedded in an extended environment that has been treated at the DFT level using periodic slab models. In our density based embedded cluster approach an effective one electron embedding operator is constructed from a periodic DFT calculation. This embedding operator is self-consistently updated in a subsequent quantum chemical cluster calculation.

The applicability of pseudopotentials in the calculation of the kinetic energy contribution to the embedding operator was investigated in detail and a local truncation criterion based on the conventional gradient expansion on the kinetic energy functional was introduced.

Our approach has been applied to the well studied adsorbate/substrate system CO/Pd(111) where we were able to calculate accurately the adsorption energy and the vertical excitation energy for the CO internal ($5\sigma \rightarrow 2\pi^*$) transition.

Furthermore, a formal extension of the embedding theory has been derived and is currently been implemented. This extension lifts the approximation of a frozen background density inherent to the present implementation of the embedding formalism. This new approach will be tested on the system CO/Pt(111) for which all currently available electronic structure methods fail to predict the correct adsorption site.

1. N. Govind, Y. A. Wang, E. A. Carter, J. Chem. Phys. **110** (1999) 7677.
2. T. Klüner, N. Govind, Y. A. Wang, E. A. Carter, Phys. Rev. Lett. **86** (2001) 5954.
3. T. Klüner, N. Govind, Y. A. Wang, E. A. Carter, J. Chem. Phys. **116** (2002) 42.

A Surrogate Hamiltonian Treatment of Laser Induced Desorption of NO/NiO(100)

S. Dittrich, C.P. Koch, D. Kröner, S. Borowski, T. Klüner, H.-J. Freund, R. Kosloff*

*Fritz Haber Research Center, The Hebrew University of Jerusalem, Israel

Introduction

A microscopic model for electronic quenching in the photodesorption of NO from NiO(100) is developed. The quenching is caused by the interaction of the excited adsorbate-substrate complex with electron-hole pairs ($O2p \rightarrow Ni3d$ charge transfer states) in the surface. The electron-hole pairs are described as a bath of two level systems which are characterized by an excitation energy and a dipole charge. Both parameters are connected to estimates from photoelectron spectroscopy and configuration interaction calculations. Within a surrogate Hamiltonian approach^{1,2} which explicitly includes the ultrashort excitation laser pulse and the bath of electron-hole pairs as a dissipative environment, the desorption dynamics was calculated using ab initio potential energy surfaces for the electronic ground and excited state.

Results

For the first time a complete ab initio description of laser induced desorption of molecules from surfaces has been achieved^{3,4}. The desorption probability and the velocity distributions were calculated in agreement with experimental results and previous stochastic wave packet calculations⁵.

Furthermore, the lifetime of the electronically excited NO^- -like intermediate was predicted to be 25 fs in perfect agreement with previous semiempirical estimates. Currently, the surrogate Hamiltonian approach is extended to include many degrees of freedom of the adsorbate-substrate complex.

1. R. Baer, R. Kosloff, J. Chem. Phys. **106** (1997) 8862.
2. C. P. Koch, T. Klüner, R. Kosloff, J. Chem. Phys. **116** (2002) 7983.
3. C. P. Koch, T. Klüner, H.-J. Freund, R. Kosloff, Phys. Rev. Lett. **90** (2003) 117601.
4. C. P. Koch, T. Klüner, H.-J. Freund, R. Kosloff, J. Chem. Phys. **119** (2003) 1750.
5. T. Klüner, H.-J. Freund, V. Staemmler, R. Kosloff, Phys. Rev. Lett. **80** (1998) 5208.

Rotational and Lateral Dynamics of the Photodesorption of CO from Cr₂O₃(0001) - A First-Principles Quantum Dynamical Study

S. Borowski, T. Klüner, S. Thiel, M. Pykavy, V. Staemmler*, H.-J. Freund

* Ruhr-Universität Bochum, Lehrstuhl für Theoretische Chemie, 44780 Bochum, Germany

Introduction

We present results of theoretical investigations on the rotational and lateral dynamics of CO molecules photodesorbing from a Cr₂O₃(0001) surface. The studies are based on high-dimensional stochastic quantum dynamical wave packet calculations employing complete first principles potential energy surfaces¹. The angular momentum distribution of the desorbing CO molecules is completely analyzed² in terms of orientation and alignment parameters $A_q^{(k)}$. Additionally, lateral velocity distributions of the desorbing CO molecules are considered with regard to both occurrence and preference of lateral velocities³. A detailed comparison of the theoretical results with experimental findings from quantum state resolved (1+1') REMPI measurements is presented^{3,4}.

Results

- (1) The measured REMPI intensity is exactly composed of the monopole moment $A_0^{(0)}$ and the quadrupole moment $A_0^{(2)}$ only as assumed in the experiments.
- (2) Confirming experimental assumptions, the calculated angular momentum distribution is dominated by cylindrically symmetric parts with a small hexadecapole moment $A_0^{(4)}$.
- (3) The calculated mean and maximal lateral velocities are in excellent quantitative agreement with experimental data obtained from the measured Doppler profiles.
- (4) A dynamical steering effect favoring a non-zero lateral velocity for small rotational states is predicted.

1. M. Pykavy, S. Thiel, T. Klüner, J. Phys. Chem. B **106** (2002) 12556.
2. S. Borowski, T. Klüner, H.-J. Freund, J. Chem. Phys., submitted.
3. S. Borowski, T. Klüner, H.-J. Freund, I. Klinkmann, K. Al-Shamery, M. Pykavy, V. Staemmler, Appl. Phys. A, in press.
4. I. Beauport, K. Al-Shamery, H.-J. Freund, Chem. Phys. Lett. **256**, 641 (1996) 641.

Department of Molecular Physics
Poster List 2003

- MP 1** **Deceleration and trapping of beams of neutral polar molecules**
H. L. Bethlem, F. M. H. Crompvoets, S. Y. T. van de Meerakker,
J. van Veldhoven, J. Küpper, G. Meijer
- MP 2** **Dynamics of neutral molecules stored in a ring**
F. M. H. Crompvoets, H. L. Bethlem, J. Küpper, D. Carty, G. Meijer
- MP 3** **Sympathetic cooling of polar molecules by cold Rubidium atoms**
S. Schlunk, A. P. Mosk, W. Schöllkopf, G. Meijer
- MP 4** **Alternate gradient focusing and deceleration of a beam of large molecules**
J. Küpper, H. L. Bethlem, G. Meijer
- MP 5** **Molecule optics using micro-structured arrays**
S. Schulz, H. Conrad, G. Meijer
- MP 6** **Motion control of molecules via non-resonant light forces**
B. Friedrich and G. Meijer
- MP 7** **Molecular physics experiments using the free electron laser FELIX**
G. von Helden, A. Fielicke, J. M. Bakker, G. Meijer
- MP 8** **Mass-selective vibrational spectroscopy of gas-phase clusters**
K. R. Asmis, M. Brümmer, C. Kaposta, G. Santambrogio, L. Wöste,
G. von Helden, G. Meijer
- MP 9** **Angular correlations in double Auger decay of Ne and Ar**
J. Viefhaus, S. Cvejanovic, A. Grum-Grzhimailo, N. Kabachnik,
S. Korica, B. Langer, T. Lischke, G. Prümper, D. Rolles, U. Becker
- MP 10** **Doppler splitting and intra-molecular scattering of Auger electrons in dissociating molecules**
G. Prümper, R. Hentges, O. Kugeler, S. Marburger, D. Rolles,
F. Burmeister, J. Viefhaus, S. Cvejanovic, U. Hergenhahn, U. Becker

- MP 11** **Enhancement of double Auger decay following plasmon excitation in C₆₀**
A. Reinköster, S. Korica, B. Langer, S. Cvejanovic, J. Viefhaus, U. Becker
- MP 12** **Selectivity in vibrationally mediated single-molecule chemistry**
J. I. Pascual, N. Lorente, Z. Song, H.-P. Rust, H. Conrad
- MP 13** **Precursor and initial stages of oxide formation on ruthenium**
R. Blume, H. Niehus, L. Gregoratti, A. Barinov, L. Aballe, M. Kiskinova, A. Böttcher, A. Lobo, S. Amarie, H. Conrad
- MP 14** **“Lower-than-2”-dimensional systems: geometric and electronic structure**
M. Hansmann, J. I. Pascual, J. Schaefer, E. Rotenberg, K. Horn
- MP 15** **Metallic quantum wells: electronic structure and “electronic growth”**
J. W. Kim, H. Dil, S. Gokhale, M. Tallarida, L. Aballe, K. Horn
- MP 16** **Bond length and bond strength in weak and strong chemisorption: N₂, CO and CO/H on a nickel surface**
D. I. Sayago, J. T. Hoefl, M. Polcik, M. Kittel, R. L. Toomes, J. Robinson, D. P. Woodruff, M. Pascal, G. Nisbet, C. L. A. Lamont

Deceleration and trapping of beams of neutral polar molecules

H. L. Bethlem, F. M. H. Crompvoets, S. Y. T. van de Meerakker, J. van Veldhoven,
J. Küpper and G. Meijer

The ability to cool and slow atoms with light has led to exciting and sometimes unforeseen results over the last years. The pay-offs have included atom interferometry, precision spectroscopy, quantum-degenerate gases, including Bose-Einstein condensates, and atom lasers. There currently is a rapidly growing interest in the physics of cold molecules as well. However, the techniques used to cool atoms cannot be applied to the cooling of molecules.

Our group has developed techniques that exploit the interaction of neutral dipolar molecules with time-varying inhomogeneous electric fields to reduce in a stepwise fashion the velocity of these molecules. This approach is very similar to the approach used in the manipulation of charged particles, but in our case the inhomogeneous charge distribution, rather than the total charge, in the molecules is used to manipulate them. We have developed a so-called 'Stark decelerator', the equivalent of a LINear ACcelerator (LINAC) for charged particles, by which one is able to transfer the high phase-space density that is present in the moving frame of a pulsed molecular beam to a reference frame at any desired velocity [1,2]. In particular, using this approach we have been able to trap neutral deuterated ammonia molecules in an electrostatic trap at a density of (better than) 10^7 mol/cm³ and at temperatures of around 25 mK [3,4]. In the first experiments the trapping time was limited to 0.3 s due to collisions with background gas (at 10^{-8} mbar) in the trapping chamber, but this can be readily improved. Currently, an up-scaled version of the decelerator is under construction, which will not only enable greatly increasing the fraction of the molecular beam that is "accepted" by the decelerator, but will also enhance the scope of dipolar molecules that can be decelerated.

The poster will present a detailed description of the operation mechanism of the molecular beam deceleration and trapping machine. Molecular beams with a computer-controlled (calibrated) velocity and with a narrow velocity distribution are produced and applied in high resolution spectroscopic studies. The extension of the deceleration and trapping technique to beams of free radicals like OH and NH will be discussed.

References

1. H.L. Bethlem, G. Berden and G. Meijer, *Phys. Rev. Lett.* **83**, 1558 (1999).
2. H.L. Bethlem, G. Berden, A.J.A. van Roij, F.M.H. Crompvoets and G. Meijer, *Phys. Rev. Lett.* **84**, 5744 (2000).
3. H. L. Bethlem, G. Berden, F.M.H. Crompvoets, R.T. Jongma, A.J.A. van Roij and G. Meijer, *Nature* **406**, 491 (2000).
4. H.L. Bethlem, F.M.H. Crompvoets, R.T. Jongma, S.Y.T. van de Meerakker and G. Meijer, *Phys. Rev. A* **65**, 053416 (2002).

Dynamics of neutral molecules stored in a ring

F. M. H. Crompvoets, H. L. Bethlem, J. Küpper, D. Carty and G. Meijer

Static inhomogeneous electric fields can be used to spatially manipulate neutral dipolar molecules. The ability to focus a molecular beam with an electrostatic hexapole lens is a clear demonstration of this principle. By bending a hexapole into a torus, a storage ring can be created. In such a toroidal trap bunches of molecules can be confined in circular orbits.

Recently, we have experimentally demonstrated a prototype storage ring for neutral molecules; packages of 10^6 deuterated ammonia molecules with a longitudinal temperature of around 10 mK were stored for up to 6 round trips in a 25 cm diameter electrostatic storage ring [1]. The absolute velocity of the molecules in the ring was about 90 m/s, which was achieved by decelerating a pulsed molecular beam in a “Stark decelerator” prior to entering the ring. The electrodes of the ring create a dipolar electric field that delivers a sufficient centripetal force to keep the slow molecules in orbit. The number of detected round trips was ultimately limited by the spreading-out of the package of molecules due to the tangential velocity width of about 5 m/s.

Although inhomogeneous electric fields by themselves can generally not be used to increase the phase-space density (Liouville’s theorem) they can be used to manipulate the phase-space distribution of the molecules. Appropriately designed fields can be used to rotate the distribution in phase-space, thereby minimizing either the longitudinal velocity spread (longitudinal cooling) or the length of the decelerated package (longitudinal focusing or bunching) at a certain position or time [2]. In order to obtain more round trips in the storage ring, we enhanced the Stark decelerator with such a buncher.

On the poster we will present the results on the storage ring, including those obtained with the improved loading scheme. By minimizing the longitudinal velocity spread with the buncher and by matching the transversal emittance of the decelerator to the acceptance of the ring with additional hexapoles, the number of detected round trips is increased to 50. The longitudinal velocity spread is reduced to 0.76 m/s which corresponds to a temperature of 0.25 mK. The dynamics of the motion of the molecular package inside the ring is investigated by temporarily superimposing a few-cycle sinusoidal AC voltage onto the DC voltages. This results in an oscillating potential well which drives the betatron oscillations of the trapped molecules, as is experimentally observed.

References

1. F. M. H. Crompvoets, H. L. Bethlem, R. T. Jongma and G. Meijer, *Nature* **411**, 174 (2001).
2. F. M. H. Crompvoets, R. T. Jongma, H. L. Bethlem, A. J. A. van Roij and G. Meijer, *Phys. Rev. Lett.* **89**, 093004 (2002).

Sympathetic cooling of polar molecules by cold Rubidium atoms

S. Schlunk, A. P. Mosk, W. Schöllkopf and G. Meijer

Molecules, in contrast to atoms, can have a permanent electric dipole moment that can lead to a dipole-dipole interaction. This anisotropic long-range interaction is expected to cause unique features in ultracold quantum-degenerate gases of polar molecules. For bosonic polar molecules the stability of a BEC-phase is predicted to depend on the orientation of the dipoles relative to the trap geometry. For fermionic polar molecules, a Fermi-degenerate gas is expected to have relatively high critical temperatures for a single-component (p-wave Cooper pairing) BCS superfluid transition [1].

Cooling and trapping of molecules is difficult because so far, laser cooling could not be demonstrated for molecules, due to their complex multiple-level structure. In addition, evaporative cooling, which has been the essential cooling technique to produce ultracold quantum-degenerate atomic vapours, has not yet been exploited in experiments with molecules. Its efficacy depends on the ratio of the rate coefficients for elastic and inelastic cold collisions. For molecule-molecule collisions as well as for most atom-molecule collisions these rate coefficients cannot be predicted by theory because of the lack of sufficiently accurate intermolecular potentials.

In this project we plan to circumvent these limitations by overlaying a trap of cold molecules with a magnetic trap for Rubidium atoms and to study cold atom-molecule collisions, i.e. the elastic and inelastic collision rates. Inelastic collisions can spoil the thermalization process between the two species, leading to loss of atoms and/or molecules. If the ratio of elastic to inelastic atom-molecule collision rates is sufficiently large, the cloud of ultracold Rb-atoms can be used as a coolant and sympathetic cooling will lower the temperature of the molecules towards the ultracold regime.

In our experimental approach the molecules will be slowed by Stark deceleration and subsequently trapped either in an electrostatic or in a magnetic trap. With this method ND₃ molecules have been trapped in an electrostatic trap at densities of $>10^7$ mol/cm³ and at temperatures of 25 mK [2]. Trapping and cooling of the Rb-atoms will be performed in a standard magneto-optical trap (MOT) loaded from a Zeeman-slower. The atoms will be cooled and trapped in the MOT where we expect densities of $> 5 \cdot 10^9$ atoms/cm³ at a temperature of 0.3 mK. After transfer to a magnetic trap and adiabatic compression effected by increasing the magnetic field, a density on the order of 10^{11} atoms/cm³ and a temperature of about 1 mK are expected. Merging the atomic and molecular traps at these densities should reveal the effects of cold atom-molecule collisions.

References

1. M. Baranov, L. Dobrek, K. Góral, L.Santos and M. Lewenstein, Phys. Scripta T102, 74 (2002).
2. H.L. Bethlem and G. Meijer, Int. Rev. Phys. Chem. 22, 73 (2003).

Alternate gradient focusing and deceleration of a beam of large molecules

J. Küpper, H. L. Bethlem and G. Meijer

Polar molecules can be decelerated using time-varying electric fields. This method is based on the notion that a molecule in a quantum state in which the dipole moment is anti-parallel to an external electric field will be attracted to regions of low electric field. Therefore, molecules in such a “low-field” seeking state will be decelerated on their way from a region of low electric field into a region of high electric field. If the electric field is switched off while the molecules are still in the region of high electric field, the molecules will not regain their lost kinetic energy. A properly timed switching of the electric fields ensures that a bunch of molecules can be kept together in the forward direction (“phase stability”). Transverse stability is achieved by using an electrode geometry that produces a minimum of the electric field on the molecular beam axis, thereby focusing the beam.

The rotational ground state of any molecule is lowered in energy by an external perturbation, and is therefore a “high-field” seeking state. It would be a major advantage if molecules in this state could be decelerated as well. In particular, this would make large polar molecules, for which all rotational states are practically high-field seeking due to the small rotational constants and the correspondingly high density of states, amenable for deceleration and trapping experiments. It might appear straightforward to apply the above described method to molecules in high-field seeking states by simply letting the molecules fly out off, instead of into, the region of a high electric field. For the motion of the molecules in the forward direction, this is indeed true. However, Maxwell’s equations do not allow for a maximum of the electric field in free space, e.g. on the molecular beam axis, and, therefore, transverse stability cannot be maintained easily; molecules in these states have the tendency to crash into the electrodes, where the electric field are the highest.

The same situation is encountered in charged particle accelerators where this problem has been resolved by applying the alternate gradient (AG) focusing method. This principle can be applied to polar molecules when using electrostatic dipole lenses. These lenses focus the molecular beam in one direction but simultaneously defocus the beam in the orthogonal direction. By alternating the orientation of these lenses, an electric field geometry with a focusing effect in both directions can be created. By switching these lenses on and off at the appropriate times, AG focusing and deceleration of a molecular beam can be achieved simultaneously [1].

First results with a prototype AG decelerator, with both metastable CO and on YbF, will be presented, and the application of this method to large organic- and bio-molecules, with a particular focus on the deceleration of a beam of benzonitrile molecules, will be discussed.

Reference

1. H.L. Bethlem, A.J.A. van Roij, R.T. Jongma, and G. Meijer, Phys. Rev. Lett. **88**, 13003 (2002).

Molecule optics using micro-structured arrays

S. Schulz, H. Conrad and G. Meijer

By utilizing the forces that polar molecules experience in inhomogeneous electric fields, a variety of molecule-optical elements have been experimentally demonstrated. Focusing of molecular beams by electrostatic hexapoles is well-known, and when time-varying electric fields are being used, as in the so-called Stark decelerator or in the AG decelerator, the laboratory velocity of molecules can be changed as well [1]. In the experiments performed thus far, the dimensions used for the various electrostatic elements are rather large, with electrodes typically being several mm apart, implying that voltages of tens of kVs need to be applied to reach sufficiently high electric fields.

In this project we will explore the possibilities of using miniaturized electric field geometries to manipulate the motion of neutral polar molecules. An electric dipole field generated by a periodic planar array of linear electrodes which have potentials with alternating sign, for instance, will act as a mirror for impinging slow polar molecules in a low-field seeking state. By reducing such a structure to a length scale of microns, the required voltages can be modest, on the order of some 100 V, while the effective electric field strengths still reach the order of 100 kV/cm. Such electric fields are sufficient to reflect, for instance, a slow beam of state-selected ammonia molecules, as readily produced by a Stark decelerator. The overall size of such a micro-mirror, which can be made to have a time-varying reflectivity when time-varying voltages are applied, will be reduced to a mm-scale. Forward extension of the design to higher complexity allows the production of “molecule gratings” with variable blaze, wave guides, as well as miniaturized molecule traps.

The design of the microstructure used as the first mirror device consists of an interdigitated array of equally spaced gold electrodes (periodicity 20 μm) deposited on a sapphire substrate. The total area of the active part of the micro-array is $2.5 \times 2 \text{ mm}^2$. An important question determining the applicability of the micro-devices concerns the maximum electric fields that can be achieved, which determines the maximum height of the electrostatic potential experienced by the molecules. In an initial test performed in a vacuum of about 5×10^{-10} mbar, we have attained a potential drop of about 400 V between adjacent electrodes, after a conditioning procedure of several hours. This corresponds to a usable electric field of 200 kV/cm, which should be sufficient to produce a complete reflection of a 25 m/s deuterated ammonia beam. This micro-array is mounted in a molecular beam machine containing a pulsed molecular beam source, a Stark decelerator and a hexapole focuser. The performance of the micro-mirror for neutral molecules will be characterized in this machine by time-resolved (2+1) Resonance Enhanced Multi Photon Ionization (REMPI) detection of the reflected ammonia molecules.

Reference

1. H.L. Bethlem and G. Meijer, *Int. Rev. Phys. Chem.* **22**, 73 (2003).

Motion control of molecules via non-resonant light forces

B. Friedrich and G. Meijer

The ability to slow, cool and trap atoms revolutionized atomic physics. We believe that molecular physics is bound to undergo a similarly dramatic transformation once adequate methods for controlling the motion of molecules are put in place. However, compared with atoms, getting a grip on molecules is much more challenging. This has mainly to do with the complex internal structure of molecules: the existence of vibrational levels precludes laser cooling and so alternative methods for cooling/slowing molecules have to be employed. Moreover, molecular anisotropy gives rise to a strong dependence of the interactions of molecules on their spatial alignment and orientation. Therefore, motion control of molecules must also include rotational degrees of freedom. In their fundamental interest, molecules even surpass atoms in important aspects; these comprise additional internal degrees of freedom, other than spherical symmetry, and both even and odd multipole moments coupled to a rotating molecular frame.

The pursuit of all aspects of motion control of molecules – slowing/cooling, and trapping and alignment/orientation – is at the core of this project. Our principal objective is to develop highly efficient methods for manipulating the velocity, position, and orientation of individual molecules at will, by applying tailored external fields. These will comprise nonresonant fields (electrostatic and radiative) as well as near-resonant radiative fields, interacting with both permanent and induced dipole moments of molecules. The fields or their combinations will be delivered either as pulses and pulse sequences or continuously, and optimal control algorithms will be implemented to enhance their desired effects.

A large part of our effort will be dedicated to various aspects of the polarizability interaction of molecules with laser fields. This is a versatile interaction, which arises for all molecules (whether polar or non-polar) and also for larger mesoscopic structures. Therefore, manipulation techniques based on the polarizability interaction are likely to become the methods of choice for most future developments in those sciences and technologies where motion control of molecules is of relevance [1].

The following themes will be pursued:

- (1) *Slowing and trapping of molecules via induced-dipole forces.* Supersonically cooled polar molecules will be slowed down in a Stark-decelerator and loaded into a nonresonant light trap. Further cooling of the trapped molecules by forced evaporation will be attempted.
- (2) *Exploration of new principles to manipulate molecules via combined nonresonant fields.* Combinations of nonresonant fields (electrostatic, magnetic, radiative) lead to new dramatic effects such as a nearly perfect orientation of the space-fixed dipole moment, which can be used to enhance the efficacy of all available motion-control techniques.
- (3) *Development of molecule optics.* In molecule optics, a matter wave of molecules is manipulated by a molecule-optical component made out of external, typically radiative, fields. In our effort, molecule-optical elements such as a lens, prism, and mirror will be implemented and their properties studied.

Reference

1. B. Friedrich and D. Herschbach, *J. Phys. Chem. A* **103**, 10280 (1999).

Molecular physics experiments using the free electron laser FELIX

G. von Helden, A. Fielicke, J. M. Bakker and G. Meijer

Over the last thirty years, lasers have revolutionized spectroscopy. The narrow bandwidth, high intensity and tunability of continuous or pulsed UV and visible lasers brought us a multitude of different schemes to interrogate gas-phase molecules. Often, the most direct information about the structure of molecular complexes and clusters is obtained via vibrational spectroscopy. A variety of techniques exist to obtain vibrational spectra of gas phase molecules, clusters and (cluster) ions. Frequently, however, these techniques are limited by the lack of availability of suitable infrared (IR) laser systems.

A highly powerful and versatile source of tunable IR radiation is the free electron laser FELIX, located at the FOM Institute for Plasmaphysics, Nieuwegein, The Netherlands. The combination of its various performance characteristics make this laser ideally suited to resonantly pump large amounts of vibrational energy into isolated gas-phase species. FELIX is continuously tunable from 2.5 to 250 microns. The light output comes in macropulses of 5 microsecond duration at a repetition rate of 10 Hz. Each macropulse contains so-called micropulses that are 300 fs to 5 ps long and spaced by 1 ns. The bandwidth is transform-limited. Macropulse energies can reach above 100 mJ.

This energy can then subsequently trigger reactions: it can lead to the emission of photons (fluorescence), to the release of fragments (dissociation) or to the ejection of electrons (ionization). In most experiments, many IR photons need to be pumped into molecules or ions to induce the desired process and the resulting ionization or fragmentation can then be monitored using mass spectrometric techniques [1]. In the experiments, the species of interest are investigated, isolated and unperturbed, by performing the measurements in the gas-phase. The species of interest cover a wide range. In one group of experiments, astrophysically relevant molecules and ions are investigated [2]. Another experiment has as its focus the structure of highly flexible biological molecules. Also, the structure, reactivities and catalytic properties of small clusters of metal or metal oxide material are investigated [3]. Recently we succeeded to measure the first IR-absorption spectra of small pure metal nano-particles as well as of molecules adsorbed on such nano-particles. By measuring the CO stretch frequency of $\text{Rh}_n\text{-CO}$ complexes in the gas-phase as a function of cluster-size and charge-state, unique information on the adsorbate binding as well as on the charge distribution in the cluster can be obtained. IR spectra of pure V_n^+ -clusters ($3 \leq n \leq 23$) showed distinct sharp resonances in the $150\text{-}450\text{ cm}^{-1}$ range. Interestingly, all clusters have very unique IR spectral features. Together with theory the spectra should allow a solid identification of the cluster structures.

The poster will give an overview of the various molecular physics experiments that we are currently involved in at the FELIX facility.

References

1. G. von Helden, D. van Heijnsbergen and G. Meijer, *J. Phys. Chem. A* **107**, 1671 (2003).
2. J. Oomens, A.G.G.M. Tielens, B.G. Sartakov, G. von Helden and G. Meijer, *Astr. J.* **591**, 968 (2003).
3. A. Fielicke, G. Meijer and G. von Helden, *J. Am. Chem. Soc.* **125**, 3659 (2003).

Mass-selective vibrational spectroscopy of gas-phase clusters

K. R. Asmis, M. Brümmer^a, C. Kaposta^a, G. Santambrogio^a, L. Wöste^a,
G. von Helden and G. Meijer

^aInstitut für Experimentalphysik, Freie Universität Berlin, Germany

In recent years much effort has been aimed at improving the sensitivity and selectivity of experimental methods to study the vibrational spectroscopy of gas phase ions. Due to the lack of widely tunable infrared (IR) light sources most of these studies have been limited to the region above 2400 cm⁻¹, *i.e.*, the spectral region of hydrogen-stretching motions and of IR-active combination bands. The application of the infrared free-electron laser FELIX, which generates tunable radiation in the 40 – 2200 cm⁻¹ region, to molecular spectroscopy has bridged this gap [1]. We have recently developed a novel technique to study the vibrational spectroscopy of mass-selected, cooled gas-phase ions [2]. Application of this technique to three selected compound classes is discussed and compared to the results of complimentary experiments on neutral mass-selected metal clusters using femtosecond negative-neutral-positive (NeNePo) spectroscopy [3].

(i) Vanadium oxide cluster cations and anions are investigated in order to aid in the interpretation of gas phase reactivity studies. Single-photon IR-spectra are measured by monitoring the dissociation yield of V_xO_y[±]He_n[±] complexes ($x, y \leq 10$, $n \leq 3$), which are formed at low ion trap temperatures, as a function of wavelength. Structural trends, and their influence on the cluster reactivity as a function of cluster size, oxidation state and charge state are discussed.

(ii) The protonated water dimer H⁺(H₂O)₂ is a prototypical system for the study of proton transfer in aqueous solution. Our experiment directly probes the shared proton region of the potential energy surface [4]. The assignments of the absorption bands based on high-level *ab initio* calculations remain controversial, highlighting the importance of intermode coupling in shared proton systems.

(iii) Halogen atom–halogen hydride cluster anions serve as transition state precursors for model proton transfer reactions. Using FELIX, we measured the first gas-phase IR spectra of Br-H-Br⁻, Br-D-Br⁻, Br-H-I and Br-D-I [5]. Additional experiments on size-selected Br⁻•(HBr)_n clusters probe the effect of solvation on the hydrogen-bonding [6]. Evidence for the localization of the H atom and destruction of the symmetric BrHBr⁻ hydrogen bond in the larger clusters is presented.

References

1. J.A. Piest, G. von Helden and G. Meijer, *J. Chem. Phys.* **110**, 2010 (1999).
2. K. R. Asmis, M. Brümmer, C. Kaposta, G. Santambrogio, G. von Helden, G. Meijer, K. Rademann and L. Wöste, *Phys. Chem. Chem. Phys.* **4**, 1101 (2002).
3. H. Hess, K.R. Asmis, T. Leisner and L. Wöste, *Eur. Phys. J. D* **16**, 145 (2001).
4. K.R. Asmis, N.L. Pivonka, G. Santambrogio, M. Brümmer, C. Kaposta, D.M. Neumark and L. Wöste, *Science* **299**, 1375 (2003).
5. N.L. Pivonka, C. Kaposta, M. Brümmer, G. von Helden, G. Meijer, L. Wöste, D.M. Neumark and K.R. Asmis, *J. Chem. Phys.* **118**, 5275 (2003).
6. N.L. Pivonka, C. Kaposta, G. von Helden, G. Meijer, L. Wöste, D.M. Neumark and K.R. Asmis, *J. Chem. Phys.* **117**, 6493 (2002).

Angular correlations in double Auger decay of Ne and Ar

J. Viefhaus, S. Cvejanovic, A. Grum-Grzhimailo, N. Kabachnik, S. Korica,
B. Langer, T. Lischke, G. Prümper, D. Rolles and U. Becker

Double Auger processes are important manifestations of strong electron correlations in processes governed by the Coulomb interaction. Although double Auger decay is discussed in the literature for a long time now, it was just recently when direct (i.e. coincident) energy and angle resolved measurements have become feasible [1].

On the experimental side the coincident investigation of the double Auger process involves the simultaneous detection of two electrons which can share the available kinetic energy in an – in principle - arbitrary way. Coincident time-of-flight electron spectroscopy is therefore a very suitable technique for double Auger analysis because electrons of all kinetic energies can be detected simultaneously. We have used monochromatic synchrotron radiation in order to photoionize the Ar 2p as well as Ne 1s inner shell with subsequent detection of the two double Auger electrons in coincidence. The results show that double Auger is indeed an important decay path for inner-shell hole states. For both Ne and Ar we see a very strong preference for asymmetric energy sharing for the two simultaneously emitted Auger electrons. This is in qualitative agreement with calculations of Amusia et al. [2].

In addition to the measurements of coincident energy distributions the method of electron-electron coincidence spectroscopy using multiple time-of-flight electron analyzers allowed us to obtain information on the angular correlations of the two double Auger electrons. In analogy with photo-double-ionization we have developed a parametrization of the angular distributions based on symmetrized dynamic amplitudes and explicitly given state-specific angular functions. In general two classes of angular patterns may be distinguished - those which have a node for the back-to-back emission of the two electrons, and those which have a maximum there. The type of the angular correlation is determined by the symmetry properties of the two-electron angular functions.

The first double-Auger angular distribution has been measured for Ar using circularly polarised light at an energy of $h\nu=270$ eV. It clearly shows the expected symmetry properties and is to a great extent similar to the He TDCS obtained for the same kinematical conditions.

References

1. J. Viefhaus, AIP Conference Proceedings **652**, 307 (2003).
2. M. Ya. Amusia, I. S. Lee and V. A. Kilin, Phys. Rev. A **45**, 4576 (1992).

Doppler splitting and intra-molecular scattering of Auger electrons in dissociating molecules

G. Prümper, R. Hentges, O. Kugeler, S. Marburger, D. Rolles, F. Burmeister, J. Viehhaus, S. Cvejanovic, U. Hergenhahn and U. Becker

Recently, Björneholm et al. [1] discovered that in the K-shell excitation of a free O₂ molecule a large number of molecules dissociate into two oxygen atoms before the core excited state does relax. Only after the two oxygen atoms have separated, one of them emits an Auger electron. Therefore, those electrons which have been emitted into the direction of the fragment ion, or antiparallel to it, show a clear separation in energy, the so called 'Doppler' splitting.

Yet, the experiment did not resolve whether the shifted Auger electron really travels along with the corresponding fragment ion. In order to reveal this emission behavior, photoelectron-fragment ion coincidence experiments are required. We have performed such an experiment at the U49/2 beamline at BESSY using a coincidence set-up consisting of a SCIENTA SES 200 electron analyzer with delay line anode and a pulsed **ion** time-of-flight spectrometer with a crossed wire position-sensitive anode placed directly opposite [2]. This novel arrangement makes high-resolution photoelectron-fragment ion coincidence experiments feasible for the first time. Thus, we were able to distinguish between electrons emitted in different directions with respect to the molecular axis of the core-excited molecule. A similar experiment on SF₆ has been performed at the BW 3 beamline of HASYLAB, using an electron time-of-flight spectrometer instead of the SCIENTA analyzer.

Both experiments yield coincidence maps between the Auger electrons and the corresponding fragment ions. The observed features in the maps show that the Doppler shift of the electron is indeed a direct result of the fragment ion momenta. Simply thinking, one could expect that the coincidences would exhibit blue-shifted electrons going along with the fragment ion and red-shifted electrons going into the opposite direction. These processes correspond to the undisturbed emission of the electron. We have discovered cross contributions, which do not belong to the directly emitted electrons but involve scattering processes, where the electron originally emitted opposite the ion is finally detected along with the ion. As a consequence, the contribution of this parallel emission channel to the electron spectrum is always larger than the contribution of the antiparallel emission channel. Interestingly, this asymmetry occurs even in the case of measurements which do not resolve the Doppler components. In our experiment this effect becomes particularly distinct for selections of the extreme ion momenta.

References

1. O. Björneholm et al., Phys. Rev. Lett. **84**, 2826 (2000).
2. G. Prümper, O. Kugeler, U. Hergenhahn, S. Marburger, D. Rolles, F. Burmeister, J. Viehhaus, R. Hentges, S. Cvejanovic and U. Becker, BESSY Highlights 2002, 22 (2003).

Enhancement of double Auger decay following plasmon excitation in C₆₀

A. Reinköster, S. Korica, B. Langer, S. Cvejanovic, J. Viefhaus and U. Becker

The valence photoionization of C₆₀ has attracted considerable interest over the last years, in particular concerning the unusual oscillatory behavior of its different partial yields [1]. In contrast, K-shell ionization has been much less considered, both experimentally and theoretically. The K-shell photoelectron spectrum of C₆₀ consists of the C(1s) mainline a variety of satellite lines and higher lying plasmon excitations. Shake-off also contributes, but the strength of this shake-off rate was so far unknown. However, complete photoelectron spectra exhibit a large fraction of continuously distributed photoelectron intensity which could either result from shake-off photoelectron emission or double Auger decay [2].

A new series of measurements of such spectra has been performed with particular emphasis on the fingerprints of all ionization, excitation and double ionization processes. This was made possible by electron time-of-flight analysis covering the whole range of kinetic energies down to zero kinetic energy.

A careful analysis of the series of spectra yielded two surprising and unexpected results:

(i) With increasing energy the plasmon intensity reaches its sudden limit faster than expected, which points to localized excitation processes rather than a delocalized relaxation in response to core-hole creation. The sudden limit intensity is as large as 30 % of the total K-shell ionization events;

(ii) performing a spectral analysis which takes all primary and secondary ionization events into account yields a double Auger rate as high as 60 % of the total Auger yield. Assuming that the main line and the related shake-off emission result predominantly in single Auger decay, K-shell photoionization associated with satellite and plasmon excitations remains as the only plausible source for such a high double Auger rate. In fact, the measured rate would mean that most of these primary ionization processes result in double Auger relaxation. The reason for this highly unusual behaviour may be the fact that satellite and plasmon excitations both populate LUMO states which are strongly delocalized and may be energetically located in the continuum of the doubly charged C₆₀²⁺ ion produced by the K-shell ionization and its subsequent core-hole refilling process. The excited electron cannot survive in this unstable situation and will consequently leave the C₆₀ ion along with the Auger electron in form of an Auger shake-off transition. These handwaving qualitative arguments, however, have to be validated by ab initio calculations.

References

1. A. Rüdell, R. Hentges, U. Becker, H. S. Chakraborty, M. E. Madjet and J. M. Rost, Phys. Rev. Lett. **12**, 125503 (2002).
2. T. Liebsch, O. Plotzke, F. Heiser, U. Hergenhahn, O. Hemmers, R. Wehlitz, J. Viefhaus, B. Langer, S.B. Whitfield and U. Becker, Phys. Rev. A **52**, 457 (1995).

Selectivity in vibrationally mediated single-molecule chemistry

J.I. Pascual^a, N. Lorente^b, Z. Song^c, H.-P. Rust and H. Conrad

^apresently: Inst. de Ciencia de Materials de Barcelona; ^bLaboratoire Collisions, Université Paul Sabatier, Toulouse, France, ^cDept. of Chemistry, Brookhaven National Laboratory, Upton, USA

Excitation of specific molecular vibration modes has been shown to strongly influence the velocity and the pathway of chemical reactions. By preparing the educt species in well-defined vibrational states one is able to enhance the reaction efficiency and to modify the distribution of the product species. Such mode-selective chemistry has been widely applied by laser excitation of vibrational modes. Lately, inelastic tunneling spectroscopy has been successfully used to excite vibrations in adsorbed molecules. In addition to the direct detection as peaks in the second derivative of the bias voltage versus tunneling current curve, cleavage of individual bonds and induced molecular motion has been observed.

In the study presented here we have investigated the NH₃ molecule adsorbed on a Cu(100) surface with our low temperature STM operating at 5 K. NH₃ adsorbs on top of a Cu atom with the threefold axis perpendicular to the surface, with a chemisorption bond strength sufficiently stable to be imaged. However, with the tip positioned directly above an individual molecule, an increase of the bias voltage above a certain level induces a cleavage of the Cu-NH₃ bond. A subsequent analysis of the related area revealed two possible events, either a translation or a desorption of the target molecule. A statistical analysis of the threshold for a larger number of events revealed a characteristic energy distribution for the onset of the processes. For low tunneling current (<0.5 nA), the threshold energy corresponds to the eigenenergy of the N-H stretch mode leading to a translation. When using deuterated ammonia, the threshold value shifted down in correspondence to the well-known isotopic shift. For higher tunneling currents (>1 nA) an additional threshold appeared with an energy corresponding to the excitation of the umbrella mode of NH₃, which lead to the desorption event.

By analyzing the reaction yield (probability of reaction per tunneling electron) as a function of tunneling current, it is possible to determine the number of excitations necessary to induce the various processes. We have identified three operative mechanisms:

A single excitation of the N-H stretch mode can only lead to a translation since the binding energy of ammonia is higher than the vibrational quantum, while the diffusion barrier is low enough. At higher current, a double excitation of the N-H stretch leads predominantly to desorption. Excitation of the umbrella mode induces desorption in a three step ladder climbing process. Intermode coupling redistributes the N-H- stretch energy to the umbrella mode excitation, which results either in translation or, if the energy is high enough, in desorption via the NH₃ inversion.

Precursor and initial stages of oxide formation on ruthenium

R. Blume^a, H. Niehus^a, L. Gregoratti^b, A. Barinov^b, L. Aballe^b, M. Kiskinova^b,
A. Böttcher^c, A. Lobo, S. Amarie and H. Conrad

^aInstitut für Physik, Humboldt-Univ. Berlin; ^bSincrotrone Trieste; ^cInst. für Phys. Chemie, Univ. Karlsruhe

The formation of RuO₂ islands grown on Ru(0001) under well-defined O₂ or NO₂ pressures and elevated temperatures has recently been extensively investigated. Even the subsequent evolution of almost closed oxide layers have been studied with the aim of understanding the established high catalytic reactivity of Ru in oxidation reactions. Nearly all available surface science techniques have been applied to explore growth modes, structure, in particular the geometry of the topmost atoms, and reactivity with regard to selected reactions.

However, the very initial stages of oxygen incorporation into the Ru substrate are still under discussion as to the existence of well-defined phases of subsurface oxygen different from oxide or to the coexistence of the saturated chemisorption oxygen layer with microscopic islands of oxide. Using TDS, UV photoelectron spectroscopy, work function measurements and reactive scattering, we have identified two evolution stages prior to formation of RuO₂ islands for low temperature (350 to 600 K) and high oxygen pressure (10⁻³ to 1000 mbar) exposures. Both oxygen phases are structurally and electronically not oxidic but show a clearly increased reactivity. The first oxygen species (O_□) adds ~0.5 MLE (monolayer equivalent) to the saturation coverage and is probably positioned at subsurface sites directly under the top Ru layer. The second form (O_□) is connected with defects at the surface, i.e. the higher the defect density (intentionally created by mild argon ion sputtering) the faster is the O_□ accumulation amounting eventually to about 1.5 to 2 MLE. Both species are created by thermally activated processes. Only in a third evolution step, nuclei of RuO₂ cluster island develop as reflected by the appearance of a narrow peak in the thermal desorption spectra developing after further exposure to the fingerprint feature of a substantially oxidized surface.

Laterally resolved XPS measurements, using the ESCAMICROSCOPY beamline at ELETTRA, revealed a preferred accumulation of an oxygen species at surface defects. Both the Ru 3d and the O 1s core level spectra of this species exhibit components, which differ significantly from chemisorbed and oxidic oxygen. Moreover, during exposure a considerable restructuring of the surface morphology has been revealed. In particular, existing surface irregularities like holes or step boundaries have been changed in shape and partially filled up. On the other hand, the islands clearly identified as RuO₂ are found to grow virtually uncorrelated with defect positions. Also, the regions in between, previously assigned to essentially undisturbed monolayer coverage do not show the characteristic Ru 3d component.

“Lower-than-2”-dimensional systems: geometric and electronic structure

M. Hansmann, J.I. Pascual, J. Schaefer, E. Rotenberg and K.Horn

Surface- and interface-related experimental investigations make an increasingly important contribution to fundamental problems in general solid state physics, and the electronic structure of novel systems continues to attract interest also from outside the surface community. Low dimensional systems offer a wealth of interesting physics [1,2] and are also of interest for future applications in microelectronics. Among the systems studied, the Ba/Si(111) system shows a (3 x 1) superstructure in LEED; based on electron counting arguments a metallic surface is predicted, whereas photoemission shows a semiconducting surface. In a combined photoemission and STM study we showed that linear chains of Ba have a local (3 x 2) structure, which explains the semiconducting nature of the surface [3]. These chains exhibit random shifts in their registry normal to the chains, giving rise to a (3 x 1) LEED pattern. This finding explains the long-standing apparent discrepancy between geometric and electronic structure, since the electron counting rule is hardly ever violated. The electronic structure of vicinal Cu surfaces, with (554) and (332) orientation, was studied by means of STM at low temperatures (4.2 K). We find that the surface state is shifted to lower binding energies by the step superlattice, and a strong peak in the density of states appears, the energy of which depends on terrace width [4]. A simple quantum well model shows that the peak appears whenever electrons comply with the resonance conditions of confinement on the terrace. The results indicate a terrace-width dependent transition from predominantly one-dimensional behaviour of the Cu surface state, to a 2D extended state for larger terrace widths.

References

1. R. Losio, K.N. Altmann and F.J. Himpsel, Phys. Rev. Lett. **85**, 808(2000); R. Losio, K.N. Altmann, A. Kirakosian, J.-L-Lin, D.Y. Petrovykh and F.J. Himpsel, Phys. Rev. Lett. **86**, 4632 (2001).
2. P. Gambardella, A. Dallmeyer, K. Maiti, M.C. Malagoli, W. Eberhardt, K. Kern and C. Carbone, Nature **416**, 301(2002).
3. J. Schaefer, S.C. Erwin, M. Hansmann, Z. Song, E. Rotenberg, S.D.Kevan, C. S. Hellberg and K. Horn, Phys. Rev. B **67**, 085411(2003).
4. M. Hansmann, J. I. Pascual, G. Ceballos, H.-P. Rust, K. Horn, Phys. Rev. B **67** , 121409 (2003).

Metallic quantum wells: electronic structure and “electronic growth”

J.W.Kim, H.Dil, S. Gokhale, M.Tallarida, L. Aballe and K.Horn

Quantum well states in thin metal films provide a rich testing ground for solid state physics in low dimensions. This field has developed rapidly within the last few years, and many metallic quantum well systems have been established, ranging from unreactive combinations of group Ib transition metals to combinations of magnetic and non-magnetic metals and reactive metal-semiconductor systems [1,2]. Our studies on Mg films showed the importance of field confinement in the metal overlayer in the region of the bulk and multipole plasmons, and this work has been extended to several artificial alloys of the Al-Mg system, to examine the influence of a change in electron density (or r_s) on the optical response [3]. By visualizing the quantum well state dispersion, we found an interaction between the electronic states in the substrate and those of the overlayer which leads to a strong deviation from the simple free-electron behaviour of $E(k_{||x}, k_{||y})$ [4]; this influence was later also found by other groups. An interesting interplay between electronic structure and growth morphology, leading to energetically preferred “magic” or “critical” thicknesses has been predicted [5], and examples for these have been found experimentally [6]. This interplay between electronic structure and morphology was also seen in our study of Pb/Cu(111): from the binding energies of quantum well states as a function of thickness we found that certain thicknesses are preferred even during low temperature growth, and the height distribution exhibits further changes when brought into thermal equilibrium by annealing. This effect is related to total energy minimisation, since the stable layers exhibit quantum well states that are further removed in energy from the Fermi level than the less stable ones.

References

1. T.-C. Chiang, Surf. Sci. Rep. **39**, 181(2000).
2. J.E.Ortega and F.J. Himpsel, Phys. Rev. Lett. **69**, 844 (1992).
3. L. Aballe, C. Rogero, K. Horn, Surf. Sci. **518**, 141 (2002); M.Tallarida et al., in preparation.
4. L. Aballe, C. Rogero, P. Kratzer, S. Gokhale and K. Horn, Phys. Rev. Lett. **87**, 156801(2001).
5. Z. Zhang, Q. Niu and C.K. Shih, Phys. Rev. Lett. **80**, 5381(1998).
6. M.Hupalo, S. Kremmer, V. Yeh, L. Berbil-Bautista, C.Z. Wang, K.M. Ho and M.C. Tringides Phys. Rev. Lett. **85**, 5158(2000); D.-A. Luh, T. Miller, J. J. Paggel, M. Y. Chou and T.-C. Chiang. Science **292**, 1131 (2001).

Bond length and bond strength in weak and strong chemisorption: N₂, CO and CO/H on a nickel surface

D.I. Sayago, J.T.Hoeft, M. Polcik, M. Kittel, R.L. Toomes^a, J. Robinson^a,
D.P. Woodruff^a, M. Pascal^b, G. Nisbet^b and C.L.A. Lamont^b
^aUniversity of Warwick ^bUniversity of Huddersfield

The general understanding of interatomic bond lengths in molecular systems has been well established for many years, and some of the general concepts of bond order have been shown to be quite effective to describe atomic chemisorption at metal surfaces. Far less attention has been paid to understanding the trends in bond lengths associated with molecular chemisorption at metal surfaces, such as the relationship between bond strength and bond length. Weak bonds are assumed to be longer than strong ones, yet there is a dearth of data to allow quantitative evaluation of this idea. Here we show, using both chemical-state specific scanned-energy-mode photoelectron diffraction (CS-PhD) experiments and density functional theory (DFT) [1] calculations, that the N-Ni distance in the c(2x2) Ni(100)/N₂ weak chemisorption system (1.81 Å) is not anomalously long as had been concluded earlier. Moreover, by comparing experimentally determined Ni-C bond lengths for CO adsorbed on Ni(100) with and without coadsorbed hydrogen, we show that CO weakly chemisorbed in the c(2x2)-CO/H phase in an atop site has a Ni-C bond length only marginally (0.06 Å) longer than when it occupies the same atop site in the strongly chemisorbed c(2x2)-CO phase despite a change in the chemisorption bond strength by a factor of 2 and more. By contrast, we show that changing the CO bonding coordination from onefold to twofold (halving the bond order) in strongly chemisorbed CO and CO/H bridging phases has a far larger effect (0.16 Å).

Our experimental determination of the local geometry of CO chemisorbed on Ni(100) in atop and bridge sites, with and without coadsorbed hydrogen, shows that while changes in chemisorption bond order lead to changes in the associated bond lengths closely consistent with simple Pauling rules, large changes in the chemisorption energy have a far more modest influence on the bond length. Similar data for the weakly chemisorbed isoelectronic N₂ species on Ni(100) reinforce the view that weak chemisorption does not lead to substantial increase in bond length, contrary to prior suggestions.

Reference

1. D.I. Sayago, J.T.Hoeft, M. Polcik, M. Kittel, R.L. Toomes, J. Robinson, D.P. Woodruff, M. Pascal, G. Nisbet and C.L.A. Lamont, *Phys. Rev. Lett.* **90**, 116104 (2003).

Department of Physical Chemistry

Poster List

- PC 1 Scanning tunneling microscopy of RuO₂(110)/Ru(0001) in UHV and at high pressures**
M. Rößler, S.H. Kim, J. Wintterlin, and G. Ertl
- PC 2 Microscale electrochemistry**
M. Binetti, M. Giacomini, M. Kock, R. Schuster, and D. Thron
- PC 3 Taming Winfree turbulence of scroll waves in excitable media**
S. Alonso, R. Kähler, F. Sagues, and A.S. Mikhailov
- PC 4 Storage of pulses and twisted spirals in oscillatory media under periodic forcing**
O. Rudzick and A.S. Mikhailov
- PC 5 Controlling spatiotemporal pattern formation in catalytic CO oxidation on Pt(110)**
C. Beta, M. Bertram, Md G. Moula, A.S. Mikhailov, H.H. Rotermund, and G. Ertl
- PC 6 From the gentle dragging of reaction waves to reaction enhancement in the CO oxidation on Pt(110)**
J. Wolff, A.G. Papathanasiou, I.G. Kevrekidis, H.H. Rotermund, and G. Ertl
- PC 7 Heartbeats of ultrathin catalysts:
Oscillatory thermomechanical instability of an ultrathin catalyst**
J. Wolff, C. Punckt, I.G. Kevrekidis, H.H. Rotermund, and G. Ertl
- PC 8 Raman spectroscopy and second harmonic generation at surfaces**
B. Pettinger, G. Picardi, B. Ren, M. Danckwerts, S.L. Horswell, and A. Kudelski
- PC 9 Effect of insulated areas on pattern formation in an electrochemical reaction**
T.G. Noh, J. Christoph, and M. Eiswirth

- PC 10 Pattern formation under desynchronizing global coupling in electrochemical systems**
F. Plenge, H. Varela, and K. Krischer
- PC 11 Chemiluminescence accompanying aggregation of Ag clusters in an Ar matrix**
W. Schulze, I. Rabin, and G. Ertl
- PC 12 InAs quantum dot formation on GaAs surfaces**
Y. Temko, T. Suzuki, M.C. Xu, and K. Jacobi
- PC 13 Surface Coordination Chemistry: Dihydrogen versus hydride complexes on RuO₂(110)**
J. Wang, C.Y. Fan, Q. Sun, K. Reuter, K. Jacobi, M. Scheffler, and G. Ertl
- PC 14 Reactions of NO and C₂H₄ on the RuO₂(110) surface**
Y. Wang, U.A. Paulus, J.F. Xu, P. Geng, K. Jacobi and G. Ertl
- PC 15 Laser temperature jump experiments with nanometer space resolution using Rhodamine 101 Anti-Stokes fluorescence from nanoseconds to milliseconds for precise measurements of temperature changes in liquid micro-environments**
S. Couderc-Azouani, J.F. Holzwarth, A. Beeby, I.P. Clark, and T. Parker
- PC 16 Carbon nanotubes: Electronic structure, charge-carrier dynamics and adsorbate kinetics of novel materials**
A. Hagen, G. Moos, H. Ulbricht, R. Zacharia, and T. Hertel
- PC 17 Ultrafast dynamics of photoinduced surface reactions and vibrational spectroscopy of adsorbates**
D.N. Denzler, S. Wagner, R. Dudek, C. Frischkorn, M. Wolf, and G. Ertl

Scanning Tunneling Microscopy of RuO₂(110)/Ru(0001) in UHV and at High Pressures

M. Röbber, S.H. Kim, J. Winterlin and G. Ertl

The catalytic oxidation of CO on Ru surfaces has become a model system for the pressure gap in heterogeneous catalysis. It has been shown that the poor activity of Ru under vacuum conditions and the very good activity at pressures of "real catalysis" can be explained by a thin film of RuO₂ that forms at high oxygen pressures and that is much more active than the metallic Ru surface. We report about STM experiments with RuO₂(110) films grown on Ru(0001) under UHV conditions and at high pressures. Titration experiments under vacuum conditions resolve the microscopic processes during reaction of CO with oxygen. The reaction of CO molecules with O atoms proceeds by reaction of CO molecules, bonded to one-fold coordinatively unsaturated sites, with neighboring bridge-bonded O atoms, and filling of bridge vacancies with CO molecules. Experiments with simultaneous CO and O₂ adsorption show that the same processes occur under steady-state reactions, too. The observations confirm conclusions from previous investigations by macroscopic techniques and simulations. In contrast to reactions on metallic surfaces, where islands play an important role, the reaction occurs statistically, a result of the special bonding character of the oxide surface. Experiments were also performed at high pressures, in which a newly developed high-pressure STM was applied for the first time. The setup consists of a small high-pressure reactor cell that houses the STM, and a conventional UHV chamber in which the samples are prepared and analyzed after STM experiments. The system achieves atomic resolution at pressures of reactive gases of up to 1 bar. Experiments on the RuO₂(110)/Ru(0001) system at oxygen pressures of 0.5 bar surprisingly show a different surface termination than predicted for the high coverage oxygen phase. The data indicate the presence of a carbonate species that accumulates on the surface. These findings may explain the reported decline in catalytic activity of ruthenium from an initial high value.

Microscale Electrochemistry

M. Binetti, M. T. Giacomini, M. Kock, R. Schuster and D. Thron

We use ultrafast electrochemistry, where the electrochemical double layer is polarized within a few nanoseconds, for (I) the study of structure formation upon very fast ordering processes and (II) the local micromachining of surfaces.

In conventional electrochemistry the time constants for the charging of the capacitance constituted by the double layer are in the range of ms, due to the relatively large distance between the electrodes and the resulting high electrolyte resistance. However, placing the electrodes at μm distances leads to polarization of the double layers within a few ns. Thus, employing the tip of the electrochemical STM as local counter electrode allows for very fast changes of the thermodynamic state of the system.

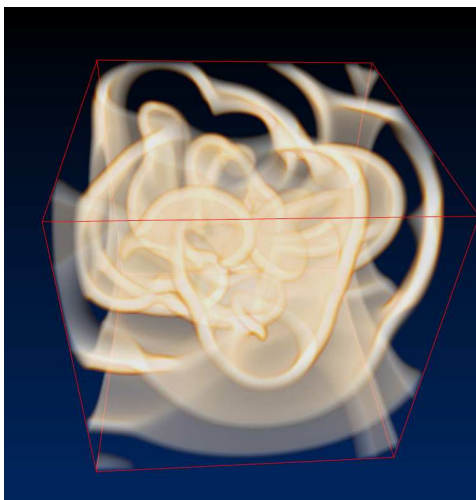
For example, upon application of a single microsecond voltage pulse to the STM tip, about half a monolayer of Au atoms from the topmost surface layer of a Au(111) surface was dissolved. The subsequent ordering process, i.e., the changes of the surface morphology were observed in-situ: The remaining Au adatoms ordered into a labyrinthine island pattern, which is indicative of the spinodal decay of an unstable adatom gas, contrary to nucleation and growth processes, usually occurring under slow changes of the state of the system.

In addition to these ordering processes, where the mesoscopic structure of the system is determined by the kinetics of the electrochemically induced phase transitions, the fast change of the electrochemical potential also allows the direct three dimensional microstructuring of surfaces. The time constant for double layer charging varies linearly with the electrolyte resistance, i.e., with the electrode distance. Upon application of ultrashort pulses of only nanosecond duration, effective charging is limited to electrode regions with distances below a few micrometers. Therefore, subsequent electrochemical reactions are confined to electrode regions in such a close proximity. This can be used for the direct three dimensional micromachining of electrode surfaces, which is demonstrated for machining of metals like Cu, Ni and stainless steel, semiconductors like p+ Si as well as for local electropolymerization of polypyrrol.

Taming Winfree Turbulence of Scroll Waves in Excitable Media

S. Alonso^a, R. Kähler^b, F. Sagues^a and A.S. Mikhailov

Scroll waves have been first observed in the chemical Belousov-Zhabotinsky reaction and are also possible in other excitable media, such as the cardiac tissue. In its transverse cross section, a scroll wave looks like a spiral. Such spirals are stacked one upon another to form a scroll-shaped pattern. The scroll rotates around a central filament characterized by zero excitation amplitude. This filament can be straight or curved; it may also form loops and close into rings. About 10 years ago, A.T. Winfree has suggested that spatiotemporal chaos (turbulence) in three-dimensional excitable media may emerge through the disordered dynamics of wave filaments. The Winfree turbulence is currently considered as one of the principal mechanisms of cardiac fibrillation.



A chaotic three-dimensional wave pattern develops through the negative-tension instability of filaments, which tend to spontaneously stretch, bend, loop, and produce an expanding tangle that fills up the volume. The figure shows an example of the complex wave pattern at an early stage of the turbulence development.

We have demonstrated [1] that such a form of wave turbulence can readily be controlled by weak nonresonant modulation of the medium excitability. Depending on the forcing frequency, either suppression or induction of turbulence can be achieved. These effects have been explained in the framework of the kinematic theory of excitation waves.

(a) Department of Physical Chemistry, University of Barcelona, Spain

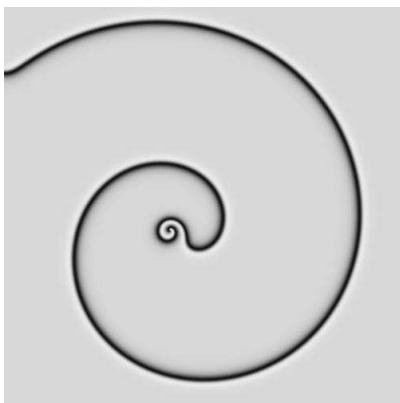
(b) Konrad-Zuse-Zentrum für Informationstechnologie, Berlin

[1] S. Alonso, F. Sagues, and A.S. Mikhailov, *Science* **229**, 1722 (2003).

Storage of Pulses and Twisted Spirals in Oscillatory Media under Periodic Forcing

O. Rudzick and A.S. Mikhailov

The purpose of chemical microengineering is to gain effective means for steering and manipulation of nonequilibrium reaction patterns on microscales. In catalytic CO oxidation on Pt surfaces, suppression of spatiotemporal chaos (chemical turbulence) by global delayed feedback and by external forcing has previously been investigated. Here, properties of regular wave patterns induced by external periodic forcing are studied. Using as a model the periodically forced Ginzburg-Landau equation, we focus attention on the behaviour of kink structures formed by 2π phase flips. Since the phases, differing by 2π , are physically identical, the kinks represent localized travelling pulses. Numerical investigations reveal that the propagation velocity of a kink train depends on its spatial period and its direction of motion can change as the period is decreased. This effect has two significant implications. We demonstrate that, by creating an appropriate heterogeneity in an oscillatory medium, part of it may serve as a kink trap. A well-defined number of pulses are stored in such a trap as a stationary pattern. When the parameters of the medium are changed, the pulses run away from the trap. The storage of pulses has been observed by us both in one- and two-dimensional geometries.



Another novel phenomenon, already possible in uniform two-dimensional oscillatory media with periodic forcing, is the formation of rotating twisted spiral waves. The center of the twisted structure (see the figure) is occupied by a small spiral wound in the direction which is opposite to that in the outside region. The twist (i.e. the switch of the direction rotation) is caused by a change in the sign of the propagation velocity of the kinks. The pattern is persistent, with some meandering taking place in the central region.

Controlling Spatiotemporal Pattern Formation in Catalytic CO Oxidation on Pt(110)

C. Beta, M. Bertram, Md G. Moula, A.S. Mikhailov, H.H. Rotermund and G. Ertl

The spatiotemporal behavior of high-dimensional distributed nonlinear systems has attracted much attention over the past decade. In particular, extensive work was devoted to spatiotemporal pattern formation in the large class of reaction-diffusion systems. More recently, the control of pattern forming processes and selective generation and stabilization of patterns came into the focus of research activities. While most of these studies are purely theoretical, the catalytic oxidation of CO on Pt(110) single crystal surfaces is one of the few systems where detailed experimental observations of these phenomena are possible.

We present experimental and theoretical results from our work on control of spatiotemporal pattern formation in the catalytic CO oxidation on Pt(110). In particular, we study the dynamics of our system under both global feedback schemes of different complexity and global periodic forcing.

Global delayed feedback as well as periodic forcing is applied in a parameter regime, where dynamics of the unperturbed system are oscillatory and, furthermore, uniform oscillations are unstable and a complex, irregular state of chemical turbulence develops. Both control approaches allow suppression of chemical turbulence and induce uniform oscillations in the system if applied with sufficient intensity. Moreover, different spatiotemporal patterns can be stabilized at intermediate control intensities close to the transition from turbulence to homogeneous oscillation. We observe intermittent turbulence, cellular structures and cluster patterns for both control schemes (1-3,5) and, in addition, standing waves with global delayed feedback (1-3) and irregular oscillatory stripes via periodic forcing (5). Besides aspects of pattern formation, we also study the stability of uniform oscillatory states induced by global delayed feedback with particular emphasis on the question of invasiveness of the feedback (4).

While the global delayed feedback in our earlier work was generated from an averaged property of the system, we recently extended our studies by investigating the effect of a length scale dependent feedback. The patterns evolving in the system are transformed in real time to a frequency domain representation, using fast Fourier transform (FFT). A feedback signal is then generated from the modulus of the Fourier coefficient corresponding to a chosen wave vector and applied to the system by modulating a global control parameter (the CO partial pressure in the reaction chamber). From our first results using this new type of feedback we have strong evidence that the developing patterns show systematic changes in their length scales depending on the choice of the wave vector in the control scheme.

- (1) M. Kim, M. Bertram, M. Pollmann, A. v. Oertzen, A.S. Mikhailov, H.H. Rotermund, and G. Ertl, *Science* **292**, 1357 (2001).
- (2) M. Bertram, C. Beta, M. Pollmann, A. S. Mikhailov, H.H. Rotermund, and G. Ertl, *Phys. Rev. E* **67**, 036208 (2003).
- (3) M. Bertram, A.S. Mikhailov, *Phys. Rev. E* **67**, 036207 (2003).
- (4) C. Beta, M. Bertram, A.S. Mikhailov, H.H. Rotermund, and G. Ertl, *Phys. Rev. E* **67**, 046224 (2003).
- (5) M. Bertram, C. Beta, H.H. Rotermund, and G. Ertl, *J. Phys. Chem. B* **107** (Sep. 03).

From the Gentle Dragging of Reaction Waves to Reaction Enhancement in the CO Oxidation on Pt(110)

J. Wolff, A.G. Papathanasiou, I.G. Kevrekidis¹, H.H. Rotermund and G. Ertl

In this poster we present results pertaining to the interaction of a pattern forming reaction with a temperature heterogeneity. This heterogeneity is generated by focusing a laser beam on a metal single crystal catalyst and manipulating its position through computer-controlled mirrors, thus enabling us to “write” spatiotemporal temperature heterogeneity patterns (1). Our two-dimensional model system is the low-pressure catalytic oxidation of CO on Pt(110), a reaction exhibiting well-understood spatiotemporal patterns. Depending on the state of the pattern forming reaction – showing pulses or not – and on the intensity (in degree K) of the heterogeneity different types of phenomena can be observed:

In the simplest case the laser spot causes the ignition of a reaction wave by a single critical “kick” at a selected surface location. The cooperativeness between two local *subcritical* perturbations separated in time and/or space is explored (2).

If some strong enough temperature heterogeneity, capable of igniting an oxygen pulse by itself, is moved along a line it may ignite waves along its path. The limiting velocities with which the laser spot can be moved across the sample and still cause the local ignition of waves are explored. They depend on the laser power and on the direction of the path (3).

For the case of the corresponding stationary temperature heterogeneity being not capable of igniting an oxygen pulse by itself, the effects of the moving laser spot on an existing reaction wave are investigated (4). In particular, we “dragged” spontaneously isothermally forming reactive pulses and fronts with speeds differing from their naturally selected ones. We examined the shapes acquired by these dragged waves and their limits of stability (that is, the range of dragging speeds for which they can exist). Through computer-aided bifurcation analysis we examined the nature of the “detachment” instability, marking the loss of the ability to drag a pulse in 1- or 2D.

1. J. Wolff, A.G. Papathanasiou, I.G. Kevrekidis, H.H. Rotermund, G. Ertl, *Science* **294**, 134-137 (2001).
2. J. Wolff, A.G. Papathanasiou, H.H. Rotermund, G. Ertl, M. Katsoulakis, X. Li, I.G. Kevrekidis, *Phys. Rev. Lett.* **90**, 148301-4 (2003).
3. J. Wolff, A.G. Papathanasiou, H.H. Rotermund, G. Ertl, X. Li, I.G. Kevrekidis, *J. Catalysis* **216**, 246–256 (2003).
4. J. Wolff, A.G. Papathanasiou, H.H. Rotermund, G. Ertl, X. Li, I.G. Kevrekidis, *Phys. Rev. Lett.* **90**, 018302 1-4 (2003).

Heartbeats of ultra thin catalysts: Oscillatory Thermomechanical Instability of an Ultrathin Catalyst

J. Wolff, C. Punckt, I.G. Kevrekidis¹, H.H. Rotermund and G. Ertl

Mechanical deformation as a result of a driving force lies at the heart of our ability to sense many different phenomena: the force on a current-carrying wire by a magnetic field and the resulting deformation underpins most traditional electric measuring instruments. In contemporary technology, the transducer may be a piezocrystal, a gel-coated microcantilever, or a polyelectrolyte gel artificial muscle. Definitive measurement requires a one-to-one relation between driving force and resulting deformation; but sometimes, the interaction exhibits an instability, and spontaneous oscillations can arise.

We have found such mechanical oscillations during the CO-oxidation on ultra-thin (~200 nm) self-supported metal single crystals, where, due to the released reaction heat, the surface responded with oscillatory extended mechanical buckling. We showed that, without any chemical reaction, already small intensities of a laser (50 mW) reflected from the middle of an ultra-thin crystal gave rise to a bent of its surface, while intensities above 300 mW resulted in quite coarse buckling, fairly similar to the observed one during the CO-oxidation.

In an extended modeling effort including groups from Princeton and Rutgers Universities and from Caltech we have been able to explore each player in this puzzle leading to the observed oscillations: the chemical kinetics, the thermochemistry and heat transport, as well as large deformation (nonlinear) elastodynamics (1). We also demonstrated how titration of a monolayer of either reactant might result in a mechanical response (like ripples) of the surface. Utilizing an interferometer for determining the bending of the surface, we could detect microscopic deformations of the catalytic foils. The present findings may lead to ultra-sensitive but affordable measurement devices for reaction rates.

¹ Dept. of Chemical Engineering, Princeton University, USA

(1) F. Cirak, J.E. Cisternas, A.M. Cuitiño, G. Ertl, P. Holmes, I.G. Kevrekidis, M. Ortiz, H.H. Rotermund, M. Schunack, J. Wolff, *Science* **300**, 1932 (2003).

Raman spectroscopy and Second Harmonic generation at surfaces

B. Pettinger, G. Picardi, B. Ren, M. Danckwerts, S.L. Horswell and A. Kudelski

Raman spectroscopy and Second Harmonic Generation are employed to study the adsorption and (catalytic) reactivity of molecules at surfaces and their dependences on the structural and electronic configuration of the substrate.

Tip enhanced Raman spectroscopy (TERS), light emission: TERS is a local, near-field Raman spectroscopy, where the 10^4 -fold Raman enhancement is provided by an optically active STM tip of Ag or Au, separated from the surface by about 1 nm. For tip radii below 100 nm, the enhanced electromagnetic field is confined within the gap between tip apex and opposing metal surface, which has a diameter of about 15 nm and smaller, thus supporting spectroscopy with nanometer resolution. The high enhancement of the Raman cross-section in the vicinity of the tip opens promising avenues towards single molecule Raman spectroscopy. TERS has been observed for dyes at Ag, Au and Pt films as well as for CN^- adsorbed at Au films. The local nature of TERS results also in a lower inhomogeneous broadening of the TERS bands. Studies on the optical resonances (from light emission induced by tunneling electrons) indicate mode structure of localized surface plasmons (G. Picardi, B. Ren).

Second harmonic generation is used to probe single crystal / electrolyte interfaces using the hanging meniscus configuration. The investigations have been extended also to faradaic reactions at these interfaces, such as periodate reduction in the presence of camphor in the electrolyte. Since the optical nonlinear response is rather insensitive to the electrochemical reaction itself, it can be used to probe structural changes of the surface induced by this reaction. It could be shown that surface reconstruction is stable under reaction at negative potentials. At more positive potentials, adsorption of periodate leads to a sudden lifting of reconstruction, an event that has no signature in current voltage curves (M. Danckwerts, S.L. Horswell).

The selective oxidation of methanol to formaldehyde at copper surfaces has been studied using mass spectrometry and Raman spectroscopy. Under specific conditions, the methanol oxidation at copper surfaces occurs in an oscillatory manner. Raman spectroscopy reveals the methoxy as the only detectable intermediate at the copper(-oxide) interface (A. Kudelski).

Effect of Insulated Areas on Pattern Formation in an Electrochemical Reaction

T. Noh, J. Christoph and M. Eiswirth

The dynamical interplay of chemical reactions is a widespread phenomenon. Not only is it the realm of electrochemistry, but it also occurs at biological membranes (e.g. in nerve cells and muscle tissue). Pattern formation in such systems is mediated by ion migration under the influence of the electric field, which can, depending on geometry, have a long interaction range enabling distant or even separate parts of the medium to communicate with each other.

The electrochemical oxidation of formic acid on a Pt ring electrode has been studied experimentally using 12 potential microprobes in order to monitor the spatiotemporal dynamics. Under oscillatory conditions with the reference electrode close to the plane of the working electrode, mainly 2 types of patterns were observed: rotating pulses and oscillatory standing waves (with the latter existing in a significantly smaller parameter region close to the Hopf bifurcation).

The Pt ring was then modified by coating several areas in a symmetric way with apiezon wax (each covering an angle of about 15-30 degrees). With 1 or 2 areas covered the standing waves were found to be stabilized (i.e. existing over a wider parameter range) with their nodes located at the insulators. Introduction of 3 insulated regions 120 degrees apart destroyed the symmetry of the standing waves, but they still persisted, with 2/3 of the electrode out of phase with the rest.

In all cases rotating pulses could still be obtained. For small overvoltages (comparable to low excitability) a pulse stopped for a moment when reaching an obstacle before jumping to the other side and continuing its propagation. This is attributed to the fact that the double layer needs some time to recharge and trigger the reaction. In contrast at higher potentials the pulse was accelerated just before encountering an obstacle and jumped over it without any noticeable delay (saltatory propagation). In these cases the coupling seemed to become rate-determining and could easily bridge the gap over the insulated area.

Theoretical studies of conductor/insulator interfaces with the reaction-migration formalism revealed that the long-range coupling can be described by a coupling function which falls off with increasing distance, but increases again close to an interface and actually diverges there (though the integral remains finite). This increased coupling close to an edge can readily explain the observed acceleration of pulses in the vicinity of the obstacles. The results may be of interest for an understanding of pulse propagation in myelinated axons, where the excitation jumps from one node of Ranvier to the next, which significantly enhances the effective propagation velocity. At least in part this acceleration may be attributed to edge effects, i.e., the increased coupling at the conductor/insulator (naked membrane/myelin sheath) interface.

Pattern formation under desynchronizing global coupling in electrochemical systems

F. Plenge, H. Varela and K. Krischer ¹

The external control of an electrochemical reaction (e.g. by means of a potentiostat or a galvanostat) often introduces a global coupling into the system, which has a decisive influence on the spatio-temporal dynamics. We present a quantitative study of the conditions under which global coupling is present in electrochemical systems and demonstrate its impact on pattern formation.

A reformulation of the evolution equation for the local electrode potential is derived in which the strength of the global coupling is given in terms of experimentally easily accessible parameters and independent of the specific electrode geometry. Furthermore, from this formulation it becomes apparent that any ohmic drop compensation introduces a negative, i.e. desynchronizing, global coupling into the system.

The impact of the global coupling on pattern formation is studied experimentally and theoretically with the hydrogen oxidation on Pt in the presence of poisons, a prototype electrochemical oscillator and a system of specific fundamental interest as well as technological relevance. A rich variety of - to a large extent novel - patterns is observed, both in experiments and simulations. The conditions under which the different patterns form are discussed and the mechanisms of their formation is elucidated employing concepts from nonlinear dynamics.

¹ Present address: Technische Universität München, Physik Dept. E19, James-Franck-Str. 1, 85748 Garching

Chemiluminescence accompanying aggregation of Ag clusters in an Ar matrix

W. Schulze, I. Rabin and G. Ertl

The agglomeration of Ag clusters resulting from codeposition of Ag and Ar atoms onto a cold substrate causes the emission of light with maximum intensities at 478 and 620 nm, respectively. These bands originate from the radiative decay of Ag_2^* and Ag_3^* , respectively. These species are created in the aggregation processes $\text{Ag}_n + \text{Ag}_m \rightarrow \text{Ag}_{n+m-2,3} + \text{Ag}_{2,3}^*$.

The yield of chemiluminescence was investigated as a function of the deposition rates of Ag and Ar at temperatures of 10 K and 30 K. The relative concentrations of (ground-state) Ag, Ag_2 , Ag_3 and Ag_8 species were monitored by means of their known fluorescence spectra, and it is concluded that the light-emitting species are created by aggregation of Ag_n clusters with $8 \leq n \leq 20$. High deposition rates of the noble gas favor the yield of light emission which is therefore not observed under 'normal' matrix isolation conditions with typical noble gas deposition rates of the order 10^{16} atoms/cm² · s. Similar effects have so far been observed with the agglomeration of Cu or Mg clusters, and it is therefore concluded that this effect is probably of quite general character.

InAs quantum dot formation on GaAs surfaces

Y. Temko, T. Suzuki, M.C Xu and K. Jacobi

With molecular beam epitaxy (MBE) and in situ scanning tunnelling microscopy (STM) we study the quantum dot (QD) formation on a variety of differently oriented GaAs surfaces. The surprising result, that at the standard GaAs(001) surface the terminating facets of the InAs QD are to more than 80% (137) surfaces and not, as always assumed, low-index (110) or (111) surfaces, was further established. From the ongoing investigation of QDs on GaAs(001), (113)A, $(\bar{1}\bar{1}\bar{3})$ B, (2 5 11)A, $(\bar{2}\bar{5}\bar{11})$ B, (114)A, $(\bar{1}\bar{1}\bar{4})$ B, (135)A, and $(\bar{1}\bar{3}\bar{5})$ B we can draw some general conclusions for the system InAs/GaAs:

- a) The QDs are rather flat, i.e., they can be better described as lenses than as pyramids. This is achieved by terminating high-index surfaces for QDs on low-index substrates and vice versa. This model works through the stable, high-index (137) and (2 5 11) surfaces discovered in our group.
- b) The shape of the QDs reflects the symmetry of the substrate as expected for epitaxial growth.
- c) The size distribution is bimodal: A large number of small, so-called coherent QDs of nearly equal size are found besides a small number of large presumably incoherent islands. The latter are assumed to incorporate dislocations at the interface, which largely reduces the strain allowing growth to larger size. Due to broken bonds and fixed charges at the dislocations these islands are thought to be optically dead.
- d) The nucleation is governed by kinetics, whereas the formation of the QD shape is near to the thermodynamic equilibrium.

Highlights of the ongoing work are the observation of dislocations at large incoherent QDs and the derivation of a model to understand the variety of QD shapes.

- J. Márquez, L. Geelhaar and K. Jacobi, Appl. Phys. Lett. **78**, 2309 (2001).
 K. Jacobi, L. Geelhaar and J. Márquez, Applied Physics A **75**, 113 (2002).
 J. Márquez, L. Geelhaar and K. Jacobi, Phys. Rev. B **65**, 165320 (2002).
 L. Geelhaar, Y. Temko, J. Márquez, P. Kratzer & K. Jacobi, Phys. Rev. B **65**, 155308 (2002).
 Y. Temko, L. Geelhaar, T. Suzuki, K. Jacobi, Surf. Sci. **513**, 328 (2002).
 T. Suzuki, Y. Temko, K. Jacobi, Surf. Sci. **511**, 13 (2002).
 T. Suzuki, Y. Temko and K. Jacobi, Appl. Phys. Lett. **80**, 4744 (2002).
 T. Suzuki, Y. Temko, and K. Jacobi, Phys. Rev. B **67**, 045315(7) (2003).
 Y. Temko, T. Suzuki, and K. Jacobi, Appl. Phys. Lett. **82**, 2142 (2003).
 K. Jacobi, Prog. Surf. Sci. **71**, 185 (2003).
 Y. Temko, T. Suzuki, P. Kratzer and K. Jacobi, Phys. Rev. B, resubmitted 17.07.03.
 Y. Temko, T. Suzuki, K. Jacobi, Appl. Phys. Lett., submitted 03.06.2003.
 T. Suzuki, Y. Temko, M.C. Xu, K. Jacobi, Surf. Sci., submitted 18.07.03.

**Surface Coordination Chemistry:
Dihydrogen versus Hydride Complexes on RuO₂(110)**

J. Wang, C.Y. Fan, Q. Sun*, K. Reuter*, K. Jacobi, M. Scheffler* and G. Ertl

Similarities between bond formation in transition metal complexes and chemisorption on solid surfaces form the basis for relations between homogeneous and heterogeneous catalysis. Coupling of hydrogen is generally associated with dissociation of the ligand. We find that hydrogen interacts in a complex manner with the two under-coordinated sites – Ru^{cus} and O^{bridge} – on the RuO₂(110) surface. Upon exposure at 85 K, H₂ instead of dissociating at Ru^{cus} weakly adsorbs as dihydrogen on top of Ru^{cus} and dissociatively interacts with O^{bridge} in forming a metastable dihydride (waterlike) complex which upon further heating transforms into the stable monohydride. The combination of low-temperature ultrahigh vacuum experiments in conjunction with density-functional theory (DFT) calculations provides detailed insights into the coordination chemistry of a solid surface which, on the other hand, exhibits remarkable correlations to complex chemistry with single transition metal atoms. Although we find strong similarities for both types of species with data from transition-metal complex chemistry, the major difference is that with the surface the two hydrogen types are associated to different sites: the dissociated β-state to O^{bridge} and the molecular α-state to Ru^{cus} atoms.

Reference:

J. Wang, C.Y. Fan, Q. Sun, K. Reuter, K. Jacobi, M. Scheffler, G. Ertl, *Angew. Chem. Int. Ed.* **42**, 2151 (2003); *Angew. Chem.* **115**, 2201 (2003).

* Theory Department

Reactions of NO and C₂H₄ on the RuO₂(110) surface

Y. Wang, U.A. Paulus, J.F. Xu, P. Geng, K. Jacobi and G. Ertl

RuO₂(110) surfaces have been prepared by exposing Ru(0001) to high doses of O₂ at 700 K. The stoichiometric RuO₂(110) surface exposes coordinatively unsaturated atoms – Ru-cus and O-bridge – and has been found to exhibit high catalytic activity for CO oxidation. The stoichiometric surface can be oxidized resulting in Ru-cus being covered by O-cus. This weakly bonded oxygen has been found to be highly reactive in oxidation of coadsorbed species, e.g., CO and CO₂. The adsorption and oxidation of NO as well as of C₂H₄ on this surface were studied by thermal desorption spectroscopy (TDS) and high-resolution electron energy-loss spectroscopy (HREELS).

NO: At low exposure (≤ 0.5 L) and 85 K, NO is adsorbed on-top of Ru-cus. After saturation of this state, NO reacts with O-bridge in forming an NO₂-type surface species which decomposes again at 250 K. At higher exposure, a small amount of N₂O-cus is formed, presumably via an (NO)₂ dimer intermediate. In parallel, a low-temperature pathway for N₂ formation is observed, which leaves the surface instantaneously between 130 and 190 K.

C₂H₄: On the stoichiometric surface, C₂H₄ adsorbs and desorbs molecularly. At 260 K, a reorientation from π - to σ -bonding is observed. On the oxidized surface C₂H₄ becomes completely oxidized through the interaction with O-cus. Under our experimental conditions an epoxide cannot be identified. A so far not identified reaction intermediate is being investigated in the ongoing study.

**Laser temperature jump experiments with nanometer space resolution
using Rhodamine 101 Anti-Stokes fluorescence from nanoseconds to
milliseconds for precise measurements of temperature changes
in liquid micro-environments**

S. Couderc-Azouani, J.F. Holzwarth, A. Beeby⁺, I.P Clark[#], T. Parker[#]

⁺University of Durham, UK, [#]Rutherford Appleton Laboratories, Chilton, Oxfordshire, UK

The measurement of temperature changes in nano-litre volumes is a serious problem, especially if both, high precision and nano-second time resolution are required.

Rhodamine 101 a water-soluble fluorescent dye whose solutions have been shown to present Anti-Stokes fluorescence at 590 nm after an excitation with a red laser (He-Ne) at 632.8 nm offers a convenient solution to the above problem. We used a pulsed dye laser with a wavelength of 633 nm and a bandwidth of 15 ns to perform time resolved measurements. The T-Jump laser (1.9 μm , 10 ns) and the 632.8 nm pulsed detection laser were aligned inside a 1 micro-meter spot of a liquid sample. We could observe a 10 % increase of the Anti-Stokes fluorescence intensity of Rhodamine 101 after the T-jump of 4 K. First the heating of the solution occurred and then the detection was performed with a variable delay between 20 ns and 100 milli-seconds. We could observe special effects caused by shock-waves produced by the fast temperature dependent expansion of the liquid sample.

This new technique of time resolved Anti-Stokes fluorescence measurements provides a convenient and precise tool to measure small temperature changes in nano-volumes of liquid samples under many different experimental conditions.

1. L.E. Erikson, J. Luminescence **5**, 1 (1972).
2. J.L. Clark, P.F. Miller and G. Rumbles, J. Phys. Chem. A **102**, 4428 (1988).
3. J.F. Holzwarth in: *Techniques and Applications of Fast Reactions in Solution*, (Eds.) W.J. Gettins and E. Wyn-Jones. Reidel Publ. Co., 1979, p. 47-59.
4. J.F. Holzwarth, A. Schmidt, H. Wolff, and R. Volk, Nanosecond Temperature Jump Technique with an Iodine Laser. J. Phys. Chem. **81**, 2300-2301 (1977).

Carbon nanotubes: Electronic structure, charge-carrier dynamics and adsorbate kinetics of novel materials

A. Hagen, G. Moos, H. Ulbricht, R. Zacharia and T. Hertel

Here, we present a detailed experimental and theoretical investigation of the optical properties of individual micelle-suspended single-wall carbon nanotubes (SWNTs) in aqueous environment. We compare the efficiency of different tensides and solvents for the exfoliation of SWNT ropes and present a quantitative interpretation of the UV-VIS-NIR spectra obtained from such exfoliated tubes. We also present a comparative study of electron-phonon interactions in materials with very weak and very large mass enhancement such as graphite and magnesiumdiboride, for example. Time-resolved photoemission is shown to be a versatile and capable tool for studying *e-ph* dynamics by a direct time domain measurement of the energy transferred between a laser-heated electron gas and the lattice. For a better understanding of the influence of adsorbates on the electronic properties of SWNTs we have also continued a systematic study of gas-surface adsorption and desorption kinetics on SWNT surfaces as well as the basal plane of graphite. The studies provide information which may become vital for a better control of nanotube solvation, wetting, doping, and their use in gas sensing applications.

Ultrafast Dynamics of Photoinduced Surface Reactions and Vibrational Spectroscopy of Adsorbates

D.N. Denzler, S. Wagner, R. Dudek, C. Frischkorn, M. Wolf and G. Ertl

In surface femtochemistry, charge and energy transfer from the substrate to the adsorbate is initiated by ultrafast-laser excitation. To gain insights and to obtain a microscopic understanding of these elementary processes, we have investigated a prototype system, the associative recombination of atomic hydrogen ($H_{ad} + H_{ad} \rightarrow H_{2,gas}$) from a Ru(001) surface. This reaction may be initiated thermally (i.e. under conditions of thermal equilibrium between all degrees of freedom), but if induced by fs-laser excitation characteristic differences are observed: (i) The hydrogen molecules coming off the surface exhibit appreciable excess kinetic energy (~ 2000 K, a value much higher than in thermal desorption), (ii) there exists a large isotope effect between H and D (which is absent in the thermal reaction), and (iii), most remarkably, desorption of the heavier isotope (D_2) is facilitated by the presence of the lighter counterpart (H_{ad}) on the surface. This dynamic promotion effect is attributed to the faster excitation of the lighter isotope due to the electronic nature of the energy transfer from the Ru surface to the hydrogen adlayer as evidenced by two-pulse correlation measurements. Furthermore, we could determine the internal energy distributions of the desorbing hydrogen molecules via state-resolved detection (REMPI – resonance enhanced multiphoton ionization). Both vibrational and rotational distributions exhibit rather high energy contents (~ 1000 – 1300 K) again exceeding thermally obtainable values.

Besides studies of femtosecond laser-induced processes en route to time-resolve a complete surface reaction ($2H + O \rightarrow H_2O$), we pursued experiments to investigate the interfacial structure of water adsorbed on Ru(001) using vibrational sum-frequency generation (SFG) spectroscopy. We apply broadband femtosecond-IR pulses, which allow the detection of vibrational spectra over the entire bandwidth of that pulse without tuning the resonance frequency. In contrast to theoretical studies (DFT) which propose a half-dissociated structure for the first bilayer (BL) of water on Ru(001), we found clear evidence that this layer consists of intact molecules. All adsorbate modes share the same coverage dependence with the peculiarity that the free OH stretch vibration vanishes at 1 BL and below. Consequently, we propose a “hydrogen-down” structure in which every second water molecule exhibits a hydrogen-metal bond.

Finally, we have revisited time-resolved pump-SFG-probe experiments on CO adsorbed on Ru. Monitoring the C-O stretch vibration, a delayed onset of a frequency shift of that mode represents an independent check of time scales for energy flow after femtosecond excitation. The sequential steps of electron-phonon coupling and subsequent phonon-mediated energy transfer into the adsorbate degrees of freedom explain our observations.

Theory Department

Poster List

Recent work done in the Theory Department and in Jörg Neugebauer's "Independent Junior Research Group" (*IG*) is displayed on 25 posters. Abstracts of 17 "selected posters" are given in the following, where those of the *IG* are indicated by the superscript ^(*IG*), as e.g. TH^(*IG*) 7.

All posters are displayed in building T and **the site** is given below (left column).

Poster Site

Poster Title and Authors

Group-IV and III-V Materials

- | | | |
|----|---|--|
| TH | 1 | Structural and Catalytic Properties of Nanoporous Carbon Studied by Density-Functional Theory
Johan M. Carlsson and Matthias Scheffler |
| TH | 3 | Indium Diffusion on Pseudomorphic In_xGa_{1-x}As Films Grown on GaAs(001)
Evgeni Penev, Sladjana Stojković, Peter Kratzer, and Matthias Scheffler |
| TH | 4 | Tight-Binding Study of the Influence of Strain on the Electronic Properties of InAs/GaAs Quantum Dots
Roberto Santoprete, Belita Koiller, Rodrigo B. Capaz, Peter Kratzer, Quincy K.K. Liu, and Matthias Scheffler |
| TH | 5 | Magnetic Properties of Thin Mn-Si Films on Si(001)
Hua Wu, Mahbube Hortamani, Peter Kratzer, and Matthias Scheffler |

Nitrides

- | | | |
|---------------------------|---|--|
| TH ^(<i>IG</i>) | 7 | Strain-Induced Metallization and Deep Electronic States around Threading Dislocations in GaN
Liverios Lymperakis and Jörg Neugebauer |
|---------------------------|---|--|

Oxygen-Metal Interactions and Metal Oxides

- TH 8 **Probing Transition Metal Oxides with Core Level Spectroscopy: Ab Initio DFT Cluster Studies for Oxygen Sites at the V₂O₅(010) Surface**
Christine Kolczewski and Klaus Hermann
- TH 9 **Stability of Pd Surface Oxides at Ambient Pressures**
Mira Todorova, Edvin Lundgren, Johan Gustafson, Jutta Rogal, Anders Mikkelsen, Jesper Andersen, Karsten Reuter, and Matthias Scheffler

Surface Phase Diagrams and Surface Chemical Reactions

- TH 12 **Adsorption and Reaction of CO, H, and H₂ at Clean and Defected Vanadium Oxide Surfaces: Ab Initio DFT Cluster Model Studies**
Christoph Friedrich and Klaus Hermann
- TH 14 **Non-Adiabatic Effects in O₂ Dissociation at Al(111)**
Jörg Behler, Sönke Lorenz, Bernard Delley, Karsten Reuter, and Matthias Scheffler
- TH 15 **Modeling Catalytic Activity with First-Principles Kinetic Monte-Carlo Simulations**
Karsten Reuter, Daan Frenkel, and Matthias Scheffler

New Methods, New Functionals

- TH^(IG) 17 **Ground State Based Formulation of the Exact Exchange Formalism (EXX)**
Matthias Wahn and Jörg Neugebauer
- TH 18 **Quasiparticle Electronic Structure and Energetics of Point Defects on Semiconductor Surfaces**
Arno Schindlmayr, Magnus Hedström, Günther Schwarz, and Matthias Scheffler
- TH 20 **Diffusion Monte Carlo Study of Small Molecules and Hydrogen Bonded Model Systems – Benchmarking Density Functionals**
Martin Fuchs, Alexander Badinski, Joel Ireta, Peter Kratzer, Claudia Filippi, and Matthias Scheffler

Biology

- TH^(IG) 21** **Structural, Energetical, and Vibrational Properties of Hydrogen Bonded Biomolecules: From Small Molecules to the α -Helix**
Lars Ismer, Joel Ireta, and Jörg Neugebauer
- TH^(IG) 22** **Mechanical Response of the α -Helix Secondary Structure under Tensile and Compressive Strain**
Joel Ireta, Jörg Neugebauer, Matthias Scheffler, Arturo Rojo, and Marcelo Galván

...and More

- TH 23** **Nanostructures at Surfaces from Substrate-Mediated Interactions**
Kristen Fichthorn, Michael L. Merrick, and Matthias Scheffler
- TH^(IG) 24** **Density Based Kinetic Monte Carlo Methods to Perform Fast Growth Simulations**
Lorenzo Mandreoli and Jörg Neugebauer

Structural and Catalytic Properties of Nanoporous Carbon Studied by Density-Functional Theory

Johan M. Carlsson and Matthias Scheffler

Dehydrogenation of ethylbenzene to form styrene is an important reaction in the chemical industry and the most common catalyst is K-promoted iron oxide [1]. However, recent theoretical work showed that the composition of iron oxide surfaces may be very different to what was hitherto believed [2]. Subsequent experimental work showed that the surface of the iron oxide catalyst gets covered by a carbon layer after a short period of use. This has been believed to severely damage the activity of the catalyst. On the other hand, the experiments had indicated that nanoporous carbon may be catalytically active [3]. Indeed, Mestl *et al.* [4] recently showed that the active dehydrogenation catalyst is the carbon material and not the iron oxide. The latter “only” serves as a catalyst to produce the active carbon structures during the induction period. Still, little is known what this structure may look alike.

We therefore studied the atomic and electronic structure of nanoporous carbon by DFT calculations. The properties of nanoporous carbon are modeled by introducing curvature and defects in graphene sheets. Our results show that the size of the vacancies depends on the environment (partial carbon pressure): The single vacancy has the lowest formation energy in an inert atmosphere, while larger vacancies become more favorable in a reactive atmosphere. Relaxation tends to pair up the undercoordinated atoms around the vacancy in order to remove dangling bonds. This mechanism is particularly efficient at the double and twelve vacancies.

The vacancies break the symmetry of the π -electron system in the graphene sheet, and in particular for the single vacancy, a semi-localized p -state is split off from the π -band. This gives a higher density of states at the Fermi level, whose character is consistent with the superstructures observed by STM in the vicinity of vacancies [5]. Tensile strain increases the bond length in the sheet and lowers the energy of the bond rotation defect. Compression induces a curvature and lowers the vacancy energy. It also leads to band broadening but does not create any localized states. This suggests that curvature itself is not enough to form a catalytically active material, but that the nanoporous carbon is activated by intrinsic (strain stabilized) defects.

(*) In collaboration with H.C. Foley, Dept. of Chemical Engineering, Pennsylvania State University, U.S.A.; D. Su and R. Schlögl, Dept. of Inorganic Chemistry, FHI.

- [1] F. Cavani and F. Trifiro, *Appl. Catal. A, General* **133**, 219 (1995).
- [2] X.-G. Wang *et al.*, *Phys. Rev. Lett.* **81**, 1038 (1998).
- [3] M.S. Kane, L.C. Kao, R.K. Mariwala, D.F. Hilscher, and H.C. Foley, *Ind. Eng. Chem. Res.* **35**, 3319 (1996).
- [4] G. Mestl, N.I. Maksimova, N. Keller, V.V. Roddatis, and R. Schlögl, *Angew. Chem. Int. Ed.* **40**, 2066 (2001).
- [5] K.F. Kelly, D. Sarkar, G.D. Halle, S.J. Oldenburg, and N.J. Halas, *Science* **273**, 1371 (1996).

Indium Diffusion on Pseudomorphic $\text{In}_x\text{Ga}_{1-x}\text{As}$ Films Grown on GaAs(001)

Evgeni Penev, Sladjana Stojković^(*), Peter Kratzer, and Matthias Scheffler

Previous experimental [1] and theoretical [2] work has shown that the early stage of InAs heteroepitaxy on GaAs(001) (sub-monolayer deposition) is characterized by surface alloying and formation of an intermixed pseudomorphic film displaying (2×3) or (1×3) reconstruction patterns. Both reconstructions are very arsenic-rich and quite similar in structure but they differ by an As dimer that is missing (desorbed) in the (1×3) structure. Frequently, experimentally prepared InGaAs films show incomplete ordering due to insufficient equilibration of the surface structure under the preparation conditions.

We use total-energy calculations within density-functional theory (DFT, PBE functional) to calculate potential energy surfaces for an In atom diffusing on a pseudomorphic InGaAs film with locally varying atomic arrangement. Using the energy barriers and prefactors from the DFT calculations, we investigate diffusion of a single In atom on a pseudomorphic film of composition $\text{In}_{2/3}\text{Ga}_{1/3}\text{As}$ as a function of temperature. Due to the complexity of the surface structure, extracting diffusion coefficients from the knowledge of the energy barriers is a non-trivial task. While diffusion coefficients on either the pure (1×3) or (2×3) reconstructed surface can be calculated analytically using the continuous-time random walk formalism, [3] the temperature and pressure range where the transition from (1×3) to (2×3) occurs is characterized by structural disorder and requires numerical methods for calculating the diffusion coefficients. We extract the diffusion coefficients from a random walk generated by a kinetic Monte Carlo simulation. The results show a drop of the diffusivity in the transition region, while the diffusion coefficients on the pure (1×3) and (2×3) surface are recovered in the simulation at high and low temperatures, respectively.

In summary, we find diffusion of In on the $\text{In}_{2/3}\text{Ga}_{1/3}\text{As}$ film to be strongly anisotropic and substantially enhanced compared to In diffusion on the GaAs(001) $c(4 \times 4)$ substrate. This will be consequential for molecular beam epitaxy and the nucleation and growth of quantum dots.

(*) Present address: CEMES/CNRS, B.P. 4347, F-31055 Toulouse Cedex, France.

[1] J.G. Belk, C.F. McConville, J.L. Sudijono, T.S. Jones, and B.A. Joyce, *Surf. Sci.* **387**, 213 (1997).

[2] P. Kratzer, E. Penev, and M. Scheffler, *Appl. Surf. Sci.* **216**, 436 (2003).

[3] J.W. Haus and K.W. Kehr, *Phys. Rep.* **150**, 263 (1987).

Tight-Binding Study of the Influence of Strain on the Electronic Properties of InAs/GaAs Quantum Dots

Roberto Santoprete^(*), Belita Koiller^(*), Rodrigo B. Capaz^(*), Peter Kratzer,
Quincy K. K. Liu^(**), and Matthias Scheffler

Nanometer-size semiconductor quantum dots (QD's) have attracted scientific interest, e.g. due to their potential applications in optoelectronic devices. Theoretical models currently employed in the study of the electronic properties of QD's are macroscopic (suited mainly for larger structures) or atomistic (mainly using pseudopotential methods). Though strain plays an important role in the QD formation, very few studies have addressed its influence in the QD bound states for electrons and holes.

We present a quantitative analysis of the influence of strain on the electronic properties of InAs/GaAs QD's [1], using Boykin's sp^3s^* empirical tight-binding model [2]. We show that this approach is reliable, faster than the pseudopotential method, and more transparent with respect to the analysis of the results in terms of the modified chemical bonding in QD's.

We report results for capped pyramid-shaped InAs QD in GaAs, with supercells containing $\sim 10^5$ atoms. The strain field is calculated by Keating's atomistic valence force field method [3]. Single-particle bound state energies (and respective wave functions) and the spatial confinement of charge inside the QD are calculated. The empirical tight-binding model enables us to analyze the influence of the bond length and bond angle deviations from the ideal InAs and GaAs zincblende structure. It also gives us the possibility to calculate single-particle bound state energies (with respective wave functions) and charge spatial confinement of an artificially strain-affected QD. By comparison with the results of the realistic dot, we find that the strain increases the energy gap between bound electron and hole states by about 25% and that the electron states become shallower and the hole states deeper. Furthermore, the influence of the dot-dot interaction on the bound states is quantitatively discussed in the case of three-dimensional QD arrays, where our method allows to analyze separately the interaction through the strain field and through wave function overlap. In the range of inter-dot distances examined here, the strain effect is both stronger and more long-ranged.

(*) Permanent address: Instituto de Física, Universidade Federal do Rio de Janeiro, Rio de Janeiro, Brazil.

(**) Permanent address: Bereich Theoretische Physik, Hahn-Meitner-Institut, Glienicke Str. 100, D-14109 Berlin.

[1] R. Santoprete, B. Koiller, R.B. Capaz, P. Kratzer, Q.K.K. Liu, and M. Scheffler, submitted to Phys. Rev. B.

[2] T. Boykin, Phys. Rev. B **56**, 9613 (1997).

[3] P. Keating, Phys. Rev. **145**, 637 (1966).

Magnetic Properties of Thin Mn-Si Films on Si(001)

Hua Wu, Mahbube Hortamani, Peter Kratzer, and Matthias Scheffler

Driven by anticipated applications of spintronics [1], considerable effort has recently been made to identify material systems that could serve as possible candidates for spintronics devices. Apart from dilute magnetic semiconductors, thin ferromagnetic metallic films are interesting to be used for injection of a spin-polarized current into the semiconductor substrate. Since both metallic Mn and Mn-Si compounds have interesting magnetic properties and are closely lattice-matched with Si [2], we choose to investigate magnetism in thin films of these materials, using the generalized gradient approximation of density functional theory and the full-potential augmented plane-wave plus local-orbital method, as implemented in the WIEN2k code.

Mn and Si have similar electronegativities, and form strong covalent bonds with each other. Therefore, upon deposition of Mn on Si(001), one could expect a variety of intermetallic phases to be formed. We investigated numerous atomic structures of pseudomorphic Mn-Si films for both their structural and magnetic properties. From our calculations we can identify the following trends: (i) While pure Mn films on Si(001) are unstable against formation of Mn bulk precipitates at the surface, a capping layer of Si strongly increases the thermodynamic stability of the films. (ii) The most stable films are found to be sandwich structures of Mn and Si layers, capped by a monolayer of Si atoms. (iii) While Mn-Mn bonding leads to antiferromagnetic coupling between the neighboring Mn spins, Mn-Si-Mn bonding can give rise to ferromagnetic coupling. Our analysis shows that the ferromagnetic coupling is due to itinerant exchange interaction [3] of the mixed Si $3s3p$ -Mn $3d$ conduction-band electrons accompanied by antiparallel coupling of the Mn and Si spins. The ferromagnetic coupling between Mn spins is found to be maximum for a sandwich consisting of two Si-Mn layers, and gets weaker for a three-layer sandwich. This finding, together with Mn spin moments of 1–2 μ_B in the film, clearly higher than in bulk MnSi, points to the role of surface effects for the magnetism of these ultra-thin films.

Moreover, the possibility of forming Si-Mn sandwich structures capped by a Si layer is supported by additional calculations, in which we demonstrate that Mn atoms can reach the subsurface site on the Si(001) surface without having to overcome substantial energy barriers.

[1] G.A. Prinz, *Physics Today* **48**, 58 (1995); *Science* **282**, 1660 (1998).

[2] G. Ctistis, U. Deffke, J.J. Paggel, and P. Fumagalli, *J. Magn. Magn. Mater.* **240**, 420 (2002).

[3] J. Kanamori and K. Terakura, *J. Phys. Soc. Japan* **70**, 1433 (2001).

Strain-Induced Metallization and Deep Electronic States around Threading Dislocations in GaN

Liverios Lymperakis and Jörg Neugebauer

Dislocations are extended defects which strongly affect electronic and structural properties of crystalline materials. A major challenge in describing dislocations is the large range of relevant length scales: While the core structure itself is rather localized the strain field is long ranged. Previous studies on dislocations in semiconductors therefore focused on isolated aspects: Density-functional theory (DFT) calculations give an accurate description of the core structure but are restricted to rather small system sizes thus excluding part of the strain field. Empirical potentials permit large-scale calculations thus allowing to accurately describe strain effects but the accuracy near the core region is rather limited. To overcome these deficiencies we have developed a multiscale approach which combines elements of DFT, empirical potentials, and continuum elastic theory and which allows to treat a system of some 10^5 atoms with *ab initio* accuracy.

Using this technique we have studied edge dislocations in GaN, a material notorious for high dislocation densities even in device-quality material. Since epitaxially grown GaN films are often highly strained the calculations have been performed for strained and unstrained GaN. Under tensile strain, characteristic of e.g. hydrogen vapor-phase epitaxy (HVPE) grown GaN, our calculations reveal a novel and hitherto not reported dislocation type. Based on the calculated atomic geometry high-resolution transmission electron microscopy (HR-TEM) image simulations have been performed. A comparison with experimental HR-TEM images of dislocations in HVPE-grown GaN gives excellent agreement [1].

Interestingly, in contrast to all previously identified dislocation structures in GaN the new structure is fully reconstructed implying that the dislocation should be electrically inactive, i.e., deep defect states should be absent. However, an analysis of the electronic structure clearly reveals the existence of deep defect states. The origin of these states is a giant local strain field which causes a metalization of bulk GaN in the vicinity of the core. An important implication of this result is that dislocations in GaN are intrinsically electrically active, i.e., independent on the specific core structure.

(*) In collaboration with T. Remmele, M. Albrecht, and H. Strunk, Universität Erlangen-Nürnberg.

[1] L. Lymperakis, J. Neugebauer, T. Remmele, M. Albrecht, and H. Strunk, submitted to Phys. Rev. Lett.

Probing Transition Metal Oxides with Core Level Spectroscopy: Ab Initio DFT Cluster Studies for Oxygen Sites at the $V_2O_5(010)$ Surface

Christine Kolczewski and Klaus Hermann

The identification and study of reactive sites at transition metal oxide surfaces is of basic scientific interest but also of great technological importance due to the use of these materials as catalysts. At the (010) surface of vanadium pentoxide, V_2O_5 , there are three differently coordinated oxygen centers (1-, 2-, 3-fold) which are available as active sites in specific oxidation reactions. Here it is interesting to know which of the sites participates in a given reaction. This requires an unambiguous identification of the oxygen sites and a characterization of their properties, both by theory and experiment. From an experimental point of view these sites can be studied at a quantitative microscopic level using high resolution electron and photon spectroscopy, such as XPS, NEXAFS, or ELNES. However, their interpretation has to be accompanied by theoretical studies to become convincing.

In the present work [1,2] we use ab initio density-functional theory (DFT) together with cluster models to calculate angular resolved 1s core level excitation spectra of the three different oxygen sites at the $V_2O_5(010)$ surface. The evaluation of the electronic excitation spectra as a function of oxygen coordination yields characteristic differences. Excitation energies and transition matrix elements (dipole-, quadrupole-type) are determined by details of the local V-O binding but also by electronic relaxation. The angular dependence of the core level spectra yields differences that are large enough to be used to discriminate between the oxygen sites. A comparison of our theoretical spectra with recent experimental NEXAFS data shows good agreement. Experimental O1s core ionization (XPS) spectra for $V_2O_5(010)$ indicate [3,4] that a discrimination of the differently coordinated oxygen centers is not possible. This is confirmed by the present theoretical study which yields ionization energies differing by less than 0.5 eV. Due to the local nature of V-O bonding the present results are also relevant for vanadium oxides with stoichiometry other than that of V_2O_5 .

[1] C. Kolczewski and K. Hermann, *J. Chem. Phys.* **118**, 7599 (2003).

[2] C. Kolczewski and K. Hermann, submitted to *Physica Scripta*, Conference Proceedings of XAFS 12.

[3] Z.M. Zhang and V.E. Henrich, *Surf. Sci.* **321**, 133 (1994).

[4] B. Tepper *et al.*, *Surf. Sci.* **496**, 64 (2002).

Stability of Pd Surface Oxides at Ambient Pressures

Mira Todorova, Edvin Lundgren^(*), Johan Gustafson^(*), Jutta Rogal,
Anders Mikkelsen^(*), Jesper Andersen^(*), Karsten Reuter, and Matthias Scheffler

An atomic-scale understanding of oxide formation at transition metal surfaces is of central importance for applications ranging from catalysis to corrosion. Roughly divided into pure on-surface adsorption, surface oxide formation, and oxide film growth, particularly the second step in the oxidation sequence is poorly understood on a microscopic level. While traditionally such initial surface oxides were considered to be closely related thin versions of the corresponding bulk oxides, recent atomic-scale characterizations, especially at Pd and Ag surfaces, revealed structures that have hardly any resemblance to the bulk counterparts. Largely influenced by a strong coupling to the underlying metal substrate [1,2], their stability range might well exceed the one of the rather weakly bound bulk oxides, and could possibly play an important role in applications like oxidation catalysis [3].

Focusing on Pd we study the oxide formation at the (100) and (111) surfaces within the framework of density-functional theory. After the formation of ordered adsorbate layers further oxidation of Pd(100) leads to a $(\sqrt{5} \times \sqrt{5})R27^\circ$ surface oxide structure before three-dimensional bulk oxide growth sets in. Motivated by new STM and high-resolution core level spectroscopy data, which are incompatible with a preceding LEED analysis of this phase [4], we propose a new, much more stable structural model: essentially a PdO(101) overlayer on Pd(100), i.e., a higher-energy facet largely stabilized by the strong coupling to the substrate [2].

Having identified the surface oxide at Pd(100) we determine its (T,p) stability range using the concept of *first-principles atomistic thermodynamics*. As expected the surface oxide represents the most stable phase for a wide range of environmental conditions, exceeding the stability range of bulk PdO by far. The corresponding overall structure of the surface phase diagram is confirmed semi-quantitatively by surface X-ray diffraction (SXRD) measurements in the pressure range up to 1 bar [5]. For temperatures below 600K the comparison with the experimental data additionally discerns a kinetic hindrance to the formation of the bulk oxide, stabilizing the $(\sqrt{5} \times \sqrt{5})R27^\circ$ surface oxide even up to ambient pressures.

(*) Permanent address: Department of Synchrotron Radiation Research, Institute of Physics, Lund University, Box 118, SE-221 00 Lund, Sweden.

- [1] E. Lundgren *et al.*, Phys. Rev. Lett. **88**, 246103 (2002)
- [2] M. Todorova *et al.*, Surf. Sci. **541**, 101 (2003).
- [3] B.L.M. Hendriksen and J.W.M. Frenken, Phys. Rev. Lett. **89**, 046101 (2002).
- [4] M. Saïdy, O.L. Warren, P.A. Thiel, and K.A.R. Mitchell, Surf. Sci. **494**, L799 (2001).
- [5] E. Lundgren *et al.*, Phys. Rev. Lett., submitted.

Adsorption and Reaction of CO, H, and H₂ at Clean and Defected Vanadium Oxide Surfaces: Ab Initio DFT Cluster Model Studies

Christoph Friedrich and Klaus Hermann

Vanadium oxides form important ingredients in industrially used catalysts for many chemical reactions. While this catalytic behavior has been known and utilized for a long time many microscopic details are still not fully understood. Experiments indicate that CO binds only weakly at the clean surface of a V₂O₅ single crystal. In contrast, CO is found to adsorb and bind more strongly at oxygen vacancy sites of the reduced surface. In addition, there is experimental evidence that local electronic excitations (introduced by X-ray or electron beam exposure) at deposited V₂O₃ nanoparticles can result in CO oxidation involving surface oxygen. H₂ is not found to bind at the V₂O₅(010) surface whereas atomic hydrogen is known to reduce the clean surface.

In the present work we have performed theoretical studies on electronic and structural details of CO, H, and H₂ interacting with differently coordinated oxygen sites O(1), O(2), and O(3) at the V₂O₅(010) surface. Electronic structure details are evaluated by ab initio density-functional theory using GGA functionals (cluster code *StoBe*) where local surface excitations are modeled by singlet to triplet cluster excitations. Energy barriers for oxidation reactions involving surface oxygen are determined both from geometry optimization methods involving Pseudo-Newton-Raphson (Murtaugh-Sargent) techniques and in some cases also from corresponding potential hypersurfaces.

Our calculations show that CO oxidation at the V₂O₅(010) surface is always connected with a rather high barrier (2.9 - 3.80 eV) for the surface ground state. However, if a local surface excitation is introduced (reducing nearby vanadium and opening oxygen valence orbitals for hybridization) the reaction barrier for CO oxidation is drastically reduced (0.4 - 1.4 eV). This is consistent with the experimental observation that local excitations can promote CO oxidation. While CO oxidation is always found to be an activated process connected with an energy barrier, CO adsorption at oxygen vacancy sites is possible without a barrier. Further, the theoretical data indicate that stable surface carbonate can be formed at the V₂O₅(010) surface. This has not been confirmed by experiment so far. H₂ dissociation at the V₂O₅ surface is found to be an activated process with high reaction barriers (2.1 - 3.2 eV) whereas formation of hydroxyl groups by adsorption of atomic hydrogen proceeds via very small barriers (0.1 - 0.3 eV). These results are consistent with recent experiments.

Non-Adiabatic Effects in O₂ Dissociation at Al(111)

Jörg Behler, Sönke Lorenz, Bernard Delley^(*), Karsten Reuter,
and Matthias Scheffler

The dissociation of O₂ at Al(111) is an important model reaction for the adsorption of simple molecules on metal surfaces – and represents the initial step in oxide formation. Numerous experiments have shown that the initial sticking probability of thermal oxygen molecules impinging onto Al(111) is only about one percent [1]. An obvious explanation would be the existence of energy barriers along the dissociation pathway, that could only be overcome by molecules of higher energy. In fact, sticking coefficients of almost unity have been measured at higher O₂ kinetic energies [1]. However, previous DFT studies did not find a sizeable energy barrier.

To investigate this problem we employ the well established “divide and conquer” approach [2]. First, the adiabatic full-potential six-dimensional potential energy surface (PES) is calculated on a grid using density-functional theory (DFT). Subsequent presentation of the PES by a neural network technique enables us to perform extensive molecular dynamics runs and reliable statistical averages. We obtain sticking coefficients close to unity for all O₂ kinetic energies – in agreement with the conclusions from preceding DFT studies, but in strong disagreement with the experimental data [1].

Concluding that essential physics is missing in the adiabatic picture we extended the standard approach by implementing a spin-constrained DFT method into the DMol³ code [3]. This approach, though similar in spirit, is an improvement over standard fixed spin moment calculations as it allows to keep the spin triplet located on the oxygen molecule while keeping the metal surface in a singlet state. With this tool we can investigate the effect of a non-adiabatic transition to the singlet ground state during dissociation, which could possibly arise from a low transition matrix element.

The resulting triplet-O₂ constrained PES exhibits energy barriers in most entrance channels towards dissociation. A non-instantaneous spin flip during the dissociation process could therefore well lead to a reduced sticking coefficient at low O₂ kinetic energies. Comparison with the experimental data enables us to discuss details of this proposed hindered triplet-singlet transition.

(*) Permanent address: Paul-Scherrer-Institut, CH-5232 Villigen PSI, Switzerland.

[1] L. Österlund, I. Zoric, and B. Kasemo, *Phys. Rev. B* **55**, 15452 (1997).

[2] A. Groß and M. Scheffler, *Phys. Rev. Lett.* **77**, 405 (1996); *Phys. Rev. B* **57**, 2493 (1998).

[3] B. Delley, *J. Chem. Phys.* **92**, 508 (1990).

Modeling Catalytic Activity with First-Principles Kinetic Monte-Carlo Simulations

Karsten Reuter, Daan Frenkel^(*), and Matthias Scheffler

The intricate bond making and breaking underlying catalytic processes requires a high accuracy in the theoretical description of each involved elementary process. Ultimately, the measurable activity of a catalyst is, however, governed by the statistical mechanics of the manifold of all these individual processes [1]. Therefore, predictive modeling needs to combine quantitatively reliable computation of all processes with an appropriate treatment of their mutual interdependencies. Within a first-principles approach this means to match electronic-structure theory with methods from statistical mechanics pushing the precision of the former into mesoscopic and even macroscopic length and time scales.

We attempt such a modeling by first-principles kinetic Monte-Carlo (kMC) simulations, i.e., using rates derived from density-functional theory. As a model system we choose the RuO₂(110) surface, which has recently received considerable attention due to its high catalytic activity for the CO oxidation reaction [1-3]. Using the computed rates from a total of 21 different elementary processes the kMC simulations consider site-specific (dissociative) adsorption, diffusion, reaction and (recombinative) desorption events for O₂ and CO at the two prominent binding sites at the RuO₂(110) surface. Within this kMC setup we can then easily follow the evolution of surface configurations up to time scales of seconds, enabling us to monitor the mesoscopic turnover rates, as well as the average surface population over the whole range of experimentally accessible gas phase conditions.

The overall structure of the derived surface phase diagram is found to be in very good agreement with our earlier predictions based on a “constrained thermodynamic equilibrium” approach [3]. Differences arise – as expected – under gas phase conditions where the system is close to a surface phase transition. It is particularly in these kinetically affected regions where we obtain high catalytic activity. In fact, the highest steady-state turnover rates occur when the phase coexistence at the surface enables a specific new reaction mechanism between O and CO, both adsorbed at cus sites, that is not operational at other temperature and pressure conditions including ultra-high vacuum.

(*) Permanent address: FOM-Institute for Atomic and Molecular Physics, Postbus 41883, NL-1009 DB Amsterdam, The Netherlands.

[1] C. Stampfl, M.V. Ganduglia-Pirovano, K. Reuter, M. Scheffler, Surf. Sci. **500**, 368 (2002).

[2] H. Over *et al.*, Science **287**, 1474 (2000).

[3] K. Reuter and M. Scheffler, Phys. Rev. Lett. **90**, 046103 (2003).

Ground State Based Formulation of the Exact Exchange Formalism (EXX)

Matthias Wahn and Jörg Neugebauer

In order to describe the exchange-potential in density-functional theory the most common approximations are based on local density approximation (LDA) or generalized density gradient approximation (GGA) functionals. However, these functionals have well known deficiencies: For example, calculations using LDA/GGA potentials systematically underestimate the bandgaps of semiconductors and insulators by as much as 40%. There are also problems in describing negative charged ions; experimentally stable ions like H^- , O^- , F^- are predicted to be unstable. Recent studies have shown that the exact treatment of the exchange-potential (EXX method) within the Kohn-Sham formalism largely compensates these deficiencies [1].

A major obstacle of this approach is that it is computationally rather expensive with respect to both memory and CPU time – in comparison with corresponding LDA/GGA calculations by about 2 to 3 orders of magnitude. The reason is that the EXX method is based on a Greens function formalism requiring the calculation of a large number of unoccupied states. This limits this approach so far on small bulk systems.

We have therefore developed an alternative formulation of the EXX method that is based on a variational principle and only requires as input ground state properties [2]. The key idea is to calculate variational derivatives by using first-order perturbation-theory. Specifically, we showed that the density induced by the non-locality of the Fock operator (the Fock induced density) is a variational quantity which can be calculated by solving the Sternheimer-equation instead of constructing the Greens function. In this formulation the calculation of unoccupied states is no longer required and the problem reduces to the minimization of a simple energy functional.

An additional advantage of the new approach is that the concept of a Fock induced density provides an intuitive and direct insight into the way EXX improves over Hartree-Fock or LDA/GGA. As a first step the method has been implemented for atoms. To test the method calculations for closed-shell atoms (beryllium and neon) have been performed which gave excellent agreement with previous studies.

[1] M. Städele, M. Moukara, J.A. Majewski, P. Vogl, and A. Görling, *Phys. Rev. B* **59**, 10031 (1999).

[2] Matthias Wahn, diploma thesis, Technische Universität Berlin (2002).

Quasiparticle Electronic Structure and Energetics of Point Defects on Semiconductor Surfaces

Arno Schindlmayr^(*), Magnus Hedström, Günther Schwarz^(**),
and Matthias Scheffler

Point defects strongly influence the transport, electronic, and optical properties of semiconductors. For this reason, the location of defect states in the band gap and the energetics of transitions between different charge states are important material characteristics. Previous theoretical studies of defect states and charge transition levels showed systematic deviations from experimental measurements, for instance in the case of the anion vacancies on the (110) surfaces of III–V semiconductors [1,2]. The discrepancy arises from the use of the local-density approximation (LDA), which misses the discontinuity of the exact exchange-correlation functional upon changes of the particle number. In order to overcome this problem, we employ many-body perturbation theory and the *GW* approximation for the electronic self-energy, which gives an accurate quantitative description of electron-transfer energies between the defect state and the reservoir.

As a first test case, we consider As vacancies on the GaAs(110) surface. Compared to the LDA, the *GW* approximation opens the band gap to the experimental value of 1.5 eV. While the occupied and unoccupied surface bands follow the shifts of the corresponding bulk bands, the position of the defect level depends strongly on its charge state. In particular, in the positive charge state, the $1a''$ vacancy state in the band gap is shifted from 0.06 to 0.65 eV above the valence-band maximum after the self-energy correction to the Kohn-Sham eigenvalues. The more complex charge-transition levels are addressed by a decomposition into two distinct energy contributions: the nonadiabatic transfer of an electron between the defect state and the reservoir, calculated within the *GW* approximation, and the subsequent lattice relaxation. The latter is given accurately by the LDA, as the electron number remains constant. For the P vacancy on InP(110), our calculation predicts a $\epsilon^{+/0}$ charge-transition level of 0.90 eV, which is several tenths of an eV higher than previous theoretical results and in close agreement with experimental data [1].

(*) Present address: Institut für Festkörperforschung, Forschungszentrum Jülich GmbH, D-52425 Jülich.

(**) Present address: Lehrstuhl für Theoretische Festkörperphysik, Universität Erlangen-Nürnberg, Staudtstr. 7, D-91058 Erlangen.

[1] Ph. Ebert *et al.*, Phys. Rev. Lett. **84**, 5816 (2000).

[2] M.C. Qian, M. Göthelid, B. Johansson, and S. Mirbt, Phys. Rev. B **66**, 155326 (2002).

Diffusion Monte Carlo Study of Small Molecules and Hydrogen Bonded Model Systems – Benchmarking Density Functionals

Martin Fuchs, Alexander Badinski, Joel Ireta, Peter Kratzer, Claudia Filippi^(*),
and Matthias Scheffler

Although widely employed and often giving useful accuracy, DFT calculations rely on approximate exchange-correlation functionals whose accuracy must be *assessed a posteriori*. Recent evidence warns that significant errors can occur for standard functionals like generalized gradient approximations (GGA) even in systems where they were expected to perform well [1]. This observation underlines the need for identifying (and correcting) such limitations. The diffusion quantum Monte Carlo (DMC) method promises to be a useful tool to this end, avoiding drawbacks of more common *ab initio* approaches: DMC provides (in principle) a highly accurate and systematically controlled treatment of many-electron correlation. At the same time, DMC remains computationally tractable even for larger systems where established quantum chemical post-Hartree-Fock approaches become impractical. However, DMC is not yet a routine tool, and experience to corroborate its robustness is still scarce.

Applying the DMC method together with pseudopotentials, we examined its performance for (i) selected first-row molecules and (ii) model systems for hydrogen bonds, the latter playing a key role in the structure and functionality of biomolecules. For the first-row molecules we obtain dissociation energies, bond geometries, and fundamental vibrational frequencies that rival quantum chemical reference data in accuracy and confirm the soundness of the approach. Still we demonstrate, for the N₂ molecule, that the fixed node approximation and approximating nonlocal pseudopotentials as local operators, can incur noticeable errors. We also note that without knowing the true result, problems like those observed for N₂ might be easily overlooked.

Regarding H-bonded systems our DMC results show that the energy barriers for proton transfer in the di-ammonium and formamide-water complexes and malon-aldehyde turn out severely underestimated within the PBE-GGA, even if the H-bond strengths are described rather well. Examining finite formamide chains, we further show that the PBE-GGA correctly predicts the increase of the H-bond strength (cooperativity) in longer chains. This result supports a recent PBE-GGA study explaining the stabilization of the α helical structure of polyalanine [2].

(*) Permanent address: Instituut Lorentz for Theoretical Physics, Universiteit Leiden, NL-2300 RA Leiden, The Netherlands.

- [1] C. Filippi, S.B. Healy, P. Kratzer, E. Pehlke, and M. Scheffler, Phys. Rev. Lett. **89**, 166102 (2002).
[2] J. Ireta, J. Neugebauer, M. Scheffler, A. Rojo, and M. Galván, J. Phys. Chem. B **107**, 1432 (2003).

Structural, Energetical and Vibrational Properties of Hydrogen Bonded Biomolecules: From Small Molecules to the α -Helix

Lars Ismer, Joel Ireta, and Jörg Neugebauer

Hydrogen bonds (hbs) and proton transfer (pt) play a key role in the functionality of biomolecules. Therefore, to gain a deeper understanding in the bio-activity of such molecules it is crucial to accurately describe their structural, energetical and vibrational properties. Previous *ab initio* studies employing density-functional theory (DFT) or quantum-chemical methods focused mainly on small hydrogen bonded molecules of at most a few tens of atoms. For larger and more realistic systems, such as e.g. models accounting for the secondary structure of proteins, values derived exclusively from *ab initio* calculations are rare, especially for vibrational properties. In the present study we have investigated vibrational and thermodynamic properties of a protein (poly-alanine) in α -helical conformation taking the secondary structure fully into account.

At the first stage we performed extensive checks on the accuracy/performance of various generalized density gradient approximation (GGA) functionals to describe hb strengths, pt barriers, atomic geometries and vibrational frequencies of small hydrogen-bonded molecules. A comparison with highly accurate quantum chemical methods (configuration interaction, coupled cluster) showed that the Perdew-Burke-Ernzerhof (PBE) functional [1] allows an accurate description of the hb strength (error ~ 1 kcal/mol) but underestimates pt barriers by ~ 5 kcal/mol. Although this error is reflected in the atomic geometries and also in the vibrational frequencies, the resulting deviations for the zero-point vibrational energies are generally rather small (~ 0.5 kcal/mol).

Based on these results we calculated the full phonon dispersion relation of an infinite poly-alanine chain in α -helical conformation using PBE and within the harmonic regime. A comparison with recent experimental results [2] shows an excellent agreement for all branches below 2000 cm^{-1} . For the high-frequency hydrogen-stretching modes, however, the calculated modes were systematically lower by $50\text{-}100\text{ cm}^{-1}$ with respect to the experimental ones. An analysis of this effect showed that it is related to the small atomic mass of hydrogen which gives rise to sizeable anharmonic contributions. Using the vibrational spectra for the first time a full *ab initio* based thermodynamic analysis of the helix could be performed.

[1] J.P. Perdew, K. Burke, and M. Ernzerhof, Phys. Rev. Lett. **77**, 3865 (1996).

[2] H. Lee and S. Krimm, Biopolymers **46**, R283 (1998).

Mechanical Response of the α -Helix Secondary Structure under Tensile and Compressive Strain

Joel Ireta, Jörg Neugebauer, Matthias Scheffler, Arturo Rojo^(*)
and Marcelo Galván^(*)

Proteins undergo constant motions and structural changes in cells. These processes might compress or tense the protein's tertiary and secondary structure. Therefore, the knowledge of the protein's mechanical properties is needed to understand their biological function. Experimentally, protein behavior under *tensile strain* has been studied by force microscopy. And the behavior under *compressive strain* has been investigated by static high-pressure and fast shock compression experiments. While such experiments give important information they are (presently) not able to provide insight into the microscopic processes.

We have therefore studied the mechanical response of a protein under tensile and compressive strain. Specifically, we investigated the response of an infinite polyalanine chain in α -helical conformation since this is the smallest realistic model of a protein. We employ density functional theory (DFT) and *ab initio* pseudopotentials with the parallel version of the FHI98md code. Exchange and correlation are described using the generalized gradient approximation in the Perdew-Burke-Ernzerhof formulation.

Calculating the response force along the helix axis as function of strain, we can identify three distinct regimes. In particular, for intermediate compression/stretch we observe plateaus. Similar behavior has been observed in experiments on polymers and biopolymers under tension [1,2], as well as in statistical mechanics models when simulating tensile strain [3,4].

The presence of such plateau is characteristic for a first order phase transition. The transition occurs for a compressive force larger than 200 pN or for a stretching force larger than 50 pN. An analysis of the hydrogen bond (hb) strength and the peptide group response to strain suggests that the phase transition under compression is driven by the interplay between hb breaking and deviation from planarity of the carbon atom of the carbonyl group (carbon pyramidalization). However, under tension the key degree of freedom driving the transition is a nitrogen pyramidalization.

(*) Permanent address: Universidad Autónoma Metropolitana-Iztapalapa, Departamento de Química, A.P. 55-534, México D.F. 09340, México.

- [1] C.G. Baumann *et al.*, *Biophys. J.* **78**, 1965 (2000).
- [2] B.J. Haupt, T.J. Senden, and E.M. Sevick, *Langmuir* **18**, 2174 (2002).
- [3] D.A. Kessler and Y. Rabin, *Phys. Rev. Lett.* **90**, 024301 (2003).
- [4] D. Marenduzzo, A. Maritan, A. Rosa, and F. Seno, *Phys. Rev. Lett.* **90**, 088301 (2003).

Nanostructures at Surfaces from Substrate-Mediated Interactions

Kristen Fichthorn^(*), Michael L. Merrick^(*), and Matthias Scheffler

Recent theoretical [1-5] and experimental [6,7] studies show that indirect interactions, mediated by the substrate, can be significant enough to influence the formation of nanostructures at surfaces. The way that these interactions influence adsorbate island formation is not understood and is the subject of this work.

We focus on understanding indirect interactions mediated by Shockley surface-state electrons. Noble-metal fcc(111) surfaces possess these surface states and the long-range, oscillatory interaction associated with them is well understood from both a theoretical [3] and experimental [6,7] standpoint. In recent, large-scale, DFT calculations [1], as well as experimental STM studies [6,7], it has been shown that these interactions yield a repulsive barrier at “intermediate” separations that prevents island nucleation and growth during thin-film epitaxy. Kinetic Monte Carlo (kMC) simulations [1,2,4,5] show that this leads to higher island densities than those expected from standard nucleation theory. Experimental work supports these predictions [7,8,9]. Here, we investigate another important ramification of “intermediate-range”, substrate-mediated interactions: their influence on the sizes and shapes of adsorbate islands that develop during thin-film epitaxy.

We examine the growth of Ag on compressively strained Ag(111) and Cu on Cu(111), using pair potentials obtained from DFT calculations for Ag [1] and a potential inferred from experiment [6,7] for Cu. We show that electronic interactions on these surfaces lead to the formation of repulsive barriers surrounding small adsorbate islands. These barriers increase with increasing island size and they depend on island shape. To investigate the ramifications of these size- and shape-dependent “island barriers” for the formation of nanostructures on surfaces, we conduct kMC simulations of thin-film growth. We show that the dependence of these barriers on island size and shape actuates sharp island-size distributions, which can be manipulated by changing growth conditions to yield selected island sizes and shapes. The existence of these interactions opens new prospects for engineering nanostructures at surfaces.

(*) Permanent address: Department of Chemical Engineering, The Pennsylvania State University, University Park, PA 16802, U.S.A.

- [1] K.A. Fichthorn and M. Scheffler, *Phys. Rev. Lett.* **84**, 5371 (2000).
- [2] A. Bogicevic *et al.*, *Phys. Rev. Lett.* **85**, 1910 (2000).
- [3] P. Hyldgaard and M. Persson, *J. Phys. Cond. Matter* **12**, L13 (2000).
- [4] S. Ovesson, A. Bogicevic, G. Wahnstrom, and B. I. Lundqvist, *Phys. Rev. B* **64**, 125423 (2001).
- [5] K.A. Fichthorn, M. Merrick, and M. Scheffler, *Appl. Phys. A* **75**, 17 (2003).
- [6] J. Repp, F. Moresco, G. Meyer, K.-H. Rieder, P. Hyldgaard, and M. Persson, *Phys. Rev. Lett.* **85**, 2981 (2000).
- [7] N. Knorr, H. Brune, M. Epple, A. Hirstein, M.A. Schneider, and K. Kern, *Phys. Rev. B* **65**, 115420 (2002).
- [8] H. Brune, K. Bromann, H. Roeder, and K. Kern, *Phys. Rev. B* **52**, R14380 (1995).
- [9] J. V. Barth, H. Brune, B. Fischer, J. Weckesser, and K. Kern, *Phys. Rev. Lett.* **84**, 1732 (2000).

Density Based Kinetic Monte Carlo Methods to Perform Fast Growth Simulations

Lorenzo Mandreoli and Jörg Neugebauer

Kinetic Monte Carlo (kMC) simulations are one of the key methods to perform growth simulations on realistic length and time scales. An advantage compared to mesoscopic/macrosopic approaches, such as rate equations or continuum models, is that all microscopic processes can be accurately included thus allowing a direct connection to *ab initio* calculations. A major problem in applying conventional kMC techniques is that the number of microscopic events and thus the computational effort scales exponentially with temperature. An analysis of typical kMC simulations showed that this effect is mainly related to calculating the full trajectory of each surface adatom. In a previous study [1] we showed how by replacing the adatom *trajectory* by an adatom *density* the short time scale needed to describe adatom events (diffusion) can be efficiently decoupled from the long time scale on which the relevant growth events occur.

To apply this approach to actual growth simulations two key problems have to be addressed: (i) Fast and accurate algorithms to calculate the adatom density propagation in time have to be developed and (ii) nucleation and attachment rates have to be calculated solely on the basis of the adatom density. We have therefore developed an intermediate scheme where the time propagation of the probability density $P_{\alpha}(x_1, t_1, x_2, t_2)$ is calculated explicitly for each individual adatom α . Here, x_1, t_1 are adsorption site and time, x_2, t_2 are site and time at which the probability is determined. An advantage of this formalism is that the probability function is *smooth in time* and requires only few steps to describe the evolution in time even at high temperatures. For typical systems the number of time steps could be reduced by two up to four orders of magnitude. An interesting feature of this method is that it is fully compatible to standard kMC calculations. In contrast to all previous density based approaches it can be also applied at low growth temperatures to describe fractal growth.

Another interesting aspect of the new approach is that it provides a formal analogy between nucleation and electron-electron interaction. This allowed us to use techniques originally developed to describe the electronic many particle systems (such as e.g. the Hartree approximation) to describe nucleation. Based on these developments an extensive set of growth simulations has been performed. Excellent agreement with kMC simulations for all relevant statistical parameters (island density, size distribution, shape) is found.

[1] L. Mandreoli, J. Neugebauer, R. Kunert, and E. Schöll, Phys. Rev. B, in print.